

Fluorinated quorum sensing inhibitors: enhancement of potency through conformational control

*Yuvixza Lizarme-Salas, Tsz Tin Yu, Caspar de Bruin-Dickason, Naresh Kumar and Luke Hunter**

SUPPORTING INFORMATION

Contents:

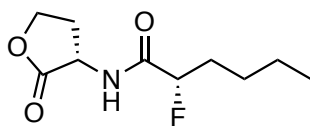
1. Synthetic reagents and instrumentation	S-2
2. Synthetic procedures and characterisation data	S-3
3. Determination of absolute configurations and optical purities	S-22
4. Selected NMR spectra	S-24
5. NMR <i>J</i> -based analysis methodology	S-68
6. DFT study	S-77
7. Biological assay details	S-83
8. Docking procedures	S-84
9. References	S-90

1. Synthetic reagents and instrumentation

Reactions were performed in oven-dried glassware at room temperature and under a nitrogen atmosphere with magnetic stirring unless stated otherwise. All commercial reagents were of synthetic grade and used as received. Reactions were monitored by thin layer chromatography (TLC) using Merck aluminum-backed silica gel 60 F254 (0.2mm) TLC plates. TLC product spots were visualised either under short-wave UV light (254 nm) or by staining with KMnO_4 and heating. Flash chromatography was performed using DAVISIL 40-63 mesh silica gel, and eluents were stated as volume-to-volume ratios. Melting points were determined using an OptiMelt melting point apparatus MPA100. IR spectra were recorded using a Cary 630 Fourier Transform Infrared (FTIR) spectrometer equipped with attenuated total reflectance (ATR) with a diamond crystal inset. NMR spectra were obtained using Bruker Avance III 300, 400 and 600 MHz instruments at 300 K. Residual solvent peaks were used as an internal reference to calibrate ^1H and ^{13}C spectra. Splitting patterns in NMR are represented by s = singlet, d = doublet, br s = broad singlet, dm = doublet of multiplets (typically for CHF protons where the 2J is easy to determine while the others are difficult). When necessary to aid in the peak assignment, 2D NMR experiments including COSY, HMBC and HSQC were performed. Coupling constants from complex spectra were obtained by Daisy simulation within the Bruker TopSpin software. In the ^{19}F NMR spectra of difluorinated substances, the α -F and β -F signals were readily distinguishable because the α -F signal typically had a simpler splitting pattern (it couples to fewer protons). HRMS results were acquired at the UNSW Bioanalytical Mass Spectrometry Facility using an Orbitrap LCQ XP Plus ion trap MS in positive ion mode using electrospray ionization (ESI). Optical rotations were measured using a Perkin Elmer model 341 polarimeter ($\lambda = 589 \text{ nm}$; $l = 1 \text{ dm}$; c expressed in grams per 100 mL).

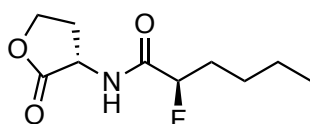
2. Synthetic procedures and characterisation data

(*S*)-2-Fluoro-*N*-((*S*)-2-oxotetrahydrofuran-3-yl)hexanamide (**2a**)



A solution of acid **5** (36.8 mg, 0.274 mmol), 1-hydroxybenzotriazole monohydrate (44.4 mg, 0.274 mmol) and *N,N'*-diisopropylcarbodiimide (0.047 mL, 0.460 mmol) in dry DMF (2.5 mL) was stirred at r.t. for 15 min. L-Homoserine lactone (47.1 mg, 0.258 mmol) was added, and the mixture was stirred at r.t. for 38 h. The mixture was concentrated under reduced pressure and the residue was dissolved in ethyl acetate (60 mL). The organic solution was washed with water (10 × 5 mL) and brine (3 × 15 mL), dried (Na₂SO₄) and concentrated onto silica under reduced pressure. The residue was subjected to column chromatography, eluting with 5:95→10:90 ethyl acetate/chloroform, to afford amide **2a** as a sticky pale yellow solid (24.9 mg, 44%); [α]_D -15.3 (*c* 0.458, CHCl₃); IR (DCM) ν_{\max} (cm⁻¹) 3285, 3079, 2953, 2870, 1774, 1656, 1548, 1384, 1270, 1181, 1065, 1018; ¹H NMR (400 MHz, CDCl₃) δ 6.92 (s, 1H, NH), 4.92 (ddd, *J* = 3.7, 7.7, 49.5 Hz, 1H, CHF), 4.59 (ddd, *J* = 6.5, 8.5, 11.3 Hz, 1H, CHHOCO), 4.47 (dd, *J* = 1.2, 13.6 Hz, 1H, NHCH), 4.29 (ddd, *J* = 6.0, 9.3, 11.3 Hz, 1H, CHHOCO), 2.81 (dddd, *J* = 1.2, 6.0, 8.5, 12.6 Hz, 1H, CHHCH₂OCO), 2.22 (ddd, *J* = 8.8, 11.6, 23.7 Hz, 1H, CHHCH₂OCO), 1.97 (m, 1H, CHFCHH), 1.83 (m, 1H, CHFCHH), 1.46–1.31 (m, 4H, CH₃CH₂CH₂), 0.90 (t, *J* = 7.2 Hz, 3H, CH₃); ¹³C{¹H} NMR (101 MHz, CDCl₃) δ 174.8, 171.1 (d, *J* = 20.3 Hz), 92.0 (d, *J* = 185.6 Hz), 66.0, 48.9, 32.1 (d, *J* = 21.1 Hz), 30.1, 26.4 (d, *J* = 2.6 Hz), 22.3, 13.8; ¹⁹F NMR (377 MHz, CDCl₃) δ -190.8 (m, 1F), ¹⁹F{¹H} NMR (377 MHz, CDCl₃) δ -190.8 (s, 1F); HRMS (ESI, +ve) C₁₀H₁₆FNO₃Na⁺ [MNa⁺] requires *m/z* 240.1006, found 240.1004.

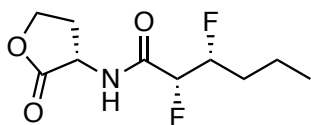
(*R*)-2-Fluoro-*N*-((*S*)-2-oxotetrahydrofuran-3-yl)hexanamide (**2b**)



The title compound was synthesised from acid *ent*-**5** on 0.182 mmol scale, in a similar fashion to that described above for amide **2a**. Amide **2b** was obtained as a sticky yellow solid (10.4 mg, 28%); [α]_D +27.0 (*c* 0.185, CHCl₃); IR (neat) ν_{\max} (cm⁻¹) 3290, 3081, 2925, 2859, 1771, 1656, 1544, 1380, 1267, 1181, 1013; ¹H NMR (400 MHz, CDCl₃) δ 6.81 (s, 1H, NH), 4.92 (ddd, *J* = 3.7, 7.7, 49.0 Hz, 1H, CHF), 4.61 (ddd, *J* = 7.5, 8.7, 11.3 Hz, 1H, CHHOCO), 4.48 (dd, *J* = 1.0, 13.7 Hz, 1H, NHCH), 4.30

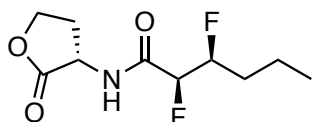
(ddd, $J = 5.9, 9.4, 11.3$ Hz, 1H, CHHOCO), 2.81 (dddd, $J = 1.0, 5.9, 8.6, 12.4$ Hz, 1H, CHHCH₂OCO), 2.21 (ddd, $J = 8.7, 11.3, 23.7$ Hz, 1H, CHHCH₂OCO), 2.07–1.79 (m, 2H, CHFCH₂), 1.50–1.32 (m, 4H, CH₃CH₂CH₂), 0.92 (t, $J = 7.2$ Hz, 3H, CH₃); ¹³C{¹H} NMR (101 MHz, CDCl₃) δ 174.7, 171.1 (d, $J = 20.0$ Hz), 92.1 (d, $J = 185.6$ Hz), 66.0, 48.8, 32.1 (d, $J = 20.0$ Hz), 30.2, 26.5 (d, $J = 2.4$ Hz), 22.3, 13.9; ¹⁹F NMR (377 MHz, CDCl₃) δ –190.7 (m, 1F); ¹⁹F{¹H} NMR (377 MHz, CDCl₃) δ –190.7 (s, 1F); HRMS (ESI, +ve) C₁₀H₁₆FNO₃Na⁺ [MNa⁺] requires m/z 240.1006, found 240.1008.

(2*R*,3*R*)-2,3-Difluoro-*N*-((*S*)-2-oxotetrahydrofuran-3-yl)hexanamide (**2c**)



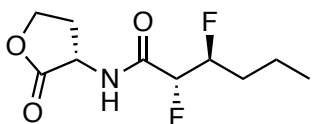
A solution of L-homoserine lactone hydrobromide (29.4 mg, 0.162 mmol) and Et₃N (0.022 mL, 0.162 mmol) in water (800 μL) was added to a solution of EDC.HCl (40.1 mg, 0.209 mmol) and acid **11** (27.0 g, 0.177 mmol) in acetonitrile (1.60 mL). The mixture was stirred at r.t. for 24 h. The mixture was concentrated under reduced pressure, and the residue was dissolved in chloroform (100 mL). The organic solution was washed with water (3 × 30 mL) and saturated aqueous NaHCO₃ (3 × 30 mL), dried (MgSO₄) and concentrated onto silica under reduced pressure. The residue was subjected to column chromatography, eluting with 98:2 hexane:methanol to afford a partially-purified sample of amide **2c**. This sample was subjected to preparative reverse phase HPLC eluting with 2:98→100:0 acetonitrile:water over 50 min, to afford pure amide **2c** as a waxy pale yellow solid (9.60 mg, 25%); [α]_D –12.5 (*c* 0.480, CHCl₃); IR (DCM) ν_{max} (cm⁻¹) 3291, 2957, 2960, 2871, 1675, 1602, 1518, 1455, 1342, 1320, 1260, 1130, 1067, 1028; ¹H NMR (400 MHz, CDCl₃) δ 6.86 (s, 1H, NH), 4.94 (dddd, $J = 1.4, 5.0, 8.9, 28.1, 45.3$ Hz, 1H, CH₂CHF), 4.87 (ddd, $J = 1.4, 29.6, 47.2$ Hz, 1H, CH₂CHFCHF), 4.69 (ddd, $J = 6.9, 7.9, 11.7$ Hz, 1H, CHHOCO), 4.48 (ddd, $J = 1.0, 8.9, 9.1$ Hz, 1H, NHCH), 4.31 (ddd, $J = 5.8, 9.1, 11.7$ Hz, 1H, CHHOCO), 2.88 (dddd, $J = 1.0, 5.8, 8.2, 13.0$ Hz, 1H, CHHCH₂OCO), 2.18 (ddd, $J = 8.9, 12.0, 23.9$ Hz, 1H, CHHCH₂OCO), 1.93 (m, 1H, CH₃CH₂CHH), 1.75–1.38 (m, 3H, CH₃CH₂CHH), 0.99 (t, $J = 7.3$ Hz, 3H, CH₃); ¹³C{¹H} NMR (101 MHz, CDCl₃) δ 174.6, 167.8 (dd, $J = 3.8, 21.0$ Hz), 92.1 (dd, $J = 5.2, 19.9$ Hz), 90.3 (dd, $J = 13.9, 19.9$ Hz), 66.1, 48.9, 32.2 (dd, $J = 4.4, 20.3$ Hz), 30.4, 18.3 (d, $J = 5.2$ Hz), 13.8; ¹⁹F NMR (377 MHz, CDCl₃) δ –197.6 (m, 1F, CH₂CHF), –208.6 (m, CH₂CHFCHF); ¹⁹F{¹H} NMR (377 MHz, CDCl₃) δ –197.6 (d, $J = 11.2$ Hz, 1F, CH₂CHF), –208.6 (d, $J = 11.2$ Hz, 1F, CH₂CHFCHF); HRMS (ESI, +ve) C₁₀H₁₅NO₃F₂Na⁺ [MNa⁺] requires m/z 258.0912, found 258.0909.

(2*S*,3*S*)-2,3-Difluoro-*N*-((*S*)-2-oxotetrahydrofuran-3-yl)hexanamide (**2d**)



The title compound was synthesised from difluorinated acid *ent*-**11** on 0.127 mmol scale, in a similar fashion to that described above for amide **2a**. Amide **2d** was obtained as a waxy yellow solid (6.30 mg, 26%); $[\alpha]_D -103$ (*c* 0.126, CHCl₃); IR (DCM) ν_{\max} (cm⁻¹) 3297, 3055, 2964, 1778, 1687, 1535, 1420, 1179, 1131, 1071, 1019; ¹H NMR (600 MHz, CDCl₃) δ 6.95 (br s, 1H, NH), 4.93 (dddd, *J* = 1.4, 4.9, 9.0, 27.0, 46.5 Hz, 1H, CH₂CHF), 4.86 (ddd, *J* = 1.4, 29.0, 47.1 Hz, 1H, CH₂CHFCHF), 4.51 (ddd, *J* = 1.4, 9.2, 9.8 Hz, 1H, CHHOCO), 4.49 (ddt, *J* = 1.4, 6.1, 13.7 Hz, 1H, NHCH), 4.30 (ddd, *J* = 6.1, 9.2, 11.2 Hz, 1H, CHHOCO), 2.83 (ddd, *J* = 1.0, 6.1, 13.7 Hz, 1H, CHHCH₂OCO), 2.30 (ddt, *J* = 1.0, 11.2, 20.9 Hz, 1H, CHHCH₂OCO), 1.93 (dddd, *J* = 1.0, 5.4, 9.2, 17.9, 18.8 Hz, 1H, CH₃CH₂CHH), 1.74–1.38 (m, 3H, CH₃CH₂CHH), 0.99 (t, *J* = 7.3 Hz, 3H, CH₃); ¹³C{¹H} NMR (151 MHz, CDCl₃) δ 174.1, 167.7 (dd, *J* = 3.4, 21.0 Hz), 91.1 (dd, *J* = 20.9, 196.3 Hz), 90.9 (dd, *J* = 18.6, 177.8 Hz), 66.0, 49.1, 32.0 (dd, *J* = 4.4, 21.0 Hz), 29.6, 18.2 (d, *J* = 5.4 Hz), 13.7; ¹⁹F NMR (565 MHz, CDCl₃) δ -197.1 (m, 1F, CH₂CHF), -208.1 (m, CH₂CHFCHF), ¹⁹F{¹H} NMR (565 MHz, CDCl₃) δ -197.1 (d, *J* = 11.4 Hz, 1F, CH₂CHF), -208.1 (d, *J* = 11.4 Hz, 1F, CH₂CHFCHF), HRMS (ESI, +ve) C₁₀H₁₅NO₃F₂Na⁺ [MNa⁺] requires *m/z* 258.0912, found 258.0910.

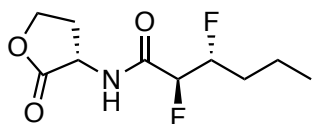
(2*R*,3*S*)-2,3-Difluoro-*N*-((*S*)-2-oxotetrahydrofuran-3-yl)hexanamide (**2e**)



The title compound was synthesised from difluorinated acid *ent*-**13** on 0.094 mmol scale, in a similar fashion to that described for amide **2a**. Amide **2e** was obtained as a waxy yellow solid (4.80 mg, 27%); $[\alpha]_D -47.6$ (*c* 0.126, CHCl₃); IR (MeOH) ν_{\max} (cm⁻¹) 3365, 2962, 2920, 2873, 2861, 1780, 1675, 1539, 1378, 1454, 1191, 1027; ¹H NMR (400 MHz, CDCl₃) δ 6.87 (s, 1H, NH), 5.12 (ddd, *J* = 1.8, 19.7, 49.1 Hz, 1H, CH₂CHFCHF), 4.91 (dddd, *J* = 1.8, 3.3, 10.0, 24.8, 47.2 Hz, 1H, CH₂CHF), 4.57 (ddd, *J* = 6.5, 8.6, 11.3 Hz, 1H, CHHOCO), 4.50 (dt, *J* = 1.1, 9.2 Hz, 1H, NHCH), 4.31 (ddd, *J* = 6.0, 9.2, 11.3 Hz, 1H, CHHOCO), 2.84 (dddd, *J* = 1.1, 6.0, 8.6, 13.0 Hz, 1H, CHHCH₂OCO), 2.22 (ddd, *J* = 8.6, 11.8, 23.4 Hz, 1H, CHHCH₂OCO), 1.89 (m, 1H, CH₃CH₂CHH), 1.64–1.37 (m, 3H, CH₃CH₂CHH), 0.96 (t, *J* = 7.1 Hz, 3H, CH₃); ¹³C{¹H} NMR (151 MHz, CDCl₃) δ 174.3, 167.0 (dd, *J* = 9.5, 20.3 Hz), 92.4 (dd, *J* = 19.8, 177.3 Hz), 91.9 (dd, *J* = 30.0, 194.0 Hz), 66.1, 49.0, 30.8 (dd, *J* = 6.0, 21.3 Hz), 30.1, 18.5 (d, *J* = 3.4 Hz), 13.8; ¹⁹F NMR (377 MHz, CDCl₃) δ -193.5 (m, 1F,

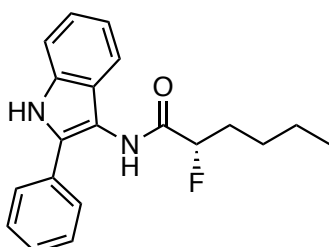
CH₂CHF), -199.6 (m, 1F, CH₂CHFCH₂F), ¹⁹F{¹H} NMR (377 MHz, CDCl₃) δ -193.5 (d, *J* = 12.8 Hz, 1F, CH₂CHF), -199.6 (d, *J* = 12.8 Hz, 1F, CH₂CHFCH₂F); HRMS (ESI, +ve) C₁₀H₁₅NO₃F₂Na⁺ [MNa⁺] requires *m/z* 258.0912, found 258.0909.

(2*S*,3*R*)-2,3-Difluoro-*N*-((*S*)-2-oxotetrahydrofuran-3-yl)hexanamide (**2f**)



The title compound was synthesised from difluorinated acid **13** on 0.187 mmol scale, in a similar fashion to that described above for amide **2a**. Amide **2f** was obtained as a sticky white solid (15.2 mg, 38%); [α]_D +15.2 (*c* 0.286, CHCl₃); IR (neat) ν_{max} (cm⁻¹) 3291, 3075, 2962, 2351, 2116, 1773, 1656, 1543, 1460, 1383, 1355, 1270, 1225, 1177, 1116; ¹H NMR (400 MHz, CDCl₃) δ 6.88 (s, 1H, NH), 5.13 (ddd, *J* = 1.9, 18.6, 49.5 Hz, 1H, CH₂CHFCH₂F), 4.92 (dddd, *J* = 1.9, 2.6, 10.0, 25.3, 47.1 Hz, 1H, CH₂CHF), 4.59 (ddd, *J* = 7.0, 8.3, 11.5 Hz, 1H, CHHOCO), 4.49 (dd, *J* = 1.1, 9.2 Hz, 1H, NHCH), 4.30 (ddd, *J* = 5.9, 9.2, 11.1 Hz, 1H, CHHOCO), 2.81 (dddd, *J* = 1.1, 5.9, 8.4, 12.6 Hz, 1H, CHHCH₂OCO), 2.24 (ddd, *J* = 8.8, 11.5, 24.0 Hz, 1H, CHHCH₂OCO), 1.89 (m, 1H, CH₃CH₂CHH), 1.62–1.39 (m, 3H, CH₃CH₂CHH), 0.96 (t, *J* = 7.2 Hz, 3H, CH₃); ¹³C{¹H} NMR (101 MHz, CDCl₃) δ 174.2, 167.0 (dd, *J* = 10.1, 20.2 Hz), 92.4 (dd, *J* = 19.8, 177.3 Hz), 92.0 (dd, *J* = 23.2, 194.1 Hz), 66.0, 48.9, 30.6 (dd, *J* = 5.9, 21.3 Hz), 29.8, 18.5 (d, *J* = 3.6 Hz), 13.7; ¹⁹F NMR (377 MHz, CDCl₃) δ -192.9 (m, 1F, CH₂CHF), -201.0 (m, CH₂CHFCH₂F), ¹⁹F{¹H} NMR (377 MHz, CDCl₃) δ -192.9 (d, *J* = 12.7 Hz, 1F, CH₂CHF), -201.0 (d, *J* = 12.7 Hz, 1F, CH₂CHFCH₂F); HRMS (ESI, +ve) C₁₀H₁₅NO₃F₂Na⁺ [MNa⁺] requires *m/z* 258.0912, found 258.0909.

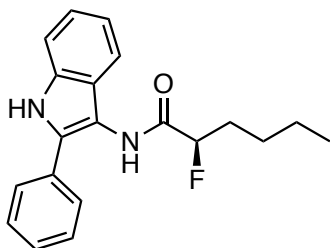
(*S*)-2-Fluoro-*N*-(2-phenyl-1*H*-indol-3-yl)hexanamide (**3a**)



A solution of acid **5** (18.9 mg, 0.141 mmol), 1-hydroxybenzotriazole monohydrate (22.8 mg, 0.141 mmol) and *N,N'*-diisopropylcarbodiimide (22.5 μ L, 0.141 mmol) in dry DMF (2.00 mL) was stirred at r.t. for 15 min. 3-Amino-2-phenylindole (27.9 mg, 0.132 mmol) was added, and the mixture was stirred at r.t. for 38 h. The mixture was evaporated under reduced pressure and the residue was

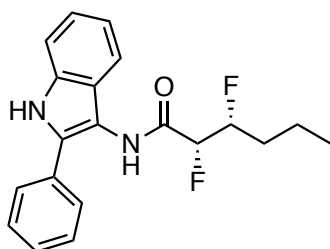
dissolved in ethyl acetate (50 mL). This organic solution was washed with water (10 × 12 mL) and brine (3 × 12 mL), dried (Na₂SO₄) and concentrated onto silica under reduced pressure. The residue was subjected to column chromatography, eluting with 5:95→10:90 ethyl acetate/hexane, to afford amide **3a** as a green oil (24.5 mg, 57%); [α]_D –8.4 (*c* 0.925, CHCl₃); IR (neat) ν_{max} (cm⁻¹) 3287, 3058, 2955, 2863, 1675, 1518, 1456, 1341, 1260, 1078, 1008; ¹H NMR (400 MHz, CDCl₃) δ 8.47 (s, 1H, NH-indole), 7.79 (d, *J* = 5.5 Hz, 1H, NHCO), 7.53–7.47 (m, 3H, ArH), 7.40–7.30 (m, 3H, ArH), 7.22–7.11 (m, 3H, ArH), 5.05 (ddd, *J* = 3.8, 7.3, 49.8 Hz, 1H, CHF), 2.19–1.94 (m, 2H, CHFCH₂), 1.60–1.52 (m, 2H, CH₃CH₂CH₂), 1.47–1.37 (m, 2H, CH₃CH₂CH₂), 0.96 (t, *J* = 7.3 Hz, 3H, CH₃); ¹³C{¹H} NMR (101 MHz, CDCl₃) δ 170.3 (d, *J* = 18.6 Hz), 134.7, 132.2, 131.2, 129.1, 128.3, 127.2, 125.6, 123.1, 120.6, 118.6, 111.5, 108.6, 92.8 (d, *J* = 186.2 Hz), 32.5 (d, *J* = 20.0 Hz), 26.6 (d, *J* = 2.7 Hz), 22.5, 14.0; ¹⁹F NMR (377 MHz, CDCl₃) δ –188.6 (m, 1F); ¹⁹F{¹H} NMR (377 MHz, CDCl₃) δ –188.6 (s, 1F); HRMS (ESI, +ve) C₂₀H₂₁OFN₂Na⁺ [MNa⁺] requires *m/z* 347.1530, found 347.1528.

(*R*)-2-Fluoro-*N*-(2-phenyl-1*H*-indol-3-yl)hexanamide (**3b**)



The title compound was synthesised from acid *ent*-**5** on 0.090 mmol scale, in a similar fashion to that described for compound **3a**. Amide **3b** was obtained as a green oil (10.9 mg, 40%). All spectroscopic data for **3b** were identical to those of compound **3a** except for the following: [α]_D +16.7 (*c* 0.190, CHCl₃); HRMS (ESI, +ve) C₂₀H₂₁OFN₂Na⁺ [MNa⁺] requires *m/z* 347.1530, found 347.1524.

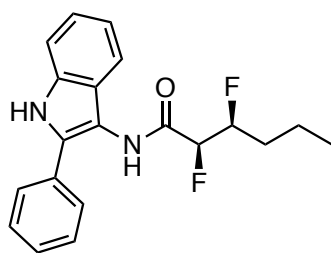
(2*R*,3*R*)-2,3-Difluoro-*N*-(2-phenyl-1*H*-indol-3-yl)hexanamide (**3c**)



A solution of acid **11** (14.0 mg, 0.092 mmol) and EDC.HCl (27.4 mg, 0.143 mmol) in dichloromethane (0.6 mL) was stirred at r.t for 15 min. A solution of 3-amino-2-phenylindole (17.0 mg, 0.082 mmol) in dichloromethane (0.6 mL) was added, and the mixture was stirred at r.t.

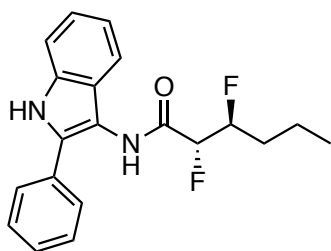
for 24 h. Dichloromethane (60 mL) was added, and the organic solution was washed with saturated aqueous solutions of K_2CO_3 (3×15 mL), Na_2CO_3 (3×15 mL) and $NaCl$ (3×15 mL). The organic layer was dried ($MgSO_4$) and concentrated onto silica under reduced pressure. The residue was subjected to column chromatography, eluting with 0:100→15:85 ethyl acetate/hexane to afford a partially purified sample of amide **3c**. This sample was subjected to preparative reverse phase HPLC eluting with 0:98→100:0 acetonitrile/water over 50 min, to afford pure **3c** as a pale purple oil (14.5 mg, 52%); $[\alpha]_D -101$ (c 0.328, $CHCl_3$); IR (DCM) ν_{max} (cm^{-1}) 3291, 3056, 2960, 2871, 1675, 1602, 1489, 1455, 1342, 1320, 1260, 1129, 1067, 1028; 1H NMR (400 MHz, $CDCl_3$) δ 8.30 (s, 1H, NH-indole), 7.82 (d, $J = 4.4$ Hz, 1H, NHCO), 7.61–7.58 (m, 2H, ArH), 7.52 (d, $J = 7.8$ Hz, 1H, ArH), 7.45–7.41 (m, 2H, ArH), 7.35 (ddd, $J = 1.2, 6.5, 8.7$ Hz, 1H, ArH), 7.31 (dt, $J = 1.2, 7.9$ Hz, 1H, ArH), 7.20 (ddd, $J = 1.3, 7.0, 14.9$ Hz, 1H, ArH), 7.14 (ddd, $J = 1.3, 7.9, 14.9$ Hz, 1H, ArH), 5.11 (dddd, $J = 1.1, 5.0, 8.9, 28.2, 45.2$ Hz, 1H, CH_2CHF), 5.07 (ddd, $J = 1.1, 30.4, 47.1$ Hz, 1H, $CH_2CHFCHF$), 2.03 (m, 1H, CH_3CH_2CHH), 1.82–1.44 (m, 3H, CH_3CH_2CHH), 1.03 (t, $J = 7.3$ Hz, 3H, CH_3); $^{13}C\{^1H\}$ NMR (101 MHz, $CDCl_3$) δ 167.1 (dd, $J = 3.3, 19.7$ Hz), 134.6, 132.3, 131.0, 129.2, 128.4, 127.2, 125.6, 123.3, 120.8, 118.9, 111.4, 108.5, 91.9 (dd, $J = 20.9, 197.9$ Hz), 91.6 (dd, $J = 18.5, 177.9$ Hz), 32.4 (dd, $J = 4.5, 21.1$ Hz), 18.4 (d, $J = 5.3$ Hz), 13.9; ^{19}F NMR (377 MHz, $CDCl_3$) δ -196.7 (m, 1F, CH_2CHF), -206.7 (m, 1F, $CH_2CHFCHF$); $^{19}F\{^1H\}$ NMR (377 MHz, $CDCl_3$) δ -196.7 (d, $J = 11.6$ Hz, 1F, CH_2CHF), -206.7 (d, $J = 11.6$ Hz, 1F, $CH_2CHFCHF$); HRMS (ESI, +ve) $C_{20}H_{20}F_2ON_2Na^+$ [MNa^+] requires m/z 365.1436, found 365.1433.

(2*S*,3*S*)-2,3-Difluoro-*N*-(2-phenyl-1*H*-indol-3-yl)hexanamide (**3d**)



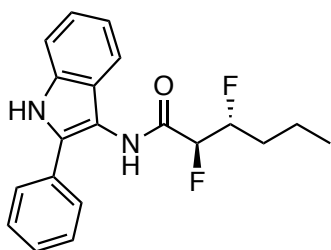
The title compound was synthesised from acid *ent*-**11** on 0.035 mmol scale, in a similar fashion to that described for compound **3c**, as a pale purple oil (4.80 mg, 50%). All spectroscopic data were identical to those of **3c** except for the following: $[\alpha]_D +293$ (c 0.071, $CHCl_3$); HRMS (ESI, +ve) $C_{20}H_{20}F_2N_2ONa^+$ [MNa^+] requires m/z 365.1436, found 365.1438.

(2*R*,3*S*)-2,3-Difluoro-*N*-(2-phenyl-1*H*-indol-3-yl)hexanamide (**3e**)



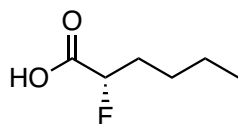
Amide **3e** was synthesised from *ent*-**13** on 0.028 mmol scale, following a similar procedure to that described above for amide **3a**. Amide **3e** was obtained as a pale green oil (6.01 mg, 65%); $[\alpha]_D^{25} +136$ (*c* 0.094, CHCl₃); **IR** (DCM) ν_{\max} (cm⁻¹) 3309, 3235, 3107, 2956, 2915, 2846, 2509, 2459, 2173, 2126, 1975, 1772, 1677, 1516, 1454, 1346, 1257, 1022; **¹H NMR** (400 MHz, CDCl₃) δ 8.26 (s, 1H, NH-indole), 7.83 (d, *J* = 3.8 Hz, 1H, NHCO), 7.61–7.59 (m, 2H, ArH), 7.50–7.44 (m, 3H, ArH), 7.41–7.34 (m, 2H, ArH), 7.24–7.14 (m, 2H, ArH), 5.31 (ddd, *J* = 1.7, 20.5, 49.2 Hz, 1H, CH₂CHFCH₂F), 5.05 (dddd, *J* = 1.7, 3.2, 10.0, 24.4, 47.7 Hz, 1H, CH₂CHF), 2.01 (m, 1H, CH₃CH₂CH₂H), 1.74–1.46 (m, 3H, CH₃CH₂CH₂H), 0.99 (t, *J* = 7.2 Hz, 3H, CH₃); **¹³C{¹H} NMR** (150 MHz, CDCl₃) δ 165.9 (dd, *J* = 8.4, 18.8 Hz), 134.6, 132.3, 131.0, 129.2, 128.6, 127.3, 125.4, 123.3, 120.9, 118.9, 111.4, 108.5, 92.8 (dd, *J* = 22.8, 195.0 Hz), 92.7 (dd, *J* = 2.8, 174.0 Hz), 31.1 (dd, *J* = 5.8, 21.4 Hz), 29.8, 18.6 (d, *J* = 3.4 Hz), 13.9; **¹⁹F NMR** (377 MHz, CDCl₃) δ -193.2 (m, 1F, CH₂CHF), -197.4 (m, CH₂CHFCH₂F), **¹⁹F{¹H} NMR** (377 MHz, CDCl₃) δ -193.2 (d, *J* = 13.0 Hz, 1F, CH₂CHF), -197.4 (d, *J* = 13.0 Hz, 1F, CH₂CHFCH₂F); **HRMS** (ESI, +ve) C₂₀H₂₀F₂N₂ONa⁺ [MNa⁺] requires *m/z* 365.1436, found 365.1433.

(2*S*,3*R*)-2,3-Difluoro-*N*-(2-phenyl-1*H*-indol-3-yl)hexanamide (**3f**)



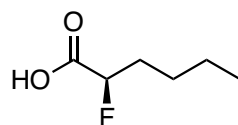
The title compound was synthesised from acid **13** on 0.085 mmol scale, in a similar fashion to that described for compound **3e**, as a yellowish oil (9.91 mg, 41%). All spectroscopic data were identical to those of **3e** except for the following: $[\alpha]_D^{25} -4.5$ (*c* 0.445, CHCl₃); **HRMS** (ESI, +ve) C₂₀H₂₀F₂N₂ONa⁺ [MNa⁺] requires *m/z* 365.1436, found 365.1408.

(*S*)-2-Fluorohexanoic acid (**5**)



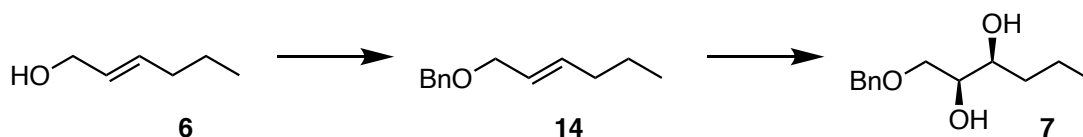
A mixture of hexanal (275 mg, 2.75 mmol), (*S*)-(-)-2,2,3-trimethyl-5-benzyl-4-imidazolidinone dichloroacetic acid^[1] (70.7 mg, 0.204 mmol), *tert*-butyl methyl ether (6.25 mL) and water (25 μ L) was stirred for 15 min. *N*-Fluorobenzenesulfonimide (593 mg, 1.88 mmol) was added, and the mixture was stirred at r.t. for 6 h. Pentane (3 mL) was added, and the resulting precipitate was filtered off to yield a solution of the α -fluoroaldehyde intermediate. To this solution was added DMF (7.5 mL) and oxone (825 mg, 2.68 mmol). This mixture was stirred at r.t. for 4.5 h. Aqueous HCl (1 M, 25 mL) was added, and the mixture was extracted with ethyl acetate (3 \times 25 mL). The combined organic layers were dried (Na_2SO_4) and concentrated onto silica under reduced pressure. The residue was subjected to column chromatography, eluting with 0:100 \rightarrow 10:90 ethyl acetate / hexane to afford the title compound as a clear oil (95.5 mg, 38% from NFSI); $[\alpha]_{\text{D}} +9.9$ (*c* 0.41, CHCl_3); **IR** (DCM) ν_{max} (cm^{-1}) 2958, 2931, 2863, 1732, 1595, 1467, 1264, 1007, 1116; **^1H NMR** (400 MHz, CDCl_3) δ 9.15 (br s, 1H, COOH), 4.95 (ddd, *J* = 4.6, 7.3, 49.0 Hz, 1H, CHF), 1.99–1.87 (m, 2H, CH_2CHF), 1.53–1.35 (m, 4H, $\text{CH}_3\text{CH}_2\text{CH}_2$), 0.92 (t, *J* = 7.2 Hz, 3H, CH_3); **$^{13}\text{C}\{^1\text{H}\}$ NMR** (101 MHz, CDCl_3) δ 176.1 (d, *J* = 24.4 Hz), 88.6 (d, *J* = 184.6 Hz), 32.0 (d, *J* = 20.7 Hz), 26.5 (d, *J* = 2.6 Hz), 22.3, 13.9; **^{19}F NMR** (377 MHz, CDCl_3) δ -192.5 (m, 1F); **$^{19}\text{F}\{^1\text{H}\}$ NMR** (377 MHz, CDCl_3) δ -192.5 (s, 1F); **MS** (ESI, +ve) $\text{C}_6\text{H}_{11}\text{FO}_2\text{Na}^+$ [MNa^+] requires *m/z* 157.06, found 157.08.

(*R*)-2-Fluorohexanoic acid (*ent*-**5**)



The title compound was synthesised from hexanal on 3.75 mmol scale, in a similar fashion to that described above for acid **5**, except using as the catalyst (*S*)-(+)-2,2,3-trimethyl-5-benzyl-4-imidazolidinone dichloroacetic acid.^[1] *Ent*-**5** was obtained as a clear oil (150 mg, 44%). All spectroscopic data were identical to those obtained for **5** except for the following: $[\alpha]_{\text{D}} +5.41$ (*c* 0.19, CHCl_3) [this should be similar, but is not, in magnitude and opposite in sign compared to **5**; the difference can be attributed to experimental error; see Section 3 of this document for a more accurate measurement of the optical purity]; **HRMS** (ESI, +ve) $\text{C}_6\text{H}_{11}\text{FO}_2\text{Na}^+$ [MNa^+] requires *m/z* 157.0635, found 157.0626.

(2*S*,3*S*)-1-(Benzyloxy)hexane-2,3-diol (**7**)

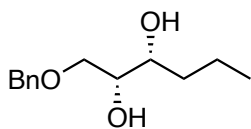


Step 1: To a suspension of sodium hydride (60% dispersion in mineral oil, 9.11 g, 228 mmol) in dry THF (500 mL) at 0 °C was added alcohol **6** (11.3 g, 112 mmol), and the mixture was stirred at 0 °C for 45 min. Benzyl bromide (52.3 g, 306 mmol) was added, and the mixture was stirred at r.t. for 24 h. Saturated aqueous NaHCO₃ (250 mL) was added, and the mixture was stirred for 30 min. The mixture was extracted with ethyl acetate (5 × 200 mL), and the combined organic layers were dried (MgSO₄) and concentrated onto silica under reduced pressure. The residue was subjected to column chromatography, eluting with 0:10→1:9 ethyl acetate/hexane, to afford intermediate compound **14** as a clear oil (19.6 g, 92%); **IR** (MeCN) ν_{\max} (cm⁻¹) 3354, 3265, 3029, 2957, 2859, 1633, 1453, 1360, 1205, 1069, 969, 735, 697; **¹H NMR** (400 MHz, CDCl₃) δ 7.46–7.33 (m, 5H, ArH), 5.83 (dt, J = 6.5, 15.4 Hz, 1H, CH=CHCH₂O), 5.73 (ddd, J = 2.2, 5.9, 15.4 Hz, 1H, CH=CHCH₂O), 4.59 (s, 2H, PhCH₂), 4.08 (ddd, J = 1.0, 2.1, 5.8 Hz, 2H, CHCH₂O), 2.18 (dt, J = 0.9, 7.0 Hz, 1H, CH₃CH₂CHH), 2.16 (dt, J = 0.6, 7.0 Hz, 1H, CH₃CH₂CHH), 1.58 (tq, J = 7.4, 14.8 Hz, 2H, CH₂CH₃), 1.05 (t, J = 7.4 Hz, 3H, CH₃); **¹³C{¹H} NMR** (101 MHz, CDCl₃) δ 138.4, 134.2, 128.1, 127.4, 127.2, 126.4, 71.6, 70.7, 34.3, 22.1, 13.5; **HRMS** (ESI, +ve) C₁₃H₁₈ONa⁺ [MNa⁺] requires m/z 213.1250, found 213.1239; spectroscopic data in accordance with literature values.^[3]

Step 2: A mixture of NaHCO₃ (12.6 g, 150 mmol), potassium carbonate (20.8 g, 150 mmol), potassium ferricyanide (49.4 g, 150 mmol), (DHQ)₂PHAL (390 mg, 0.001 mol), *tert*-butanol (125 mL) and water (125 mL) was stirred at r.t. for 30 min then cooled to 0 °C. Osmium tetroxide (0.5% solution in water, 7.6 mL, 0.15 mmol) and methanesulfonamide (4.76 g, 50.0 mmol) were added, and the mixture was stirred at 0 °C for 1 h. Alkene **14** (9.51 g, 50.0 mmol) was added, and the mixture was stirred at 0 °C for 24 h. A second portion of osmium tetroxide (0.5% solution in water, 7.6 mL, 0.15 mmol) was added, and stirring was continued to give a total reaction time of 52 h. Sodium sulfite (75.6 g, 600 mmol) was added, and the mixture was stirred at r.t. for 1 h. The mixture was extracted with ethyl acetate (4 × 200 mL) and dichloromethane (4 × 250 mL), and the combined organic layers were dried (MgSO₄) and concentrated onto silica. The residue was subjected to flash chromatography eluting with 0:4→1:3 ethyl acetate/hexane to give diol **7** as a clear waxy solid (10.2 g, 91%); $[\alpha]_D$ -23.5 (c 0.255, CHCl₃); **m.p.** 42.0–45.3 °C; **IR** (neat) ν_{\max} (cm⁻¹) 3610, 3544, 3000, 2958, 2284, 2250, 1631, 1439, 1374, 1038; **¹H NMR** (300 MHz, CDCl₃) δ 7.38–7.28 (m, 5H, ArH), 4.58 (d, J = 11.9 Hz, 1H, PhCHH), 4.53 (d, J = 11.9, Hz, 1H, PhCHH), 3.64–3.56 (m, 4H, CHOH-CHOH-CH₂), 2.78 (d, J = 4.6 Hz, 1H, OH), 2.61 (d, J = 4.1 Hz, 1H, OH), 1.83–1.41 (m, 4H,

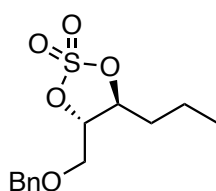
CH₃CH₂CH₂), 0.93 (t, *J* = 7.0 Hz, 3H, CH₃); ¹³C{¹H} NMR (75 MHz, CDCl₃) δ 137.8, 128.6, 128.0, 127.9, 73.8, 72.9, 72.5, 72.1, 35.7, 18.9, 14.1; HRMS (ESI, +ve) C₁₃H₂₀O₃Na⁺ [MNa⁺] requires *m/z* 247.1305, found 247.1297.

(2*R*,3*R*)-1-(Benzyloxy)hexane-2,3-diol (*ent*-7)



The title compound was synthesised from alkene **14** on 48.4 mmol scale, in a similar manner to that described above for diol **7**, except using as the catalyst (DHQD)₂PHAL. Diol *ent*-7 was obtained as a clear waxy solid (9.83 g, 91%). All spectroscopic data were identical to those obtained for diol **7** except for the following: [α]_D +6.1 (*c* 0.16, CHCl₃); **m.p.** 45.3–45.5 °C; HRMS (ESI, +ve) C₁₃H₂₀O₃Na⁺ [MNa⁺] requires *m/z* 247.1305, found 247.1297.

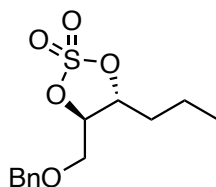
(4*S*,5*S*)-4-((Benzyloxy)methyl)-5-propyl-1,3,2-dioxathiolane 2,2-dioxide (**8**)



Thionyl chloride (1.58 mL, 21.9 mmol) was added to a solution of diol **7** (2.46 g, 11.0 mmol) and pyridine (2.52 mL, 32.9 mmol) in dichloromethane (80 mL) at 0 °C, and the resulting mixture was stirred at 0 °C for 1 h. Saturated aqueous CuSO₄ (80 mL) was added, and the mixture was extracted with dichloromethane (5 × 80 mL). The combined organic layers were dried (MgSO₄) and concentrated to give an intermediate cyclic sulfite compound. This intermediate was dissolved in acetonitrile (75 mL) and dichloromethane (75 mL) and the solution was cooled to 0 °C. Sodium metaperiodate (4.55 g, 21.9 mmol), ruthenium chloride hydrate (~15 mg) and water (120 mL) were added, and the mixture was stirred at 0 °C for 1 h. Diethyl ether (400 mL) was added, and the mixture was washed with water (400 mL), saturated aqueous NaHCO₃, (2 × 300 mL) and brine (2 × 300 mL). The organic layer was dried (MgSO₄) and concentrated to give the title compound as a dark orange oil (3.05 g, 97%); ¹H NMR (400 MHz, CDCl₃) δ 7.40–7.31 (m, 5H, ArH), 4.84 (ddd, *J* = 3.6, 8.0, 8.8 Hz, 1H, HCSO₄CH), 4.65 (dt, *J* = 4.5, 8.0 Hz, 1H, HCSO₄CH), 4.64 (d, *J* = 12.0, Hz, 1H, CHHPh), 4.58 (d, *J* = 12.0 Hz, 1H, CHHPh), 3.76 (d, *J* = 4.5 Hz, 2H, CH₂OBn), 1.87 (dddd, *J* = 5.1, 9.5, 18.5, 23.8 Hz, 1H, CH₃CH₂CHH), 1.71 (dddd, *J* = 3.6, 6.2, 9.5, 14.3 Hz, 1H, CH₃CH₂CHH), 1.62–1.42

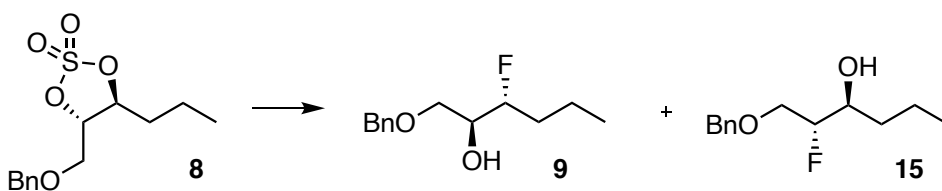
(m, 2H, CH₃CH₂CH₂), 0.97 (t, $J = 7.4$ Hz, 3H, CH₃); ¹³C{¹H} NMR (101 MHz, CDCl₃) δ 136.9, 128.8, 128.4, 128.0, 84.8, 84.5, 74.0, 67.3, 34.4, 18.6, 13.6; HRMS (ESI, +ve) C₁₃H₁₈O₅SNa⁺ [MNa⁺] requires m/z 309.0767, found 309.0752.

(4*R*,5*R*)-4-((Benzyloxy)methyl)-5-propyl-1,3,2-dioxathiolane 2,2-dioxide (*ent*-**8**)



The title compound was synthesised from *ent*-**7** on 43.1 mmol scale, in a similar manner to that described above for cyclic sulfate **8**. Cyclic sulfate *ent*-**8** was obtained as a dark orange oil (10.4 g, 84%); all spectroscopic data identical to those reported above for **8**.

(2*S*,3*R*)-1-(Benzyloxy)-3-fluorohexan-2-ol (**9**)



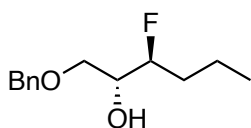
A mixture of TBAF (1M solution in THF, 21.3 mL, 21.3 mmol) and acetonitrile (150 mL) was dried over 4Å molecular sieves then added *via* cannula to an ice-cold flask containing cyclic sulfate **8** (3.05 g, 10.7 mmol). The resulting mixture was stirred at r.t. for 12 h, then concentrated to give a clear brown oil. This residue was dissolved in a mixture of sulfuric acid (1.74 mL), water (320 μL) and tetrahydrofuran (150 mL), and the resulting solution was stirred at r.t. overnight. Brine (200 mL) and water (200 mL) were added, and the mixture was extracted with dichloromethane (5 × 200 mL). The combined organic layers were dried (MgSO₄) and concentrated onto silica. The crude product was subjected to flash chromatography eluting with 1:3:6→2:3:5 ethyl acetate / dichloromethane / hexane to give, separately, compound **9** as a clear yellow liquid (1.67 g, 69%) and the regioisomeric sideproduct **15** (6%).

Data for **9**: [α]_D +9.50 (c 1.05, CHCl₃); IR (DCM) ν_{\max} (cm⁻¹) 3541, 3029, 2951, 2928, 2870, 2324, 1955, 1728, 1604, 1453, 1363, 1314, 1248, 1209, 1089, 1027; ¹H NMR (300 MHz, CDCl₃) δ 7.41–7.29 (m, 5H, ArH), 4.60 (d, $J = 12.0$ Hz, 1H, CHHPh), 4.56 (d, $J = 12.0$ Hz, 1H, CHHPh), 4.47 (dddd, $J = 4.1, 6.4, 7.4, 48.4$ Hz, 1H, CFH), 3.83 (dddd, $J = 3.5, 5.2, 6.4, 17.2$ Hz, 1H, CHOH), 3.67 (ddd, $J = 2.2, 3.5, 9.7$ Hz, 1H, OBnCHH), 3.58 (ddd, $J = 1.8, 6.4, 9.7$ Hz, 1H, OBnCHH), 2.70 (d, $J = 5.2$ Hz,

1H, OH), 1.77–1.34 (m, 4H, CH₃CH₂CH₂), 0.97 (t, *J* = 7.3 Hz, 3H, CH₃); ¹³C{¹H} NMR (75 MHz, CDCl₃) δ 137.8, 128.6, 128.0, 127.9, 93.4 (d, *J* = 170.4 Hz), 73.7, 71.7 (d, *J* = 24.3 Hz), 70.5 (d, *J* = 5.4 Hz), 33.3 (d, *J* = 20.5 Hz), 18.4 (d, *J* = 3.3 Hz), 14.0; ¹⁹F NMR (283 MHz, CDCl₃) δ –192.6 (s, 1F); ¹⁹F{¹H} NMR (283 MHz, CDCl₃) δ –192.6 (m, 1F); HRMS (ESI, +ve) C₁₃H₁₉FO₂Na⁺ [MNa⁺] requires *m/z* 249.1261, found 249.1248.

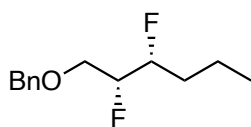
Data for **15**: [α]_D –7.46 (*c* 0.134, CHCl₃); ¹H NMR (300 MHz, CDCl₃) δ 7.39–7.27 (m, 5H, ArH), 4.61 (d, *J* = 11.9 Hz, 1H, CHHPh), 4.57 (d, *J* = 11.9 Hz, 1H, CHHPh), 4.50 (ddd, *J* = 3.4, 8.0, 47.5 Hz, 1H, CHF), 3.88 (s br, 1H, CHOH), 3.81 (ddd, *J* = 5.1, 11.4, 25.0 Hz, 1H, CHFCHH), 3.75 (ddd, *J* = 3.4, 11.4, 25.0 Hz, 1H, CHFCHH), 2.15 (s, 1H, OH), 1.62–1.34 (m, 4H, CH₃CH₂CH₂), 0.94 (t, *J* = 6.9 Hz, 3H, CH₃); ¹³C{¹H} NMR (76 MHz, CDCl₃) δ 137.7, 128.6, 128.0, 127.9, 94.4 (d, *J* = 174.2 Hz), 73.8, 71.2 (d, *J* = 22.8 Hz), 69.3 (d, *J* = 22.9 Hz), 34.8 (d, *J* = 4.4 Hz), 18.8, 14.1; ¹⁹F NMR (283 MHz, CDCl₃) δ –192.8 (m, 1F); ¹⁹F{¹H} NMR (283 MHz, CDCl₃) δ –192.8 (s, 1F); HRMS (ESI, +ve) C₁₃H₁₉FO₂Na⁺ [MNa⁺] requires *m/z* 249.1261, found 249.1248.

(2*R*,3*S*)-1-(Benzyloxy)-3-fluorohexan-2-ol (*ent*-**9**)



The title compound was synthesised from *ent*-**8** on 21.4 mmol scale, in a similar fashion to that described for **9**. Compound *ent*-**9** was obtained as a clear yellow liquid (3.18 g, 66%). All spectroscopic data were identical to those obtained for **9** except for the following: [α]_D –8.68 (*c* 0.43, CHCl₃); HRMS (ESI, +ve) C₁₃H₁₉FO₂Na⁺ [MNa⁺] requires *m/z* 249.1261, found 249.1255.

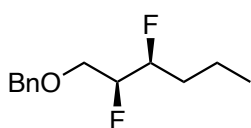
((((2*R*,3*R*)-2,3-Difluorohexyl)oxy)methyl)benzene (**10**)



A mixture of fluorohydrin **9** (508 mg, 2.24 mmol) and neat Deoxo-Fluor™ (3.32 mL, 0.018 mol) was stirred at 70 °C in a Teflon vessel for 24 h. The mixture was cooled to 0 °C, diluted with dichloromethane, and concentrated onto silica. The crude product was subjected to flash chromatography eluting with 2:73:125 acetone / dichloromethane / hexane to give, separately, difluoroalkane **10** as a pale yellow oil (208 mg, 41%) and recovered fluorohydrin **9** (105 mg, 21%). Data for **10**: [α]_D +10.6 (*c* 1.09, CHCl₃); IR (DCM) ν_{max} (cm⁻¹) 3030, 2959, 2872, 1726, 1453, 1365,

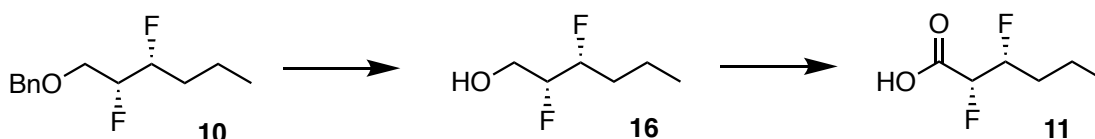
1268, 1205, 1105, 1027; $^1\text{H NMR}$ (400 MHz, CDCl_3) δ 7.40–7.28 (m, 5H, ArH), 4.64 (m, 2H, CHFCHF), 4.60 (apparent s, 2H, CH_2Ph), 3.79 (dd, $J = 1.0, 5.0$ Hz, 1H, CHFCHHO), 3.79 (dd, $J = 1.0, 4.8$ Hz, 1H, CHFCHHO), 1.81 (m, 1H, $\text{CH}_3\text{CH}_2\text{CHH}$), 1.67–1.43 (m, 3H, $\text{CH}_3\text{CH}_2\text{CHH}$), 0.98 (d, $J = 7.4$ Hz, 3H, CH_3); $^{13}\text{C}\{^1\text{H}\}$ NMR (101 MHz, CDCl_3) δ 137.7, 128.6, 128.0, 127.9, 92.2 (dd, $J = 19.7, 179.0$ Hz), 91.5 (dd, $J = 19.7, 174.9$ Hz), 73.8, 68.6 (dd, $J = 7.0, 24.9$ Hz), 32.3 (dd, $J = 5.0, 20.8$ Hz), 18.3 (d, $J = 4.9$ Hz), 13.9; $^{19}\text{F NMR}$ (377 MHz, CDCl_3) δ -198.7 (m, 1F), -202.5 (m, 1F); $^{19}\text{F}\{^1\text{H}\}$ NMR (377 MHz, CDCl_3) δ -198.7 (d, $J = 10.6$ Hz, 1F), -202.5 (d, $J = 10.6$ Hz, 1F); HRMS (ESI, +ve) $\text{C}_{13}\text{H}_{18}\text{OF}_2\text{Na}^+$ [MNa^+] requires m/z 251.1218, found 251.1217.

(((2*S*,3*S*)-2,3-Difluorohexyl)oxy)methyl)benzene (*ent*-**10**)



The title compound was synthesised from fluorohydrin *ent*-**9** on 2.24 mmol scale, in a similar fashion to that described above for **10**. Difluoroalkane *ent*-**10** was obtained as a clear yellow oil (256 mg, 50%). All spectroscopic data were identical to those obtained for **10** except for the following: $[\alpha]_{\text{D}}$ -6.11 (c 0.60, CHCl_3); HRMS (ESI, +ve) $\text{C}_{13}\text{H}_{18}\text{F}_2\text{ONa}^+$ [MNa^+] requires m/z 251.1218, found 251.1212.

(2*R*,3*R*)-2,3-Difluorohexanoic acid (**11**)

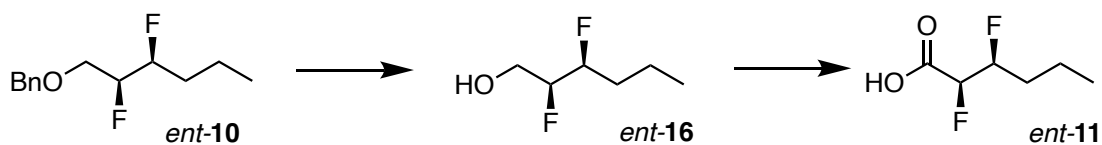


Step 1: Compound **10** (190 mg, 0.832 mmol) was dissolved in ethyl acetate (3 mL), and Pd/C (10%, 120 mg, 0.113 mmol) was added to this solution. The mixture was stirred under H_2 atmosphere at r.t. for 48 h. The mixture was filtered through a layer of Celite and washed with ethyl acetate. The filtrate was concentrated under moderately reduced pressure (NB. the product is volatile under high vacuum!) to yield alcohol **16** as a white crystalline solid (140 mg, 100%); **m.p.** 59.8–60.2 °C; IR (MeCN) ν_{max} (cm^{-1}) 3731, 3307, 2355, 2137, 2017, 1647, 1016; $^1\text{H NMR}$ (300 MHz, CDCl_3) δ 4.77–3.39 (m, 2H, CHFCHF), 3.98–3.76 (m, 2H, CH_2OH), 2.03 (s, 1H, OH), 1.89–1.41 (m, 4H, $\text{CH}_2\text{CH}_2\text{CH}_3$), 0.97 (t, $J = 7.2$ Hz, CH_3); $^{13}\text{C}\{^1\text{H}\}$ NMR (76 MHz, CDCl_3) δ 94.7–90.6 (m, $2 \times \text{CHF}$), 61.8 (dd, $J = 7.2, 23.8$ Hz), 32.4 (dd, $J = 5.1, 21.0$ Hz), 18.2 (d, $J = 4.9$ Hz), 13.8; $^{19}\text{F NMR}$ (283 MHz, CDCl_3) δ -198.5 (m, 1F, $\text{CHFCHFCH}_2\text{O}$), -205.0 (m, 1F, $\text{CHFCHFCH}_2\text{O}$); $^{19}\text{F}\{^1\text{H}\}$ NMR

(283 MHz, CDCl₃) δ -198.5 (d, J = 10.8 Hz, CHFCH₂FCH₂O), -205.0 (d, J = 10.8 Hz, CHFCH₂FCH₂O); **MS** (ESI, +ve) C₆H₁₂F₂ONa⁺ [MNa⁺] requires m/z 161.07, found 161.08.

Step 2: Alcohol **16** (153 mg, 1.11 mmol) was dissolved in acetonitrile (4 mL) and dichloromethane (4 mL), and the solution was cooled to 0 °C. Sodium metaperiodate (473 mg, 2.21 mmol), ruthenium chloride hydrate (~ 0.015 g) and water (5.8 mL) were added, and the mixture was warmed to r.t. and stirred for 24 h. The mixture was filtered through Celite and washed with acetonitrile. The filtrate was concentrated under moderately reduced pressure to afford acid **11** as a volatile greenish solid (160 mg, 95%); **IR** (neat) ν_{\max} (cm⁻¹) 3383, 3154, 1710, 1666, 1459, 1224, 1135, 1081; **¹H NMR** (300 MHz, CDCl₃) δ 5.84 (br s, 1H, COOH), 4.94 (ddd, J = 1.8, 29.2, 47.1 Hz, 1H, CHF₂COOH), 4.92 (dddd, J = 1.8, 4.7, 8.9, 25.6, 45.7 Hz, 1H, CH₂CHF), 1.95 (m, 1H, CH₃CH₂CHH), 1.81–1.40 (m, 3H, CH₃CH₂CHH), 1.00 (t, J = 7.3 Hz, 3H, CH₃); **¹³C{¹H} NMR** (76 MHz, CDCl₃) δ 171.3 (dd, J = 4.3, 25.8 Hz), 91.5 (dd, J = 19.9, 179.1 Hz), 88.5 (dd, J = 21.3, 194.6 Hz), 32.0 (dd, J = 4.2, 20.8 Hz), 18.3 (d, J = 5.3 Hz), 13.8; **¹⁹F NMR** (283 MHz, CDCl₃) δ -195.2 (m, 1F, CH₂CHF), -209.0 (m, 1F, CHF₂COOH); **¹⁹F{¹H} NMR** (283 MHz, CDCl₃) δ -195.2 (d, J = 10.0 Hz, 1F, CH₂CHF), -209.0 (d, J = 10.0 Hz, 1F, CHF₂COOH); **HRMS** (ESI, +ve) C₆H₁₀F₂O₂Na⁺ [MNa⁺] requires m/z 175.0541, found 175.0530.

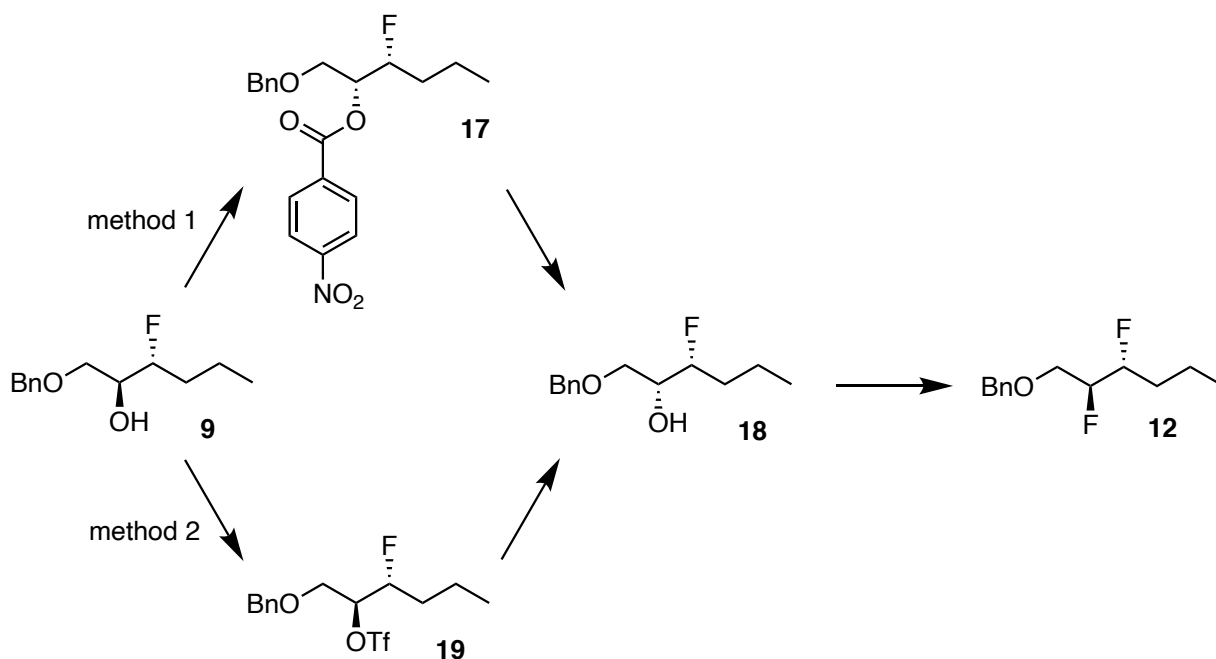
(2*S*,3*S*)-2,3-Difluorohexanoic acid (*ent*-**11**)



Step 1: The alcohol *ent*-**16** was synthesised from *ent*-**10** on 1.23 mmol scale, in a similar fashion to that described for **16**. Alcohol *ent*-**16** was obtained as a white crystalline solid (170 mg, 100%). All spectroscopic data were identical to those obtained for **16** except for the following: **m.p.** 55.4–55.9 °C (air dried only); **HRMS** (ESI, +ve) C₆H₁₂F₂ONa⁺ [MNa⁺] requires m/z 161.0748, found 161.0739.

Step 2: The acid *ent*-**11** was synthesised from *ent*-**16** on 0.195 mmol scale, in a similar fashion to that described for **11**. Compound *ent*-**11** was obtained as a volatile yellow oil (29.3 mg, 99%). All spectroscopic data were identical to those of **11** except for the following: **HRMS** (ESI, +ve) C₆H₁₀F₂O₂Na⁺ [MNa⁺] requires m/z 175.0541, found 175.0538.

(((2*S*,3*R*)-2,3-Difluorohexyl)oxy)methyl)benzene (**12**)



Method 1:

Step 1: A mixture of fluorohydrin **9** (45.9 mg, 0.203 mmol), triphenylphosphine (210 mg, 0.801 mmol), 4-nitrobenzoic acid (134 mg, 0.801 mmol) and tetrahydrofuran (1 mL) was stirred at 0 °C for 15 min. Diethyl azodicarboxylate (0.13 mL, 0.80 mmol) was added dropwise, and the mixture was stirred at 0 °C for 15 min. The mixture was warmed to r.t. and stirred for 48 h. The mixture was concentrated *in vacuo*, and the residue was dissolved in ether (1 mL) and the solution allowed to stand overnight, whereupon a yellow precipitate formed. Hexane (2 mL) was added, and the mixture was sonicated for 15 min. The yellow solid was filtered off and washed with 1:1 hexane / ether (25 mL). The filtrate was concentrated onto silica and subjected to flash chromatography eluting with 0:10→3:7 hexane / dichloromethane to afford the ester **17** as a clear oil (32.1 mg, 42%); $[\alpha]_D^{25} +13.0$ (*c* 0.945, CHCl₃); **IR** (MeCN) ν_{\max} (cm⁻¹) 2959, 2871, 1724, 1605, 1525, 1453, 1345, 1265, 1098, 1013; **¹H NMR** (400 MHz, CDCl₃) δ 8.31–8.23 (m, 4H, *p*-NO₂-C₄H₄), 7.34–7.28 (m, 5H, ArH), 5.39 (dddd, *J* = 3.6, 5.3, 5.9, 22.7 Hz, 1H, CHFCH-OCO), 4.84 (ddt, *J* = 3.6, 9.4, 47.7 Hz, 1H, CHF), 4.60 (d, *J* = 12.0 Hz, 1H, CHHPh), 4.52 (d, *J* = 12.0 Hz, 1H, CHHPh), 3.80 (ddd, *J* = 1.0, 5.2, 10.5 Hz, 1H, CHHOBn), 3.75 (ddd, *J* = 1.0, 6.0, 10.5 Hz, 1H, CHHOBn), 1.76–1.41 (m, 4H, CH₃CH₂CH₂), 0.94 (d, *J* = 7.2 Hz, 3H, CH₃); **¹³C{¹H} NMR** (101 MHz, CDCl₃) δ 164.2, 150.8, 137.7, 135.3, 131.1, 128.6, 128.0, 127.8, 123.7, 91.3 (d, *J* = 175.7 Hz), 74.4 (d, *J* = 18.9 Hz), 73.5, 68.0 (d, *J* = 6.5 Hz), 33.1 (d, *J* = 20.9 Hz), 18.4 (d, *J* = 4.3 Hz), 13.9; **¹⁹F NMR** (377 MHz, CDCl₃) δ -196.8 (m, 1F); **¹⁹F{¹H} NMR** (377 MHz, CDCl₃) δ -196.8 (s, 1F); **HRMS** (ESI, +ve) C₂₀H₂₂FO₅Na⁺ [MNa⁺] requires *m/z* 398.1374, found 398.1370.

Step 2: To a flask containing the ester **17** (14.1 mg, 0.04 mmol) at 0 °C was added methanol (5 mL) and potassium carbonate (5.8 mg, 0.042 mmol). The mixture was stirred at 0 °C for 2 h then at r.t. for 1 h. The mixture was concentrated and the residue was dissolved in dichloromethane (10 mL), and the organic solution was washed with water (3 mL) and brine (3 mL). The organic layer was dried (MgSO₄) and concentrated onto silica under reduced pressure. The residue was subjected to column chromatography, eluting with 0:100→15:85 ethyl acetate / hexane, to afford the alcohol **18** as a clear oil (7.60 mg, 90%); [α]_D +11.2 (*c* 0.626, CHCl₃); **IR** (MeOH) ν_{max} (cm⁻¹) 3438, 3029, 2958, 2930, 2871, 2016, 1721, 1454, 1364, 1271, 1100, 1028; **¹H NMR** (400 MHz, CDCl₃) δ 7.39–7.30 (m, 5H, ArH), 4.54 (ddt, *J* = 3.7, 9.1, 48.5 Hz, 1H, CHF), 4.59 (d, *J* = 12.0 Hz, 1H, OCH₂HPh), 4.55 (d, *J* = 12.0 Hz, 1H, OCH₂HPh), 3.81 (dddd, *J* = 3.7, 4.4, 6.5, 21.3 Hz, 1H, CHOH), 3.60 (ddd, *J* = 0.7, 4.7, 9.7 Hz, 1H, CHHOBn), 3.56 (ddd, *J* = 0.7, 6.7, 9.7 Hz, 1H, CHHOBn), 1.85–1.40 (m, 4H, CH₂CH₂CH₃), 0.95 (t, *J* = 7.1 Hz, 3H, CH₃); **¹³C{¹H} NMR** (101 MHz, CDCl₃) δ 137.9, 128.6, 128.0, 127.9, 93.6 (d, *J* = 170.8 Hz), 73.7, 71.9 (d, *J* = 19.9 Hz), 70.8 (d, *J* = 5.9 Hz), 33.0 (d, *J* = 20.9 Hz), 18.5 (d, *J* = 4.7 Hz), 14.0; **¹⁹F NMR** (377 MHz, CDCl₃) δ -198.0 (m, 1F); **¹⁹F{¹H} NMR** (377 MHz, CDCl₃) δ -198.0 (s, 1F); **HRMS** (ESI, +ve) C₁₃H₁₉FO₂Na⁺ [MNa⁺] requires *m/z* 249.1261, found 249.1259.

Step 3: A mixture of alcohol **18** (205 mg, 0.906 mmol) and Deoxo-FluorTM (50% in toluene, 2.30 mL, 6.21 mmol) in a Teflon vessel was stirred at 70 °C for 24 h. The mixture was cooled to 0 °C, diluted with dichloromethane, and concentrated onto silica. The crude product was subjected to flash chromatography eluting with 0:20→1:19 ethyl acetate / hexane to give difluoroalkane **12** as a pale yellow oil (208 mg, 41%); [α]_D +18.9 (*c* 0.264, CHCl₃); **IR** (DCM) ν_{max} (cm⁻¹) 3219, 2925, 2860, 1982, 1728, 1456, 1270, 1123, 1076; **¹H NMR** (400 MHz, CDCl₃) δ 7.40–7.30 (m, 5H, ArH), 4.79–4.53 (m, 2H, CHFCHF), 4.63 (d, *J* = 12.0 Hz, 1H, PhCHH), 4.59 (d, *J* = 12.0 Hz, 1H, PhCHH), 3.78 (dd, *J* = 2.1, 5.2 Hz, 1H, CHHOBn), 3.72 (dd, *J* = 2.1, 5.2 Hz, 1H, CHHOBn), 1.76–1.41 (m, 4H, CH₃CH₂CH₂), 0.98 (d, *J* = 7.3 Hz, 3H, CH₃); **¹³C{¹H} NMR** (101 MHz, CDCl₃) δ 137.8, 128.6, 127.9, 127.8, 92.5 (dd, *J* = 25.7, 176.2 Hz), 91.2 (dd, *J* = 25.0, 171.6 Hz), 73.7, 68.5 (dd, *J* = 5.7, 22.0 Hz), 32.7 (dd, *J* = 3.9, 20.6 Hz), 18.2 (d, *J* = 3.4 Hz), 13.9; **¹⁹F NMR** (377 MHz, CDCl₃) δ -194.6 (m, 1F, CHFCHFCH₂O), -196.5 (m, 1F, CHFCH₂O); **¹⁹F{¹H} NMR** (377 MHz, CDCl₃) δ -194.6 (d, *J* = 13.7 Hz, 1F, CHFCHFCH₂O), -196.5 (d, *J* = 13.7 Hz, 1F, CHFCH₂O); **HRMS** (ESI, +ve) C₁₃H₁₈F₂ONa⁺ [MNa⁺] requires *m/z* 251.1218, found 251.1216.

Method 2 [unexpected result]:

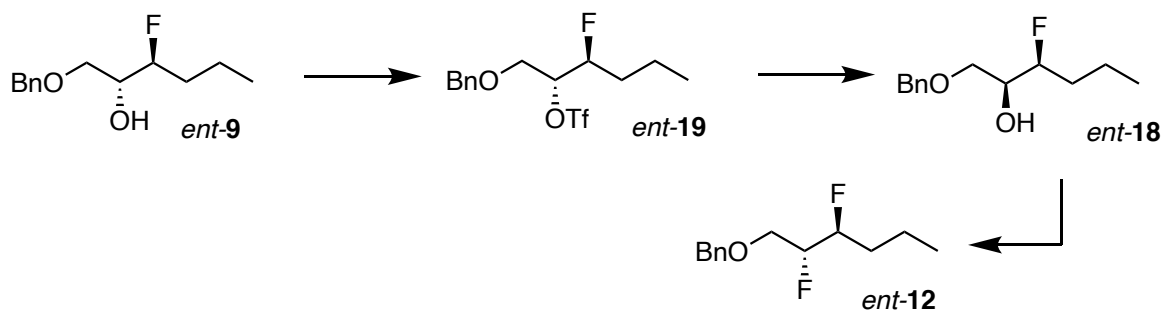
Step 1: To a solution of fluorohydrin **9** (900 mg, 3.99 mmol) in dry DCM (50 mL) at 0 °C was added triflic anhydride (1.20 mL, 7.13 mmol) and pyridine (500 μ L, 6.13 mmol). The mixture was stirred at 0 °C for 8 h. The mixture was diluted with ether (400 mL) and the organic solution was washed

with water (3 × 100 mL) and brine (3 × 100 mL). The organic layer was dried (MgSO₄) and concentrated under reduced pressure to afford triflate **19** as a brown oil (1.42 g, 99%); [α]_D +9.5 (c 0.28, CHCl₃); **IR** (neat) ν_{max} (cm⁻¹) 3030, 2960, 2937, 2873, 1733, 1454, 1413, 1209, 1144, 1098, 1027; **¹H NMR** (300 MHz, CDCl₃) δ 7.40–7.31 (m, 5H, ArH), 5.06 (ddd, J = 3.3, 7.9, 16.7 Hz, 1H, CHOTf), 4.75 (ddt, J = 3.3, 9.8, 47.3 Hz, 1H, CFH), 4.61 (d, J = 12.0 Hz, 1H, PhCH $\underline{\text{H}}$), 4.56 (d, J = 12.0 Hz, 1H, PhCH $\underline{\text{H}}$), 3.78 (dd, J = 1.2, 11.4 Hz, 1H, CH-OTf-CH $\underline{\text{H}}$), 3.73 (dd, J = 1.2, 6.5 Hz, 1H, CH-OTf-CH $\underline{\text{H}}$), 1.80–1.37 (m, 4H, CH₃CH $\underline{2}$ CH $\underline{2}$), 0.96 (t, J = 7.1 Hz, 3H, CH₃); **¹³C{¹H} NMR** (76 MHz, CDCl₃) δ 137.0, 128.7, 128.2, 127.9, 91.2 (d, J = 177.0 Hz), 87.6 (d, J = 23.5 Hz), 73.8, 66.9 (d, J = 7.1 Hz), 32.4 (d, J = 20.9 Hz), 18.4 (d, J = 3.5 Hz), 13.7; **¹⁹F NMR** (283 MHz, CDCl₃) δ -74.8 (d, J = 2.8 Hz, 3F, CF₃), -192.9 (m, 1F, CHF); **¹⁹F{¹H} NMR** (283 MHz, CDCl₃) δ -74.8 (d, J = 2.8 Hz, 3F, CF₃), -192.9 (q, J = 2.8 Hz, 1F, CHF).

Step 2: Cesium fluoride (760 g, 5.02 mmol) was added to a solution of triflate **19** (900 g, 2.51 mmol) in dry DMF (40 mL), and the mixture was stirred at 50 °C for 24 h. The mixture was concentrated under reduced pressure. The residue was diluted with ethyl acetate (350 mL), and the organic solution was washed with water (10 × 100 mL), dried (MgSO₄) and concentrated onto silica. The residue was subjected to flash chromatography eluting with 0:100→15:85 ethyl acetate / hexane to give alcohol **18** (32%, presumably formed through reaction with adventitious water), along with its corresponding formate ester (340 mg, 53%) which was converted into a second crop of **18** through hydrolysis as in Method 1, Step 2 above. Spectroscopic data for **18** were identical to the sample obtained via Method 1 above.

Step 3: As in Method 1.

(((2*R*,3*S*)-2,3-Difluorohexyl)oxy)methyl)benzene (*ent*-**12**)

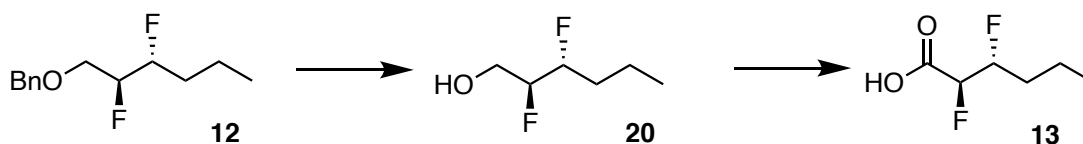


Step 1: The triflate *ent*-**19** was synthesised from *ent*-**9** on 4.42 mmol scale, in a similar fashion to that described above for **19**. Triflate *ent*-**19** was obtained as a brown oil (1.57 g, 99%). All spectroscopic data were identical to those reported for **19**, except for the following: [α]_D -21.3 (c 0.40, CHCl₃).

Step 2: The fluorohydrin *ent*-**18** was synthesised from *ent*-**19** on 4.38 mmol scale, in a similar fashion to that described above for **18**. Fluorohydrin *ent*-**18** was obtained as a clear yellow oil (0.52 g, 56%), along with its corresponding formate ester (31%) which was converted into a second crop of *ent*-**18** as described above for the enantiomeric series. All spectroscopic data for *ent*-**18** were identical to those reported for **18**, except for the following: $[\alpha]_D -7.23$ (*c* 0.47, CHCl₃); **HRMS** (ESI, +ve) C₁₃H₁₉FO₂Na⁺ [MNa⁺] requires *m/z* 249.1261, found 249.1257.

Step 3: Difluoroalkane *ent*-**12** was synthesised from *ent*-**18** on 0.661 mmol scale, in a similar fashion to that reported for **12**. Difluoroalkane *ent*-**12** was obtained as a brown oil (208 mg, 41%) alongside recovered *ent*-**18** (70 mg, 46%). All spectroscopic data for *ent*-**12** were identical to those reported for **12**, except for the following: $[\alpha]_D +7.9$ (*c* 0.510, CHCl₃); **HRMS** (ESI, +ve) C₁₃H₁₈ONa⁺ [MNa⁺] requires *m/z* 251.1218, found 251.1214.

(2*S*,3*R*)-2,3-Difluorohexanoic acid (**13**)

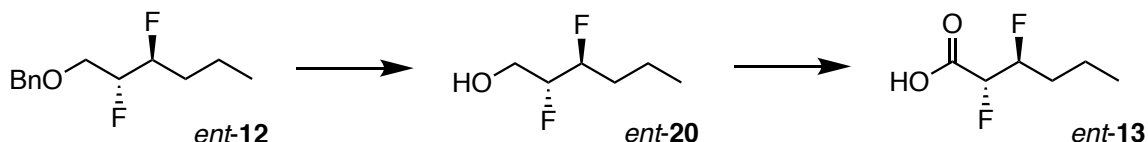


Step 1: Alcohol **20** was synthesised from benzyl ether **12** on 0.876 mmol scale, in a similar fashion to that described above for **16**. Alcohol **20** was obtained as a volatile white crystalline solid (108 mg, 89%); **m.p.** 56.2–56.4 °C (air-dried sample); **IR** (MeOH) ν_{\max} (cm⁻¹) 2359, 2341, 1646, 1405, 1110, 1014; **¹H NMR** (400 MHz, CDCl₃) δ 4.66 (dddd, *J* = 4.4, 5.9, 7.7, 10.9, 48.0 Hz, CHFCHFOH), 4.52 (dddt, *J* = 4.4, 5.6, 12.6, 47.5 Hz, CHFCHFOH), 3.92 (dd, *J* = 1.7, 4.4 Hz, 1H, CHHOH), 3.86 (dd, *J* = 1.7, 4.4 Hz, 1H, CHHOH), 1.87 (br s, 1H, OH), 1.75–1.41 (m, 4H, CH₂CH₂CH₃), 0.97 (t, *J* = 7.3 Hz, CH₃); **¹³C{¹H} NMR** (101 MHz, CDCl₃) δ 93.6 (dd, *J* = 26.4, 173.2 Hz), 90.8 (dd, *J* = 25.6, 171.1 Hz), 61.6 (dd, *J* = 5.1, 21.4 Hz), 33.1 (dd, *J* = 3.6, 20.5 Hz), 18.2 (d, *J* = 3.5 Hz), 13.9; **¹⁹F NMR** (377 MHz, CDCl₃) δ -195.3 (m, 1F, CHFCHFCH₂O), -199.8 (m, 1F, CHFCH₂O); **¹⁹F{¹H} NMR** (377 MHz, CDCl₃) δ -195.3 (d, *J* = 13.8 Hz, 1F, CHFCHFCH₂O), -199.8 (d, *J* = 13.8 Hz, 1F, CHFCH₂O); **HRMS** (ESI, +ve) C₆H₁₂F₂ONa⁺ [MNa⁺] requires *m/z* 161.0748, found 161.0743.

Step 2: Acid **13** was synthesised from alcohol **20** on 0.301 mmol scale, in a similar fashion to that described for **11**. Acid **13** was obtained as a volatile green solid (41.5 mg, 91%); **IR** (neat) ν_{\max} (cm⁻¹) 3324, 2945, 2832, 2535, 2223, 2121, 1643, 1437, 1408, 1112, 1016; **¹H NMR** (400 MHz, CDCl₃) δ 5.97 (br s, 1H, COOH), 5.11 (ddd, *J* = 2.4, 17.9, 49.0 Hz, 1H, CHF₂COOH), 4.87 (dddd, *J* = 2.4, 9.8, 22.0, 46.9 Hz, 1H, CH₂CHF), 1.92 (m, 1H, CH₃CH₂CHH), 1.64–1.40 (m, 3H, CH₃CH₂CHH), 0.96 (t, *J* = 7.2 Hz, 3H, CH₃); **¹³C{¹H} NMR** (101 MHz, CDCl₃) δ 169.9 (dd, *J* =

10.4, 24.1 Hz), 92.1 (dd, $J = 21.5, 178.5$ Hz), 89.3 (dd, $J = 24.1, 191.6$ Hz), 31.1 (dd, $J = 5.3, 21.0$ Hz), 18.3 (d, $J = 3.7$ Hz), 13.7; ^{19}F NMR (377 MHz, CDCl_3) δ -191.3 (m, 1F, CH_2CHF), -201.7 (m, 1F, CHFCOOH); $^{19}\text{F}\{^1\text{H}\}$ NMR (377 MHz, CDCl_3) δ -191.3 (d, $J = 14.0$ Hz, 1F, CH_2CHF), -201.7 (d, $J = 14.0$ Hz, 1F, CHFCOOH); HRMS (ESI, +ve) $\text{C}_6\text{H}_{10}\text{F}_2\text{O}_2\text{Na}^+$ [MNa^+] requires m/z 175.0541, found 175.0548.

(2*R*,3*S*)-2,3-Difluorohexanoic acid (*ent*-13)



Step 1: Alcohol *ent*-20 was synthesised from benzyl ether *ent*-12 on 0.656 mmol scale, in a similar fashion to that described for **16**. Alcohol *ent*-20 was obtained as a volatile white crystalline solid (90.1 mg, 99%). All spectroscopic data were identical to those reported for **20** except for the following: **m.p.** 55.9–56.4 °C (air-dried sample); HRMS (ESI, +ve) $\text{C}_6\text{H}_{12}\text{F}_2\text{ONa}^+$ [MNa^+] requires m/z 161.0748, found 161.0738.

Step 2: Acid *ent*-13 was synthesised from alcohol *ent*-20 on 0.229 mmol scale, in a similar fashion to that described for **11**. Acid *ent*-13 was obtained as a volatile green solid (29 mg, 83%). All spectroscopic data were identical to those reported for **13** except for the following: HRMS (ESI, +ve) $\text{C}_6\text{H}_{11}\text{F}_2\text{O}_2^+$ [MH^+] requires m/z 153.0722, found 153.0715.

3. Determination of absolute configurations and optical purities

The absolute configurations of **5**, *ent-5*, **7** and *ent-7* were assigned according to the precedence established in the original synthetic methods publications.^{[1],[2]}

The $^{19}\text{F}\{^1\text{H}\}$ NMR spectra of **2a** and **2b** (Figure S1) reveal that these compounds have diastereomeric ratios of 21:1 and 20:1, respectively. Compounds **2a** and **2b** were synthesised by coupling a precursor acid (**5** or *ent-5*) with homoserine lactone. The homoserine lactone reagent was enantiomerically pure, therefore the diastereomeric ratios of **2a** and **2b** are equal to the enantiomeric ratios of **5** and *ent-5* (assuming no separation of diastereomers during purification of **2a** and **2b**; a safe assumption because care was taken to collect all relevant column fractions). The enantiomeric ratios for **5** and *ent-5* (*i.e.* 21:1 and 20:1, respectively) are also carried forward to the final target compounds **3a** and **3b**.

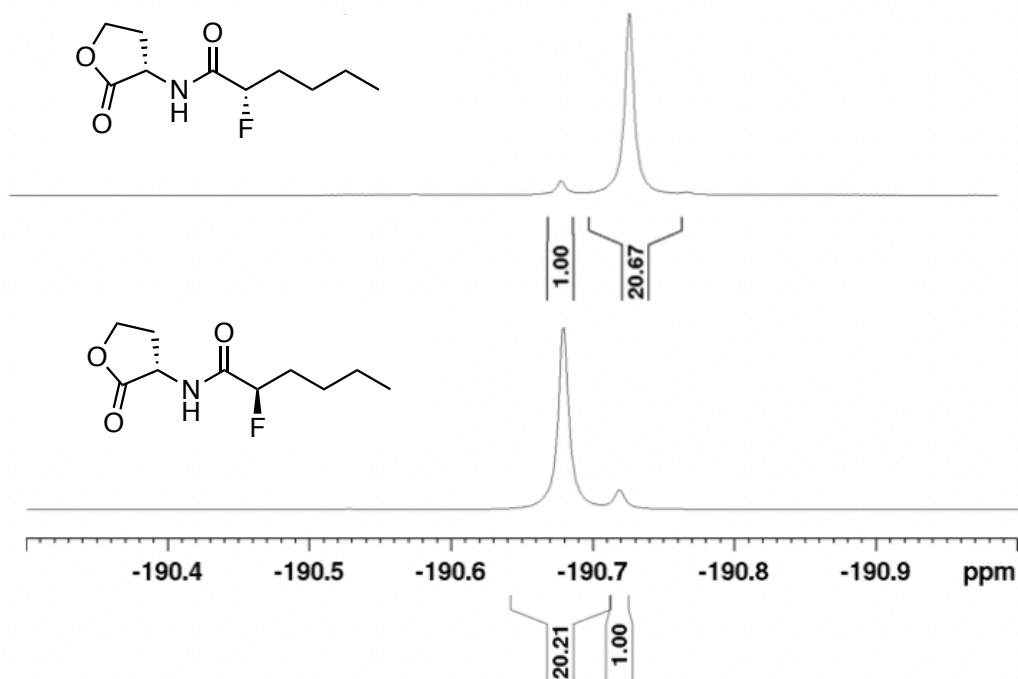


Figure S1: $^{19}\text{F}\{^1\text{H}\}$ NMR analysis reveals the diastereomeric ratios of **2a** and **2b**, which allows the enantiomeric ratios of **3a** and **3b** to be inferred.

The $^{19}\text{F}\{^1\text{H}\}$ NMR spectra of **2e** and **2f** (Figure S2) reveal that these compounds have diastereomeric ratios of 56:1 and 42:1, respectively. Similar ratios are seen for **2c** and **2d** (data not shown). Therefore, it is inferred that the precursor diols *ent-7* and **7** had enantiomeric ratios of 56:1 and 42:1, respectively. It follows that the final target compounds **3d** and **3e** have an enantiomeric ratio of 56:1, and the final target compounds **3c** and **3f** have an enantiomeric ratio of 42:1.

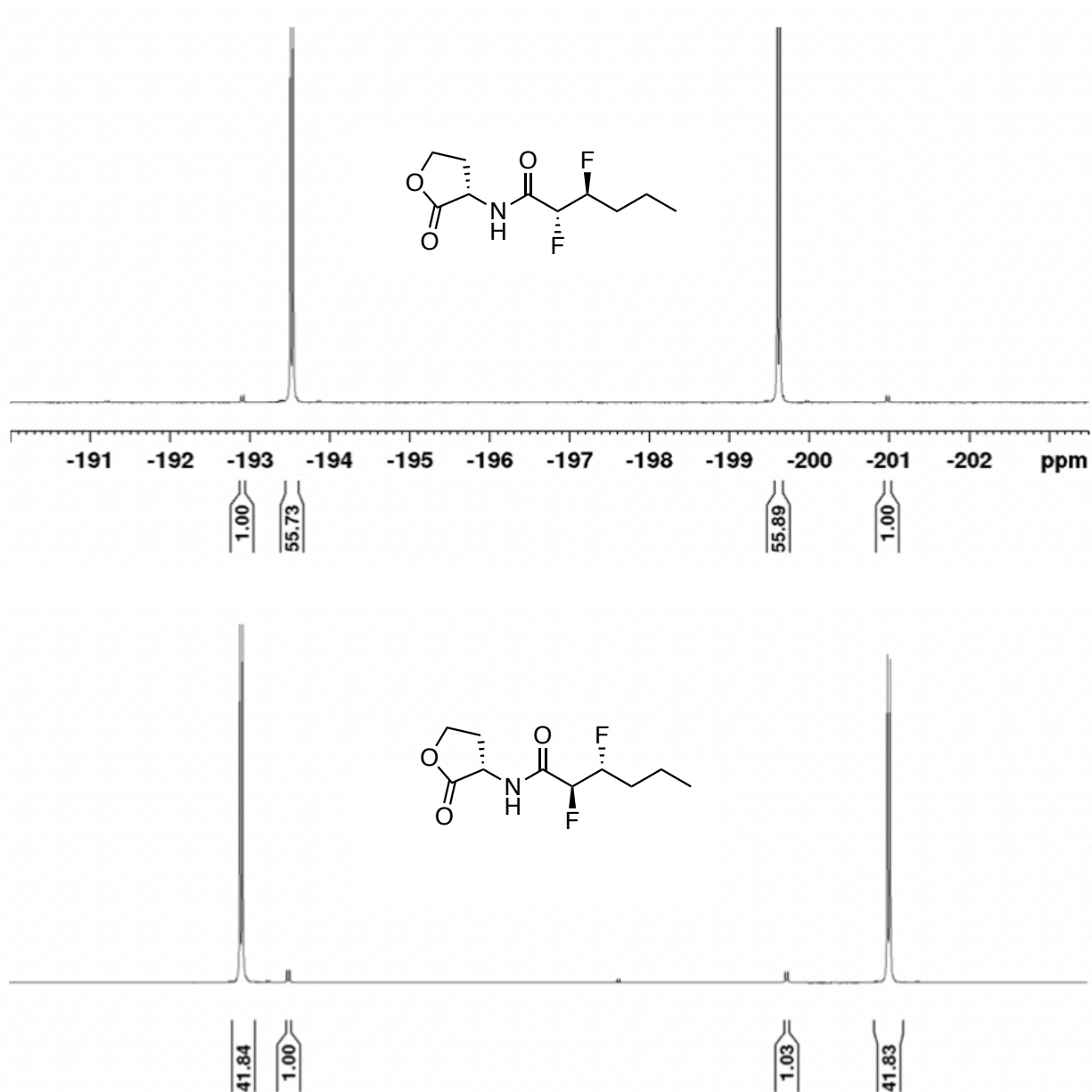
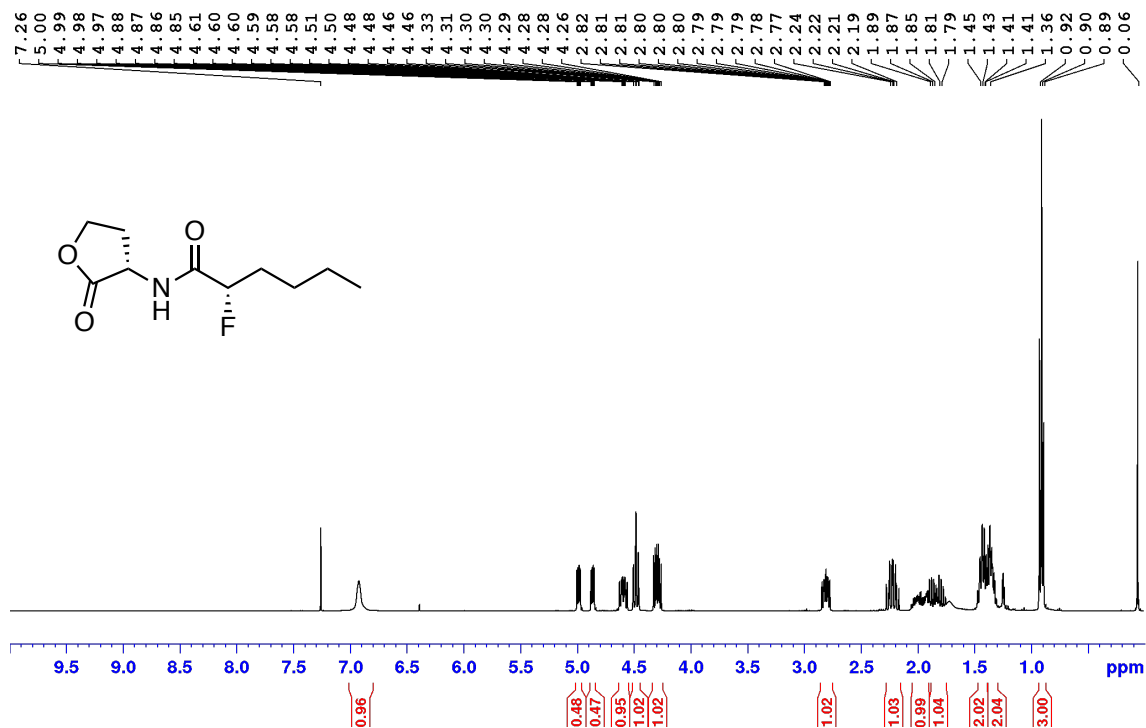


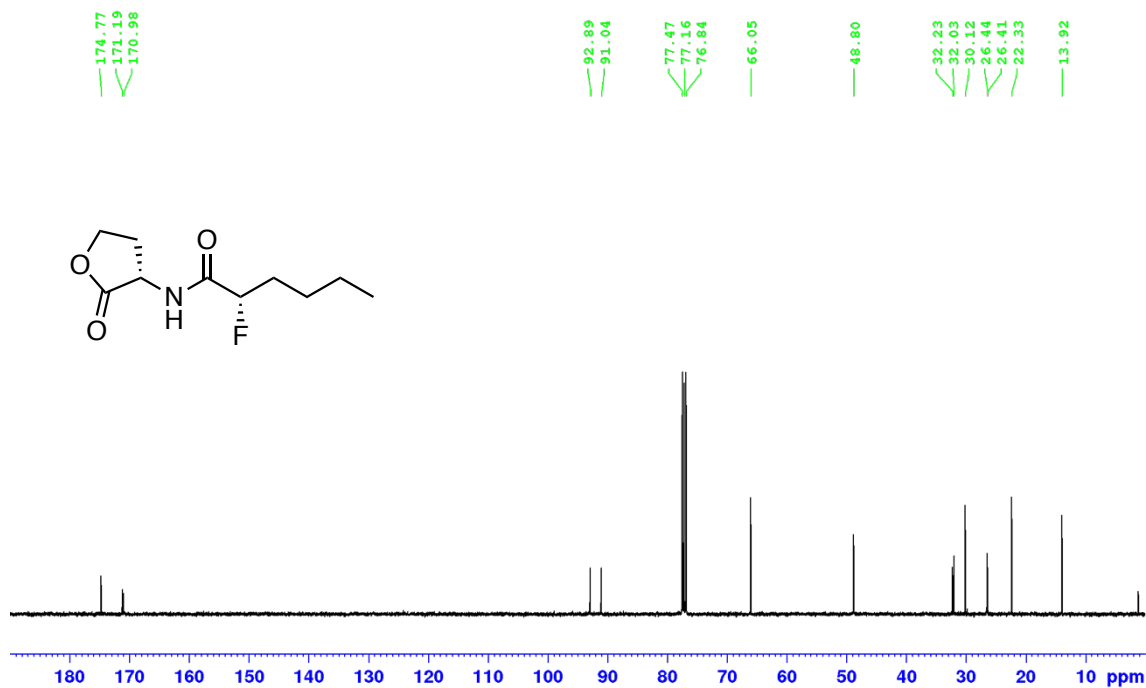
Figure S2: $^{19}\text{F}\{^1\text{H}\}$ NMR analysis reveals the diastereomeric ratios of **2e** and **3f** (shown) and the diastereomeric ratios of **2c** and **3d** (not shown), which allows the enantiomeric ratios of **3c**, **3d**, **3e** and **3f** to be inferred.

4. Selected NMR spectra

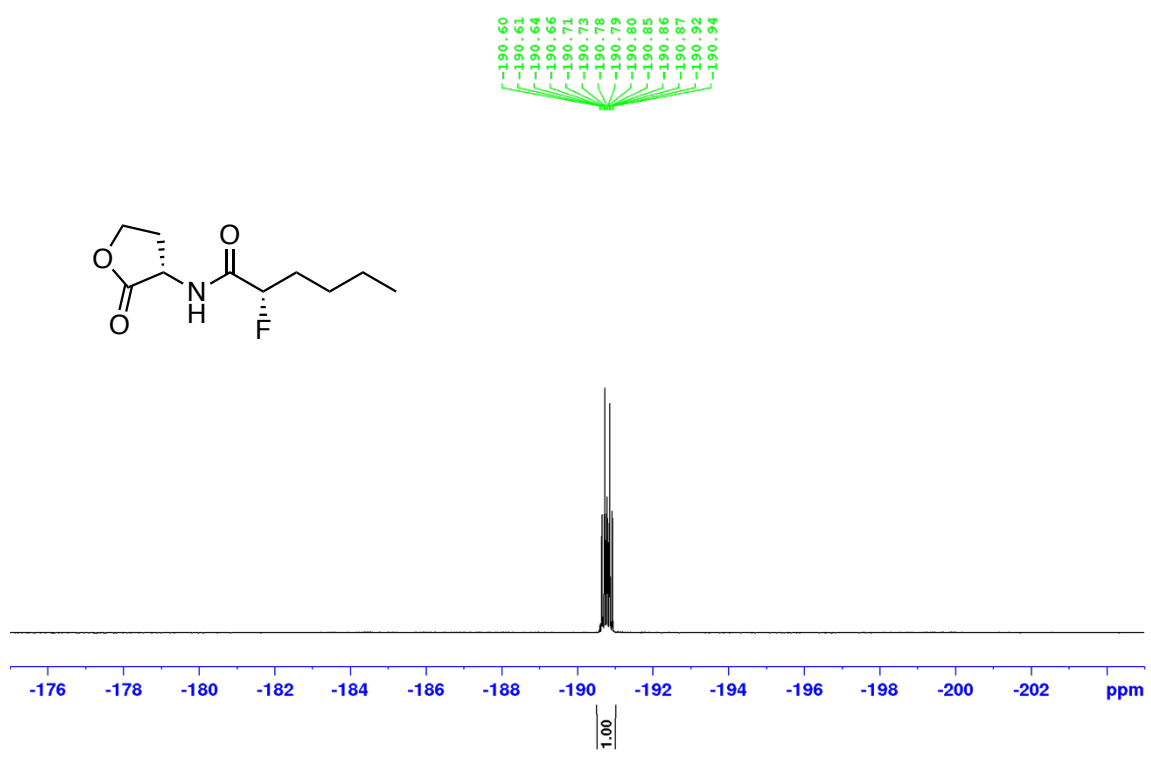
^1H NMR (400 MHz, CDCl_3) of **2a**



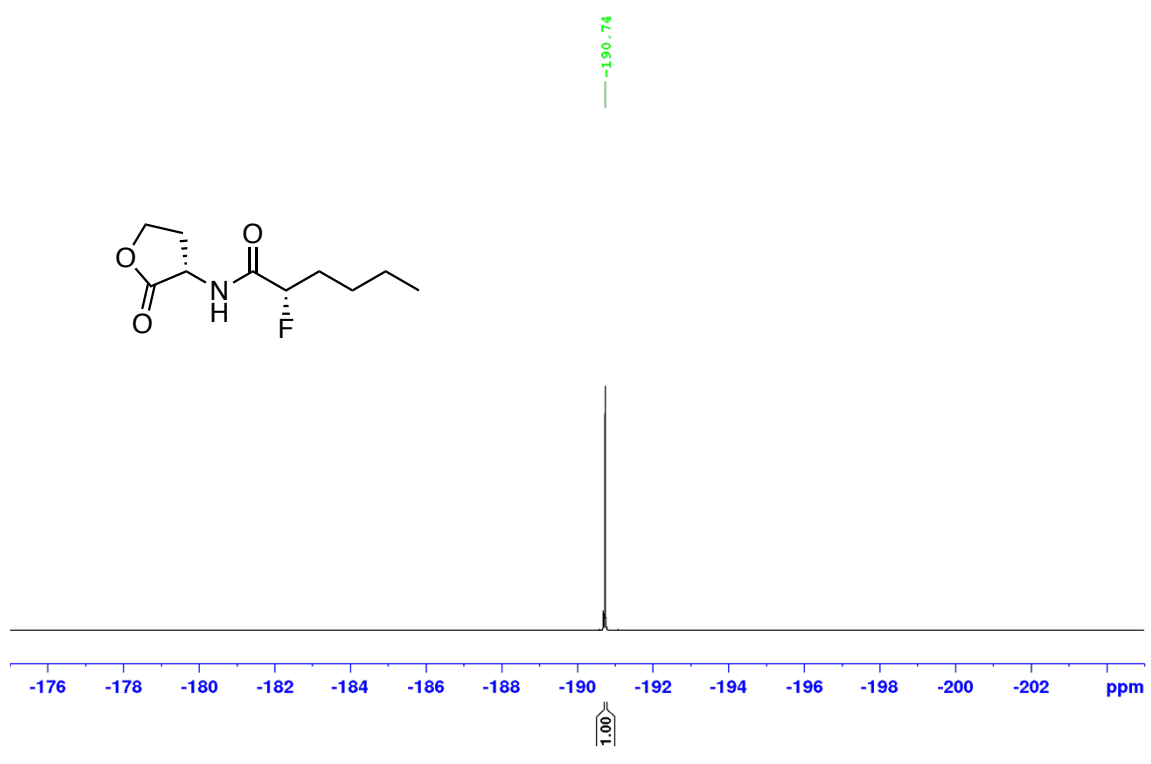
$^{13}\text{C}\{^1\text{H}\}$ NMR (101 MHz, CDCl_3) of **2a**



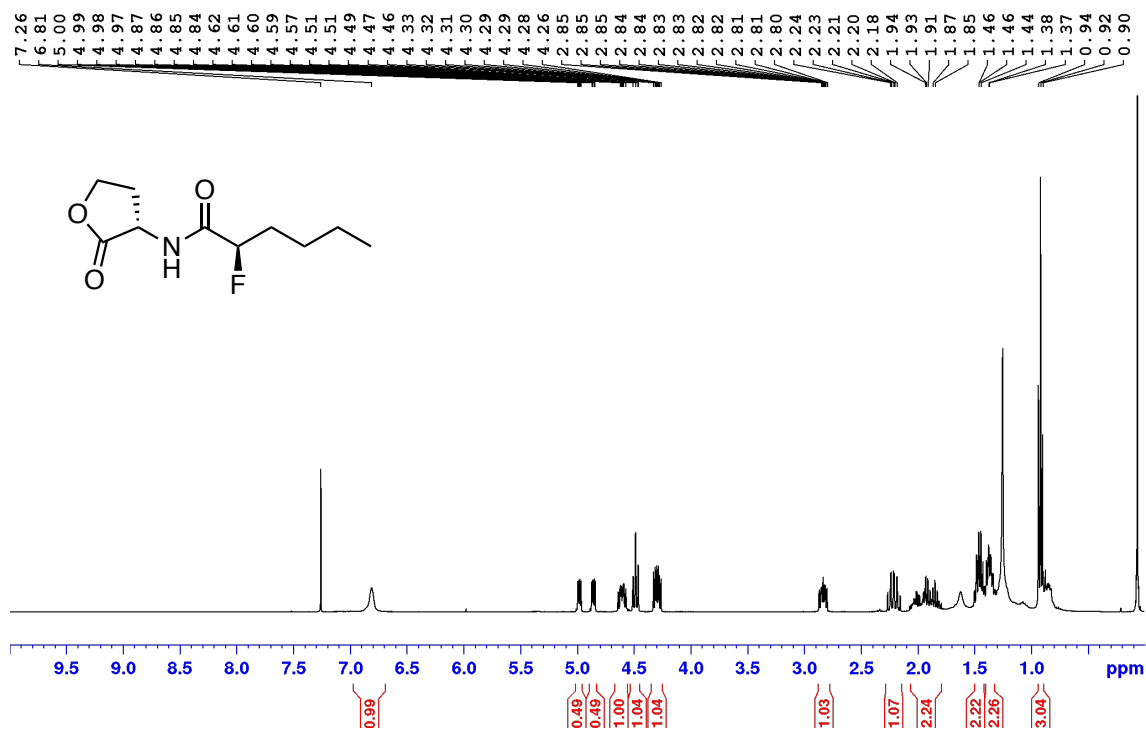
^{19}F NMR (377 MHz, CDCl_3) of **2a**



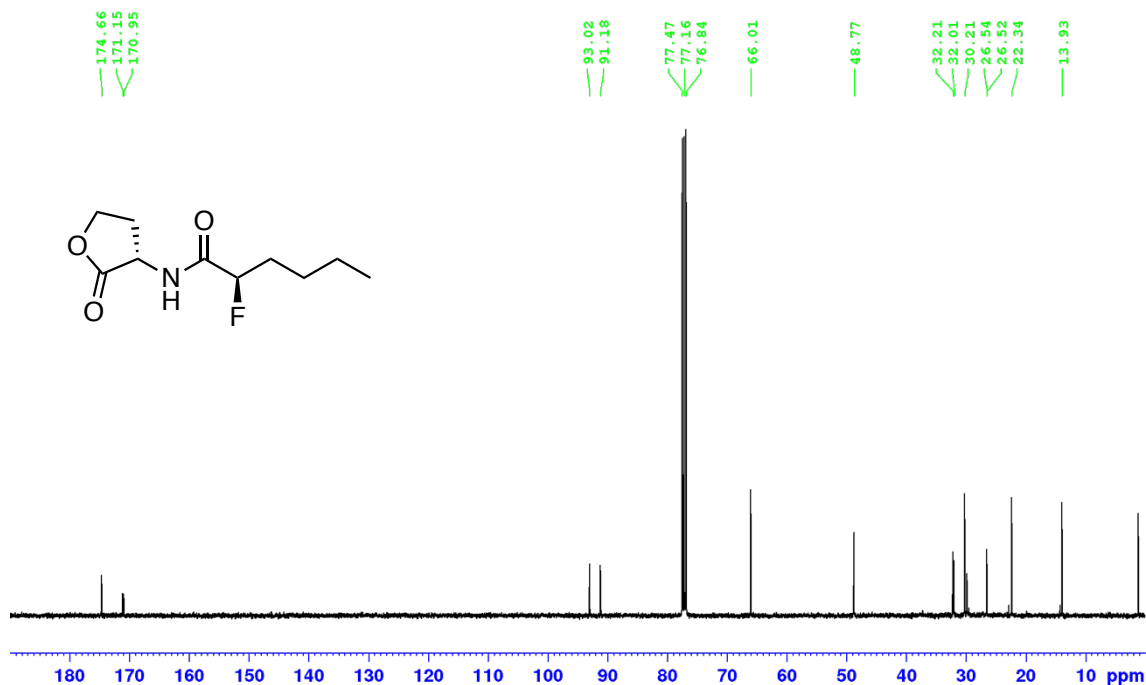
$^{19}\text{F}\{^1\text{H}\}$ NMR (377 MHz, CDCl_3) of **2a**



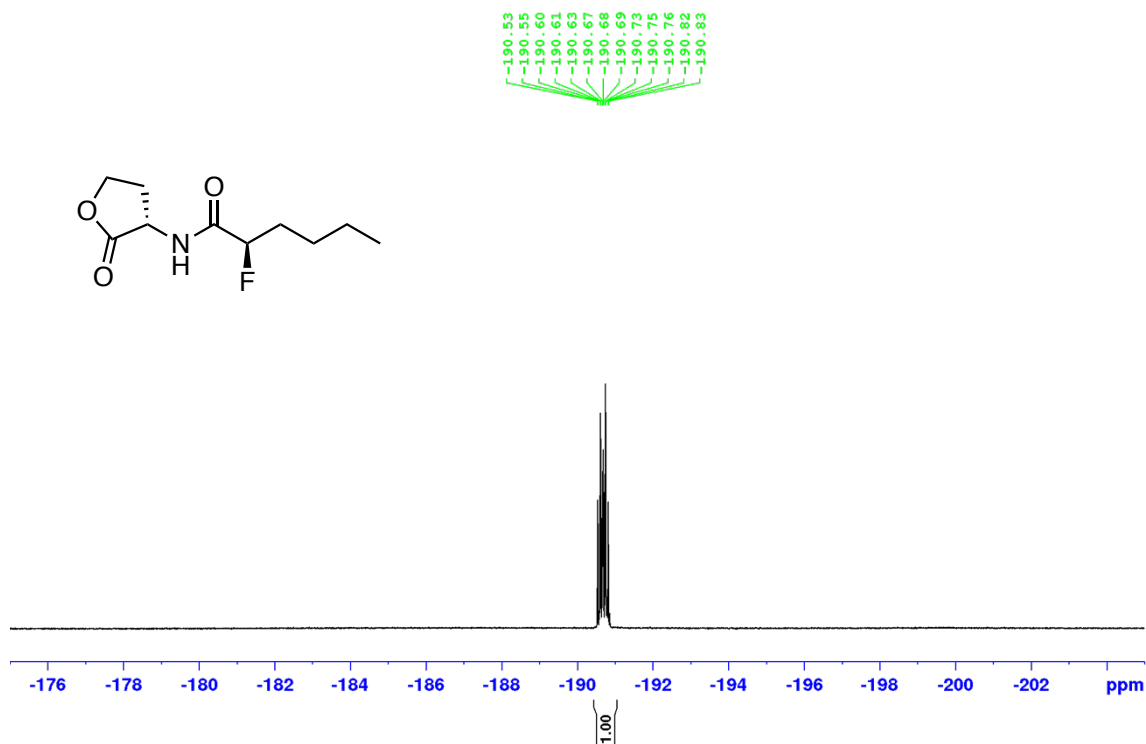
^1H NMR (400 MHz, CDCl_3) of **2b**



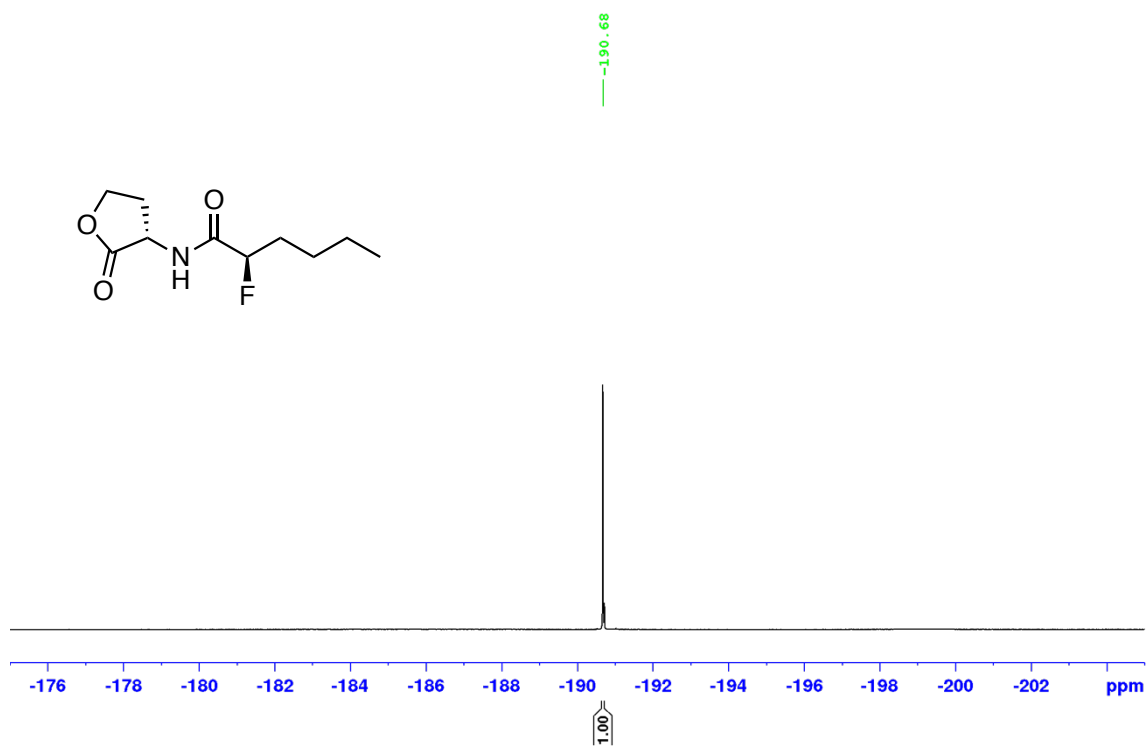
$^{13}\text{C}\{^1\text{H}\}$ NMR (101 MHz, CDCl_3) of **2b**



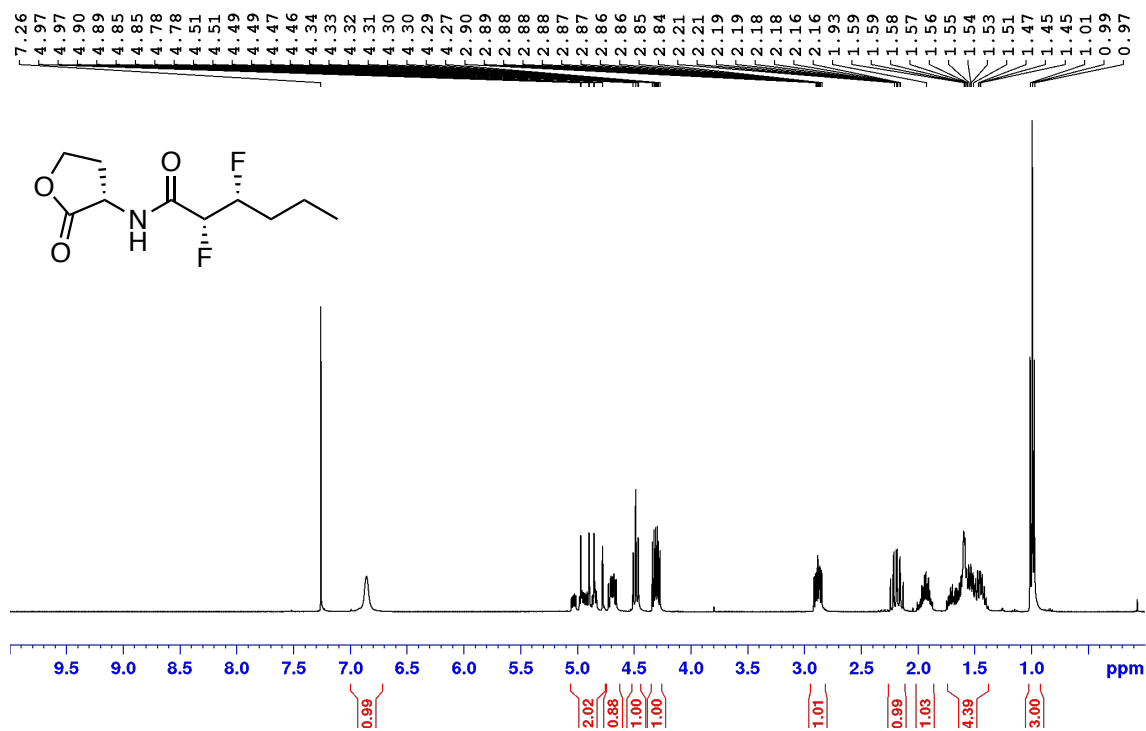
^{19}F NMR (377 MHz, CDCl_3) of **2b**



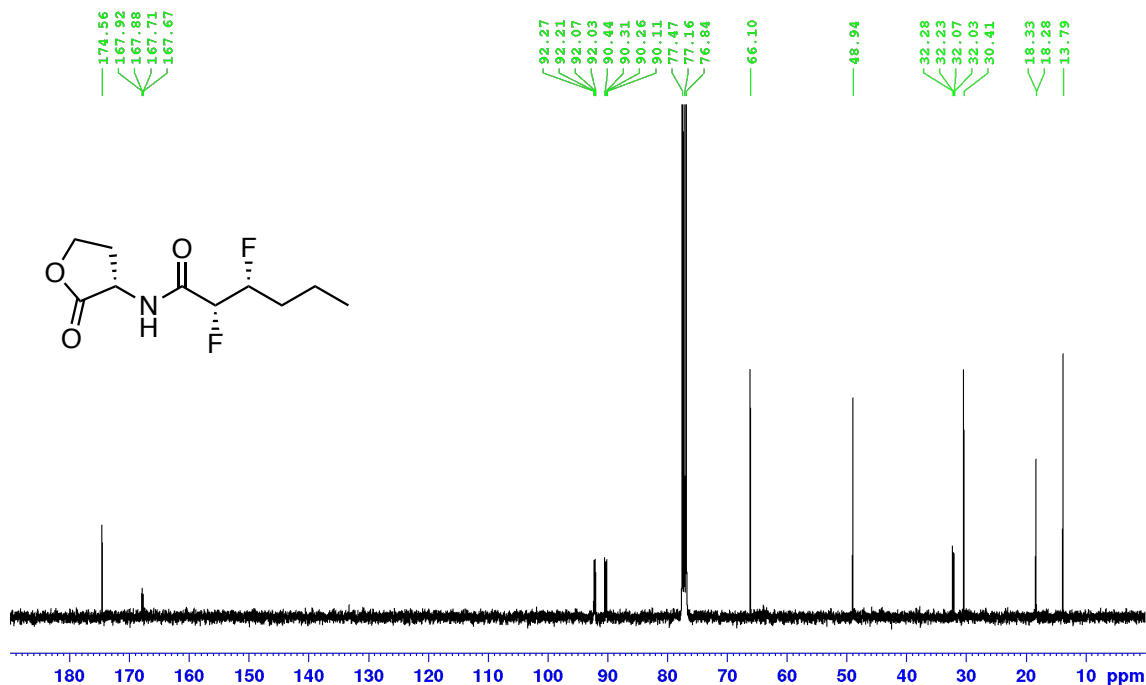
$^{19}\text{F}\{^1\text{H}\}$ NMR (377 MHz, CDCl_3) of **2b**



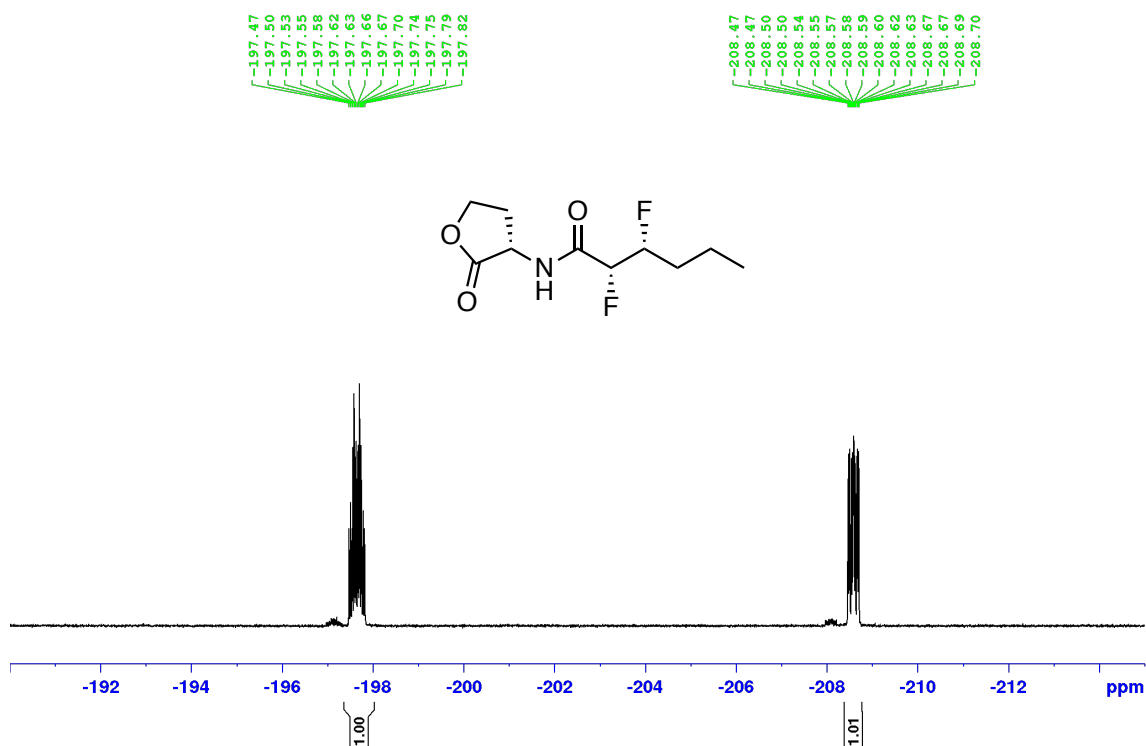
^1H NMR (400 MHz, CDCl_3) of **2c**



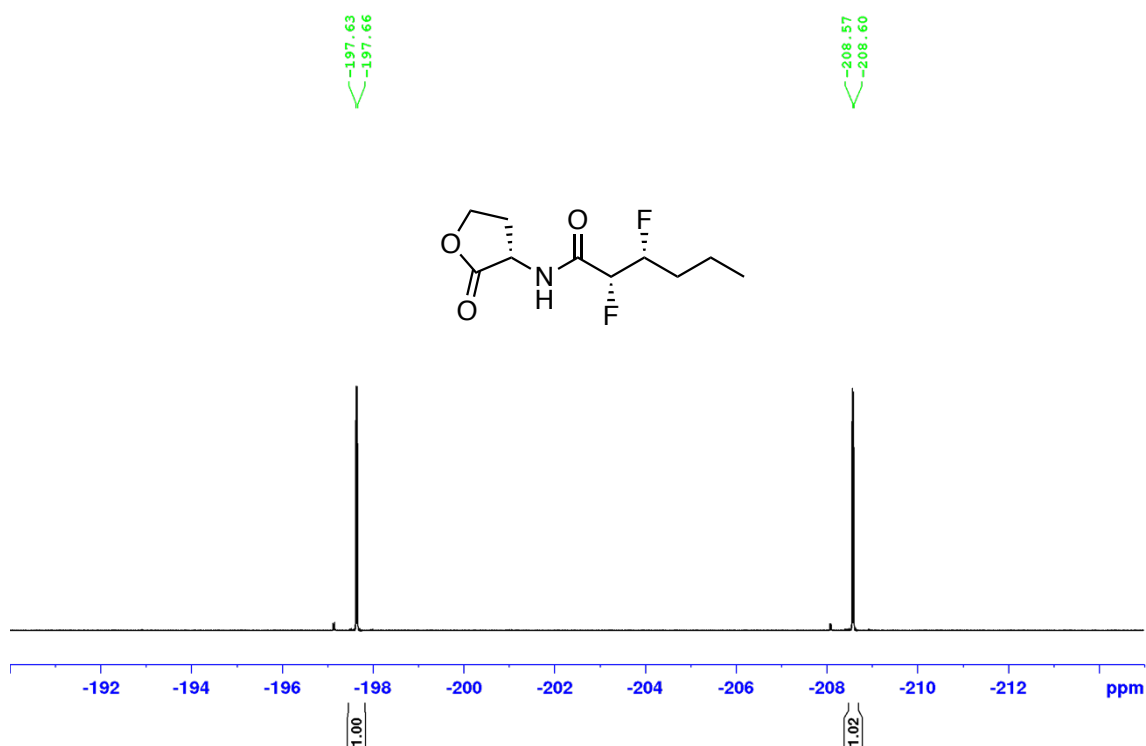
$^{13}\text{C}\{^1\text{H}\}$ NMR (101 MHz, CDCl_3) of **2c**



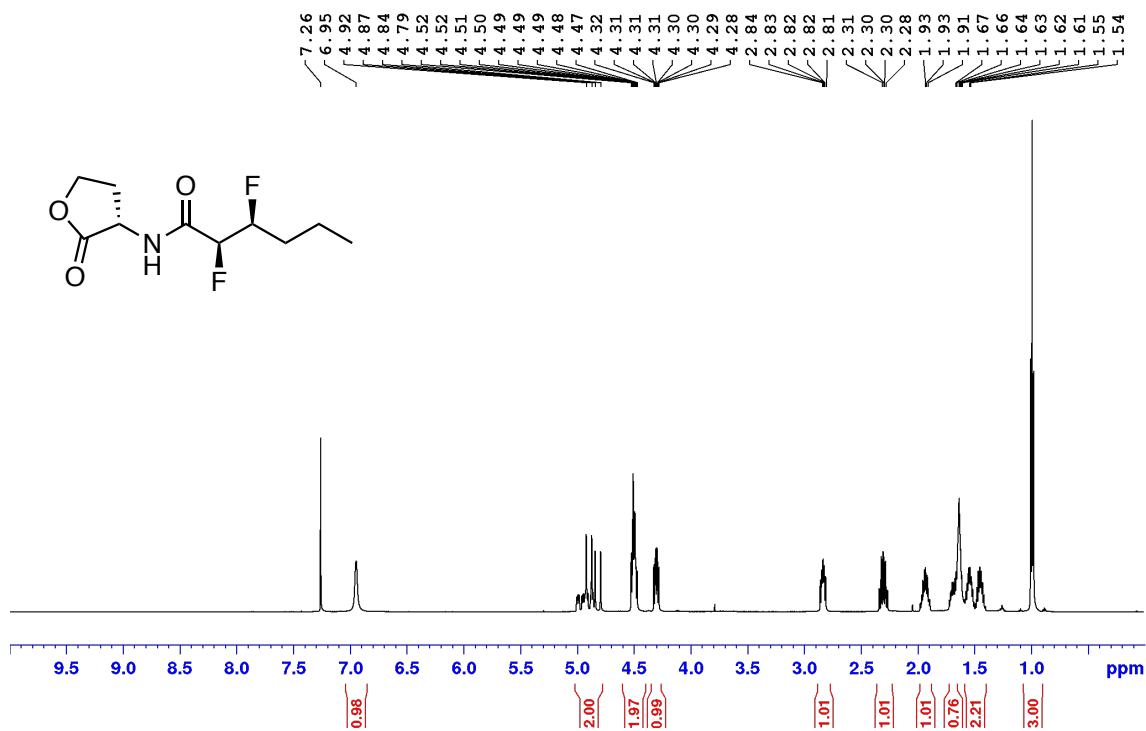
^{19}F NMR (377 MHz, CDCl_3) of **2c**



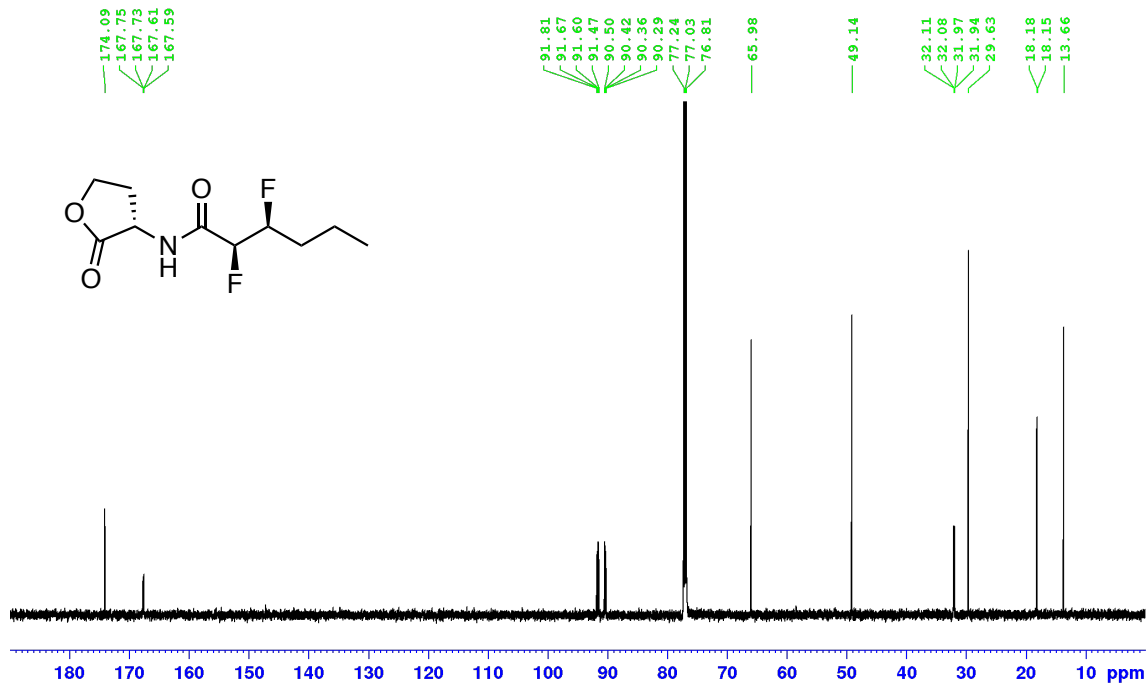
$^{19}\text{F}\{^1\text{H}\}$ NMR (377 MHz, CDCl_3) of **2c**



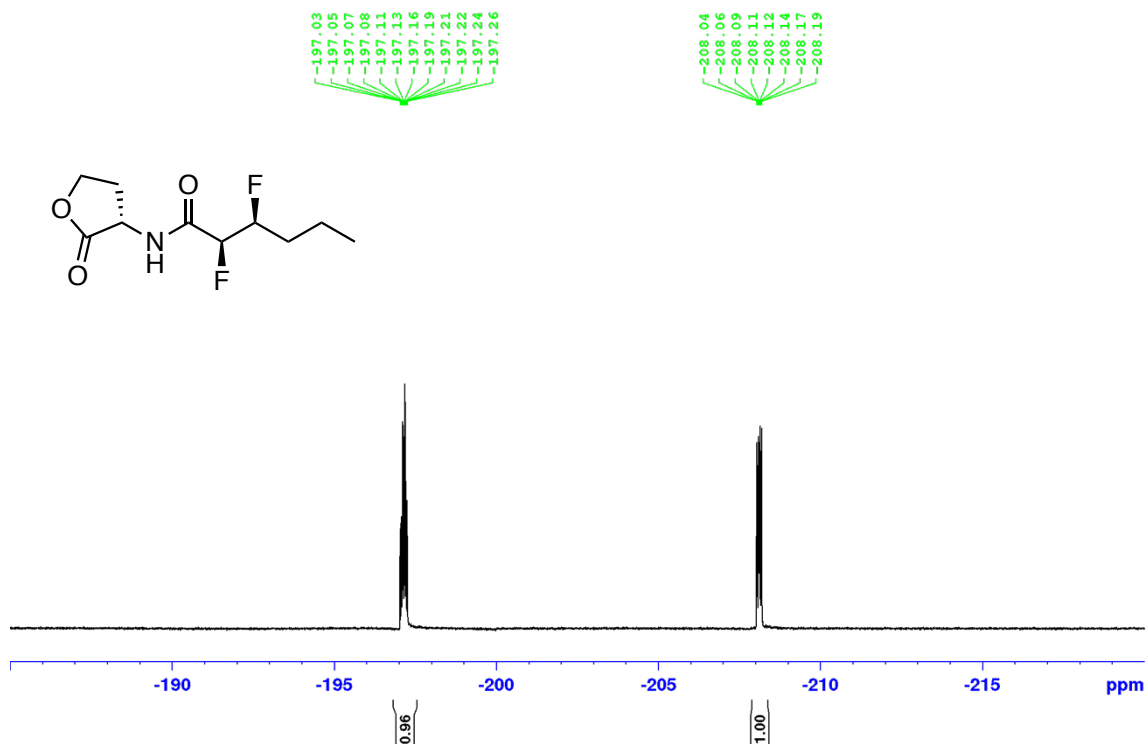
^1H NMR (600 MHz, CDCl_3) of **2d**



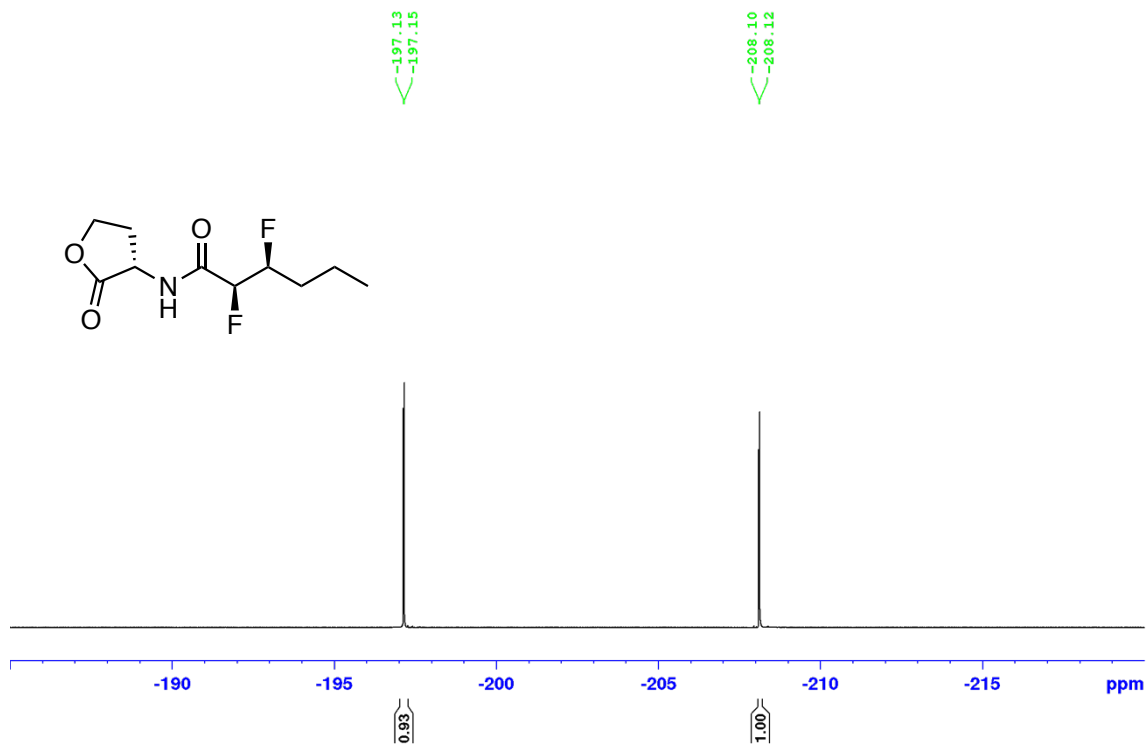
$^{13}\text{C}\{^1\text{H}\}$ NMR (151 MHz, CDCl_3) of **2d**



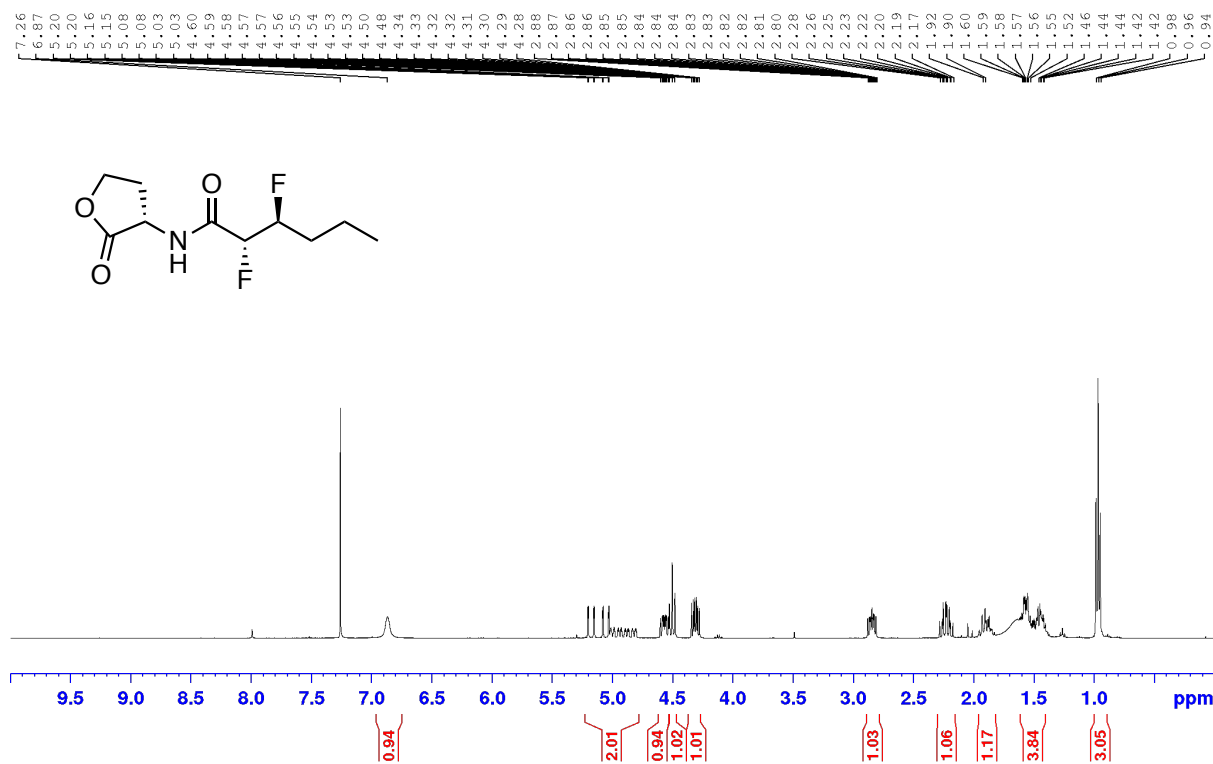
^{19}F NMR (565 MHz, CDCl_3) of **2d**



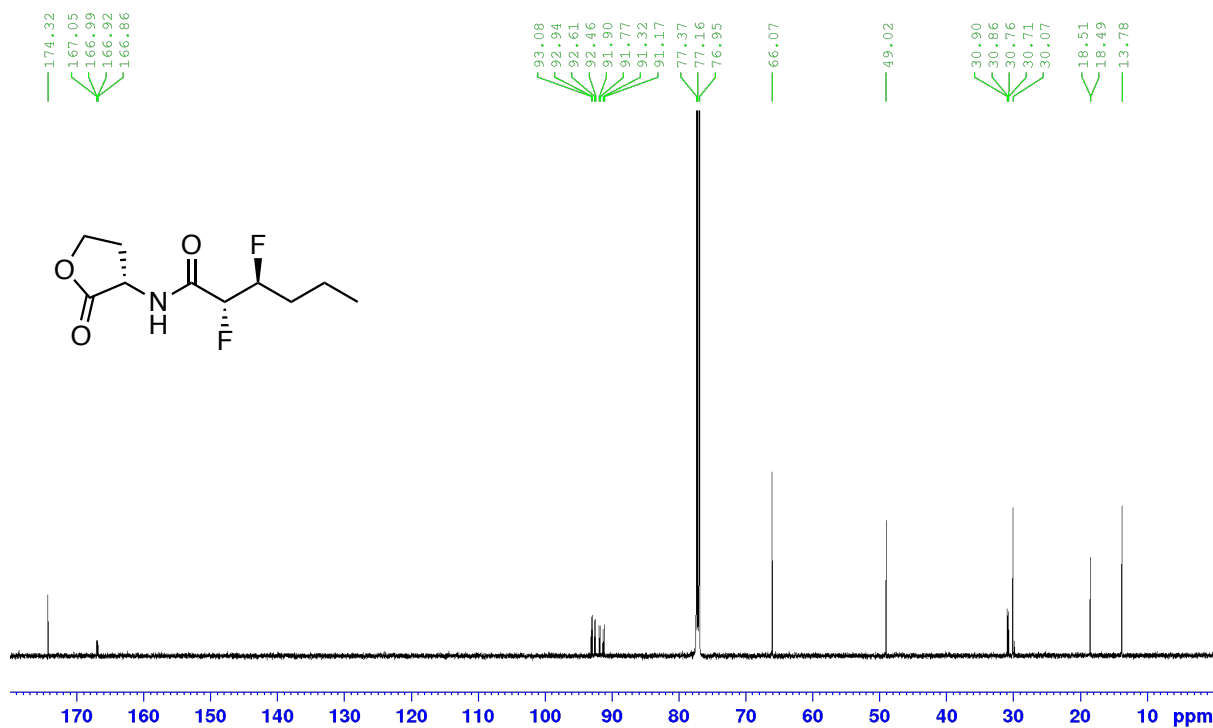
$^{19}\text{F}\{^1\text{H}\}$ NMR (565 MHz, CDCl_3) of **2d**



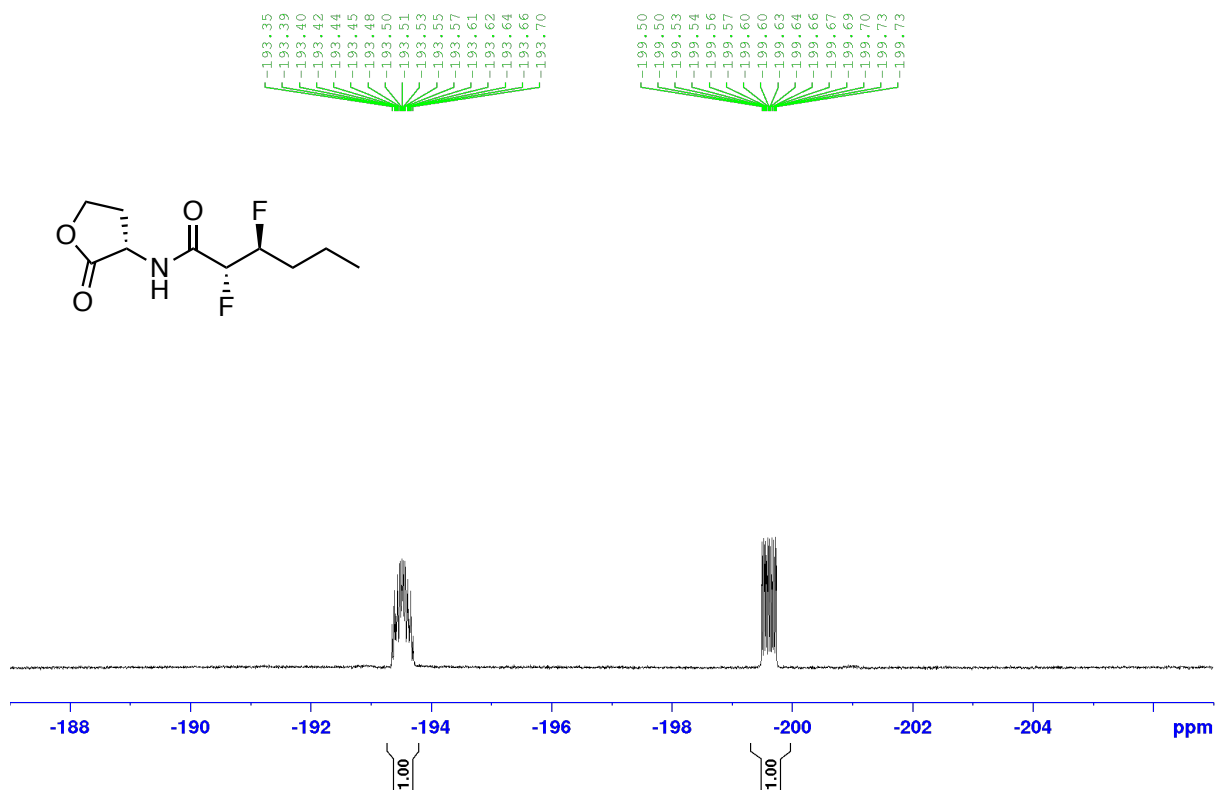
^1H NMR (400 MHz, CDCl_3) of **2e**



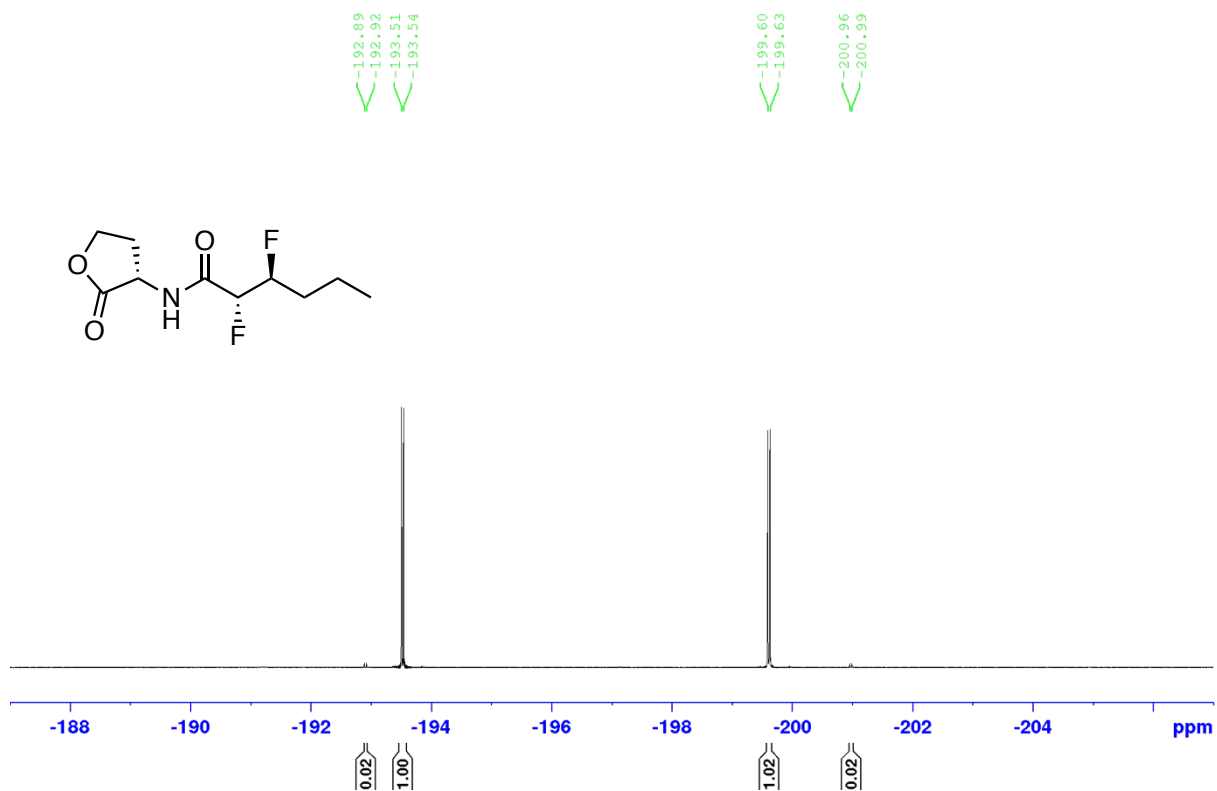
$^{13}\text{C}\{^1\text{H}\}$ NMR (151 MHz, CDCl_3) of **2e**



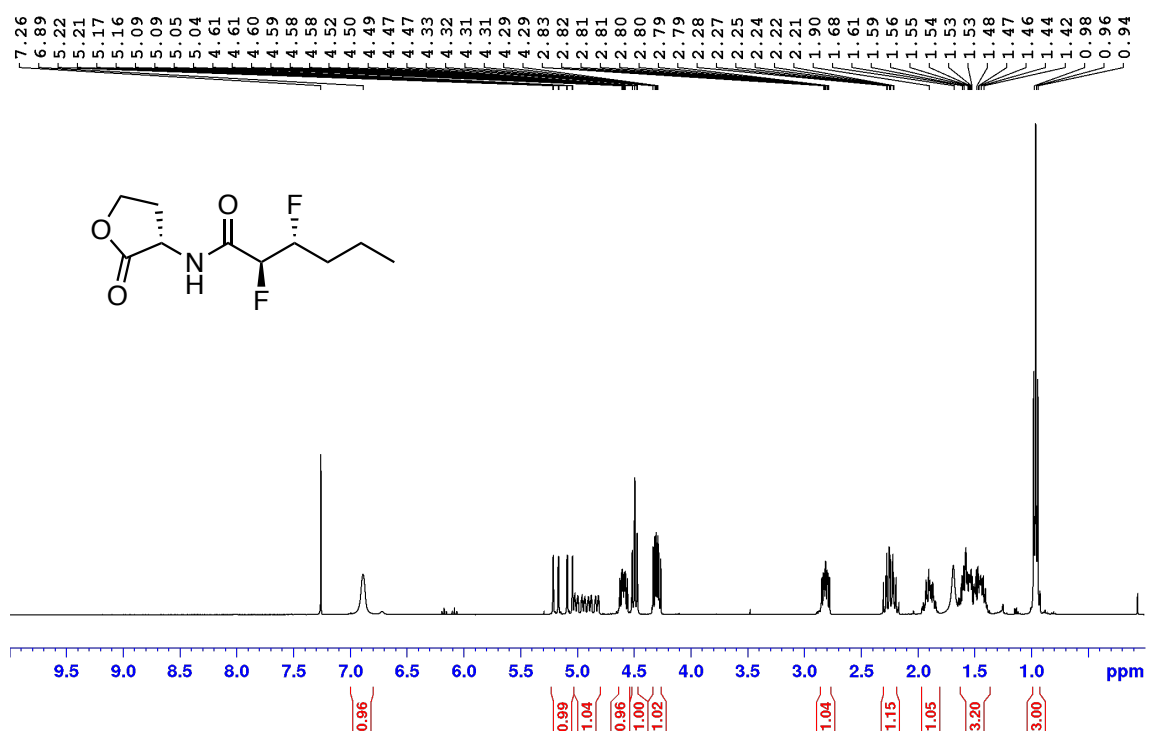
¹⁹F NMR (377 MHz, CDCl₃) of 2e



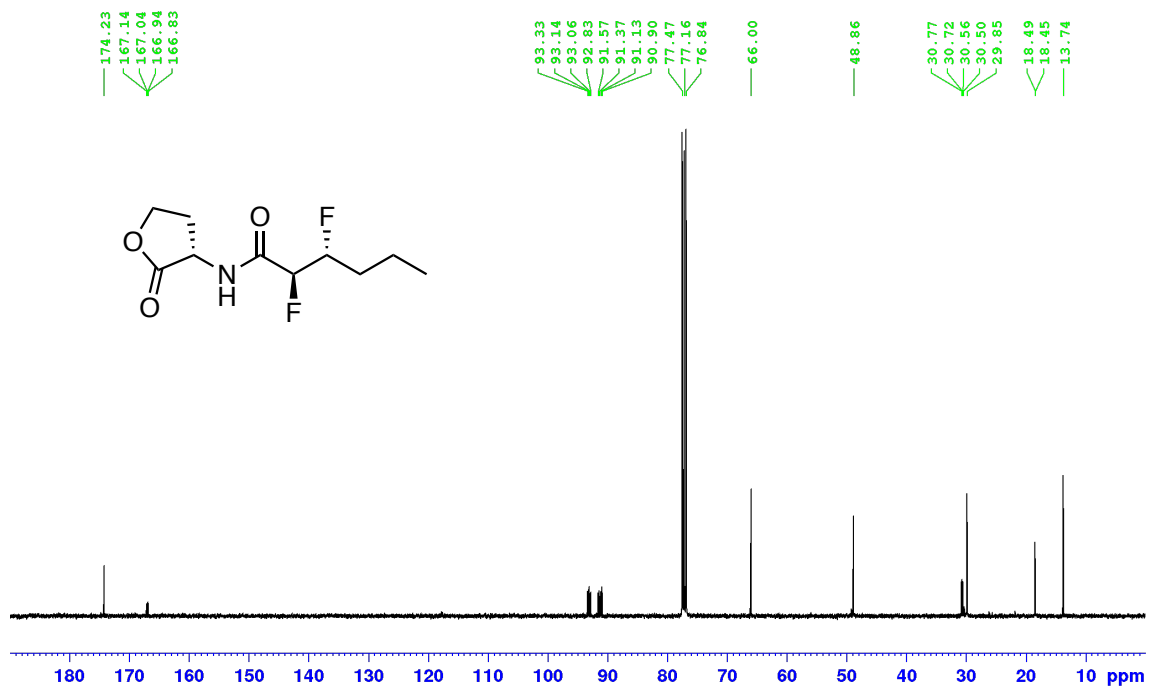
¹⁹F {¹H} NMR (377 MHz, CDCl₃) of 2e



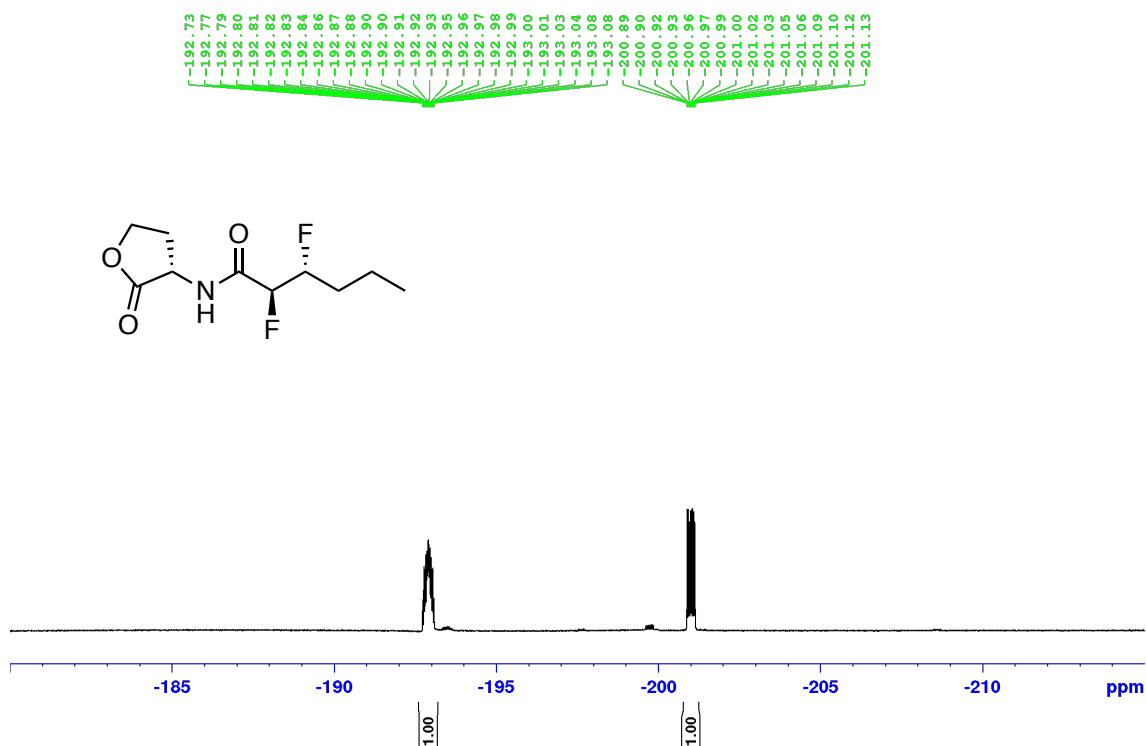
^1H NMR (400 MHz, CDCl_3) of **2f**



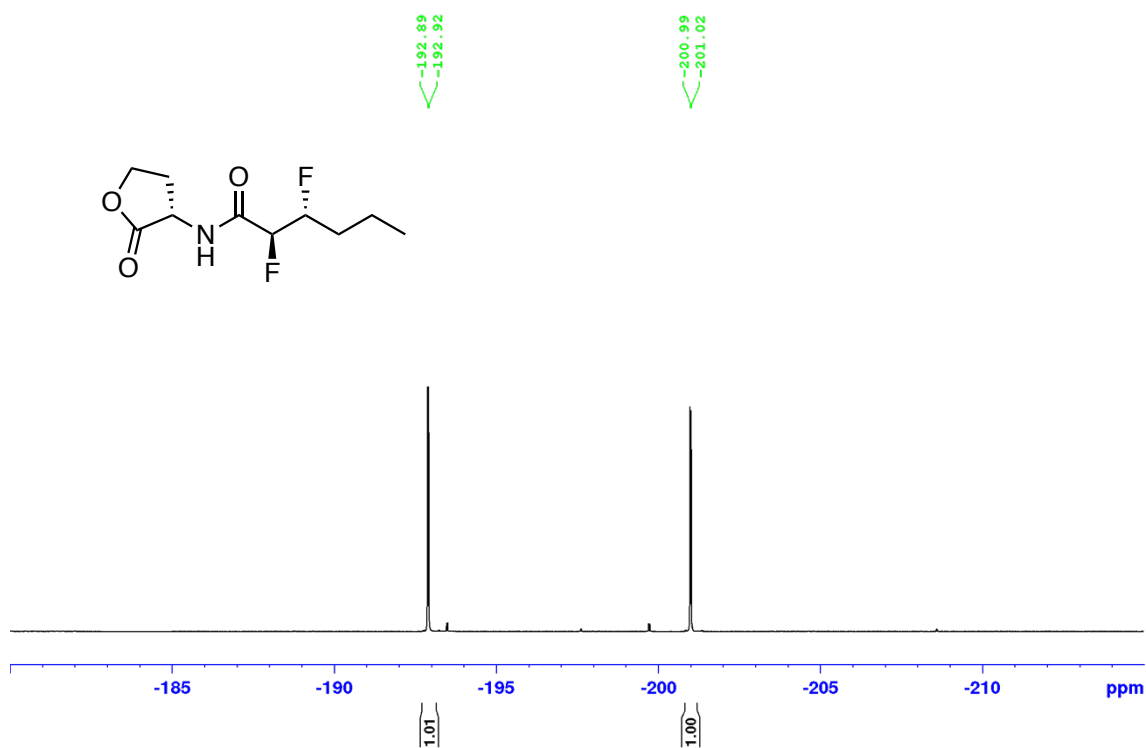
$^{13}\text{C}\{^1\text{H}\}$ NMR (101 MHz, CDCl_3) of **2f**



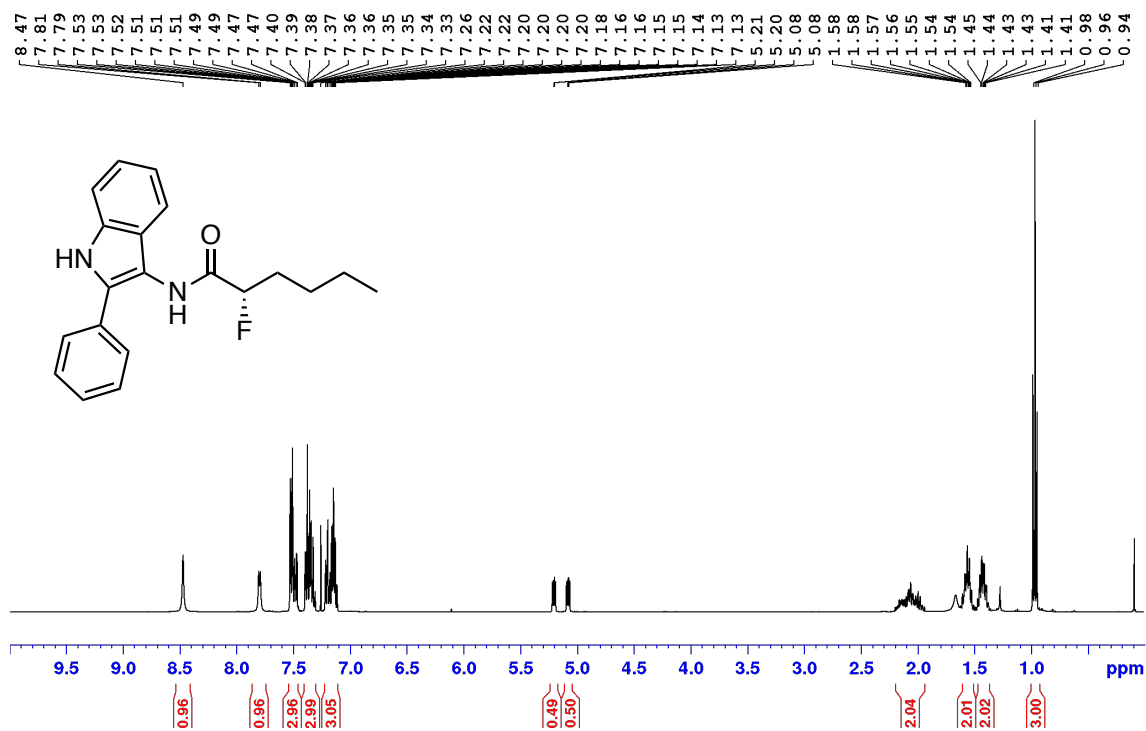
^{19}F NMR (377 MHz, CDCl_3) of **2f**



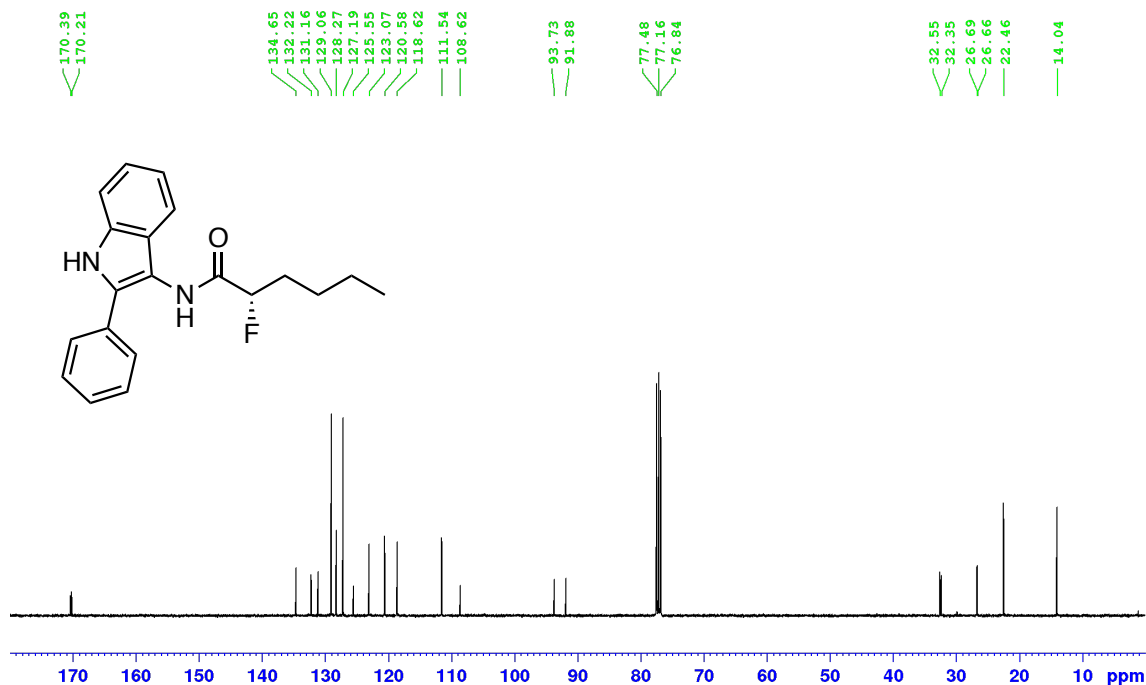
^{19}F $\{^1\text{H}\}$ NMR (377 MHz, CDCl_3) of **2f**



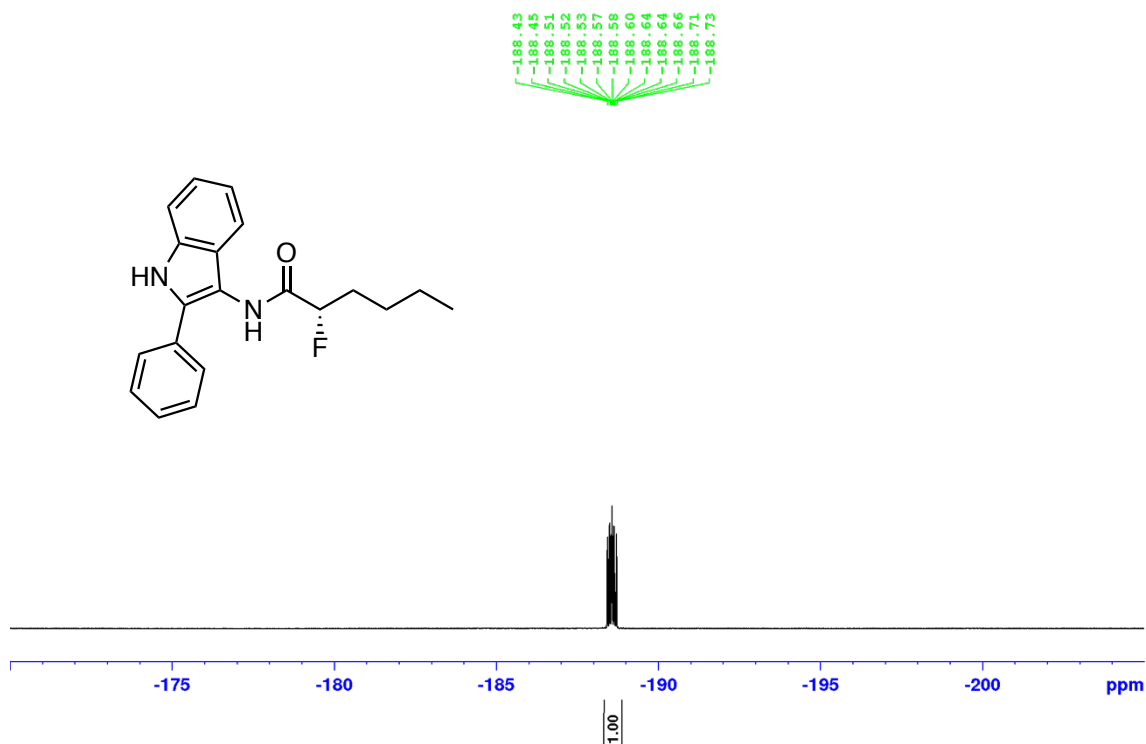
¹H NMR (400 MHz, CDCl₃) of **3a**



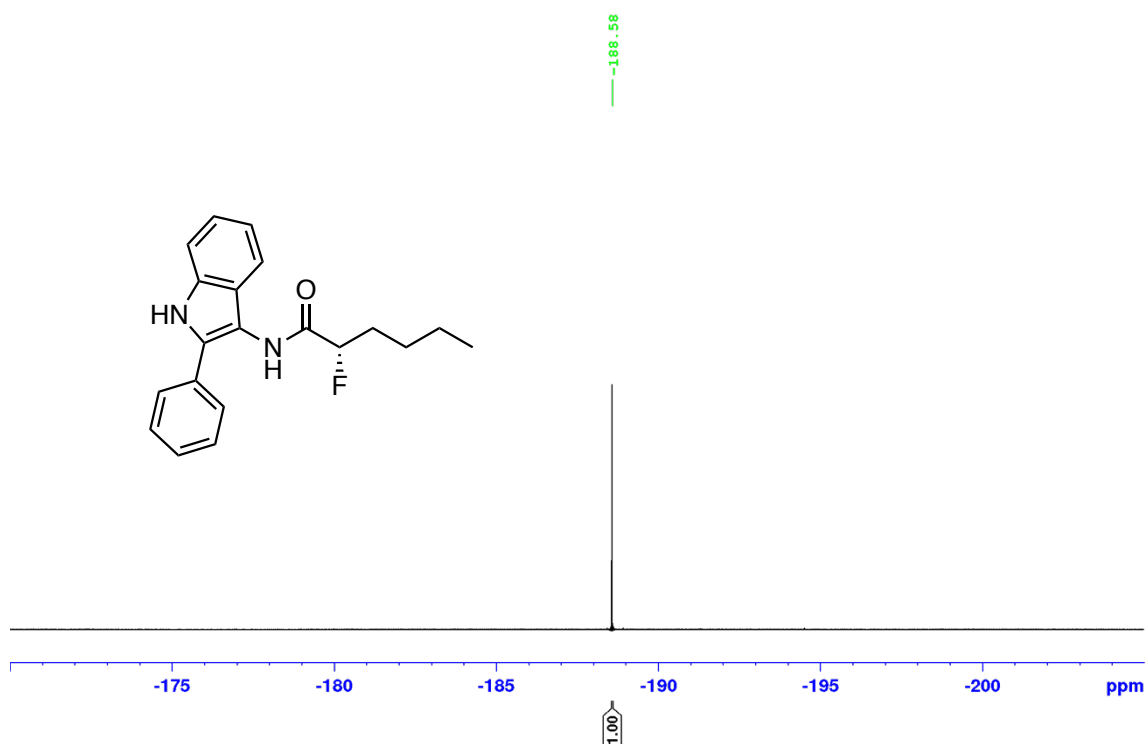
¹³C{¹H} NMR (151 MHz, CDCl₃) of **3a**



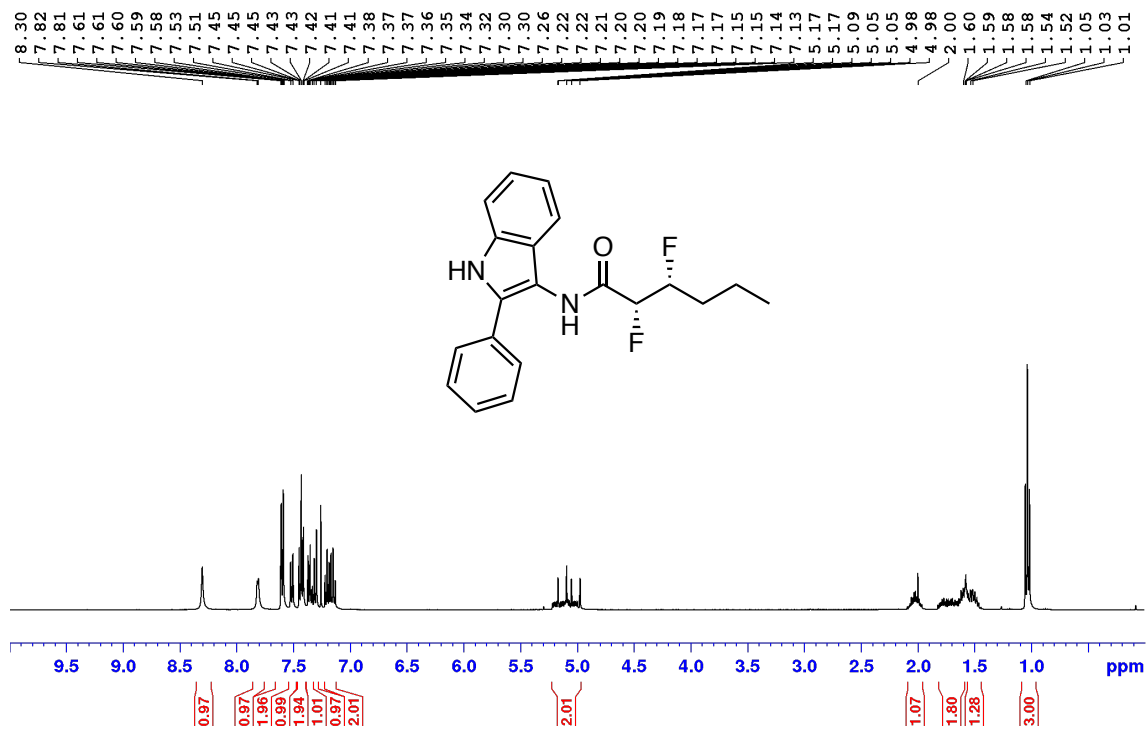
^{19}F NMR (377 MHz, CDCl_3) of **3a**



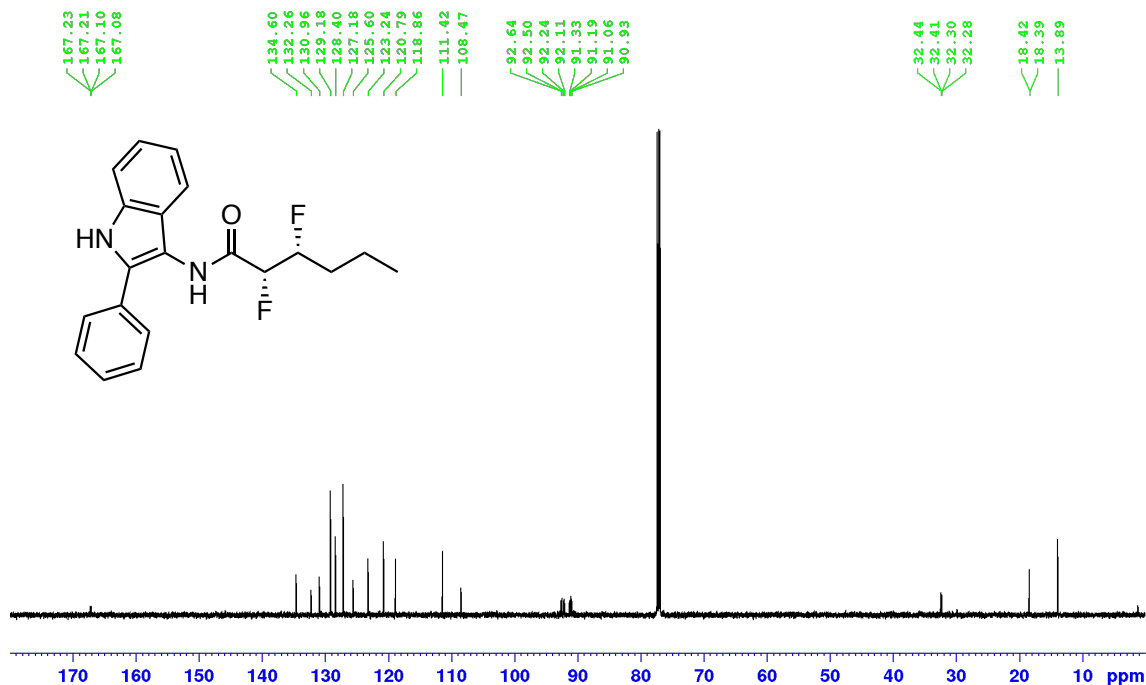
$^{19}\text{F}\{^1\text{H}\}$ NMR (377 MHz, CDCl_3) of **3a**



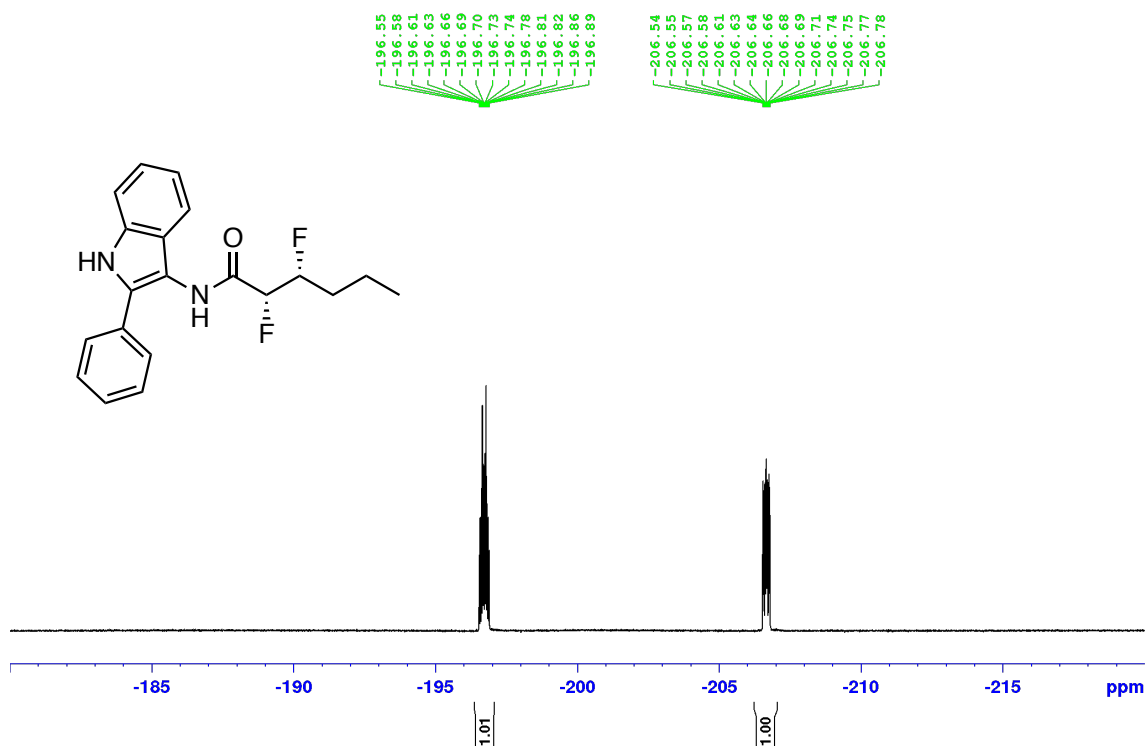
¹H NMR (400 MHz, CDCl₃) of **3c**



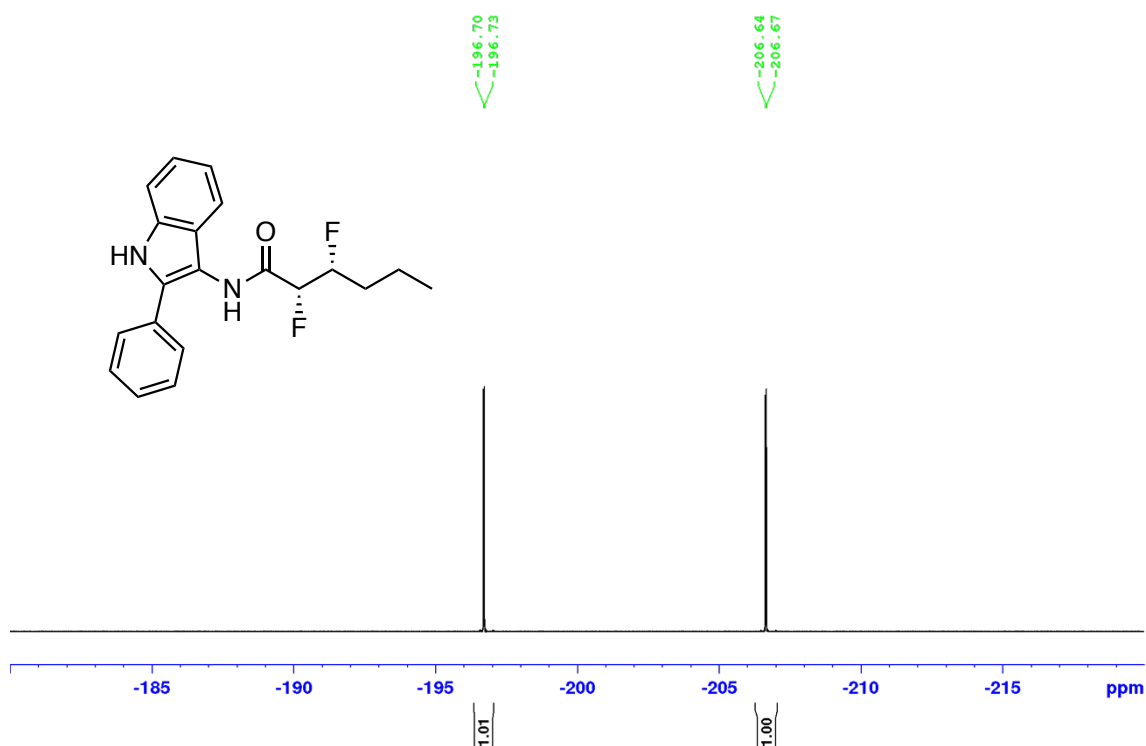
¹³C{¹H} NMR (151 MHz, CDCl₃) of **3c**



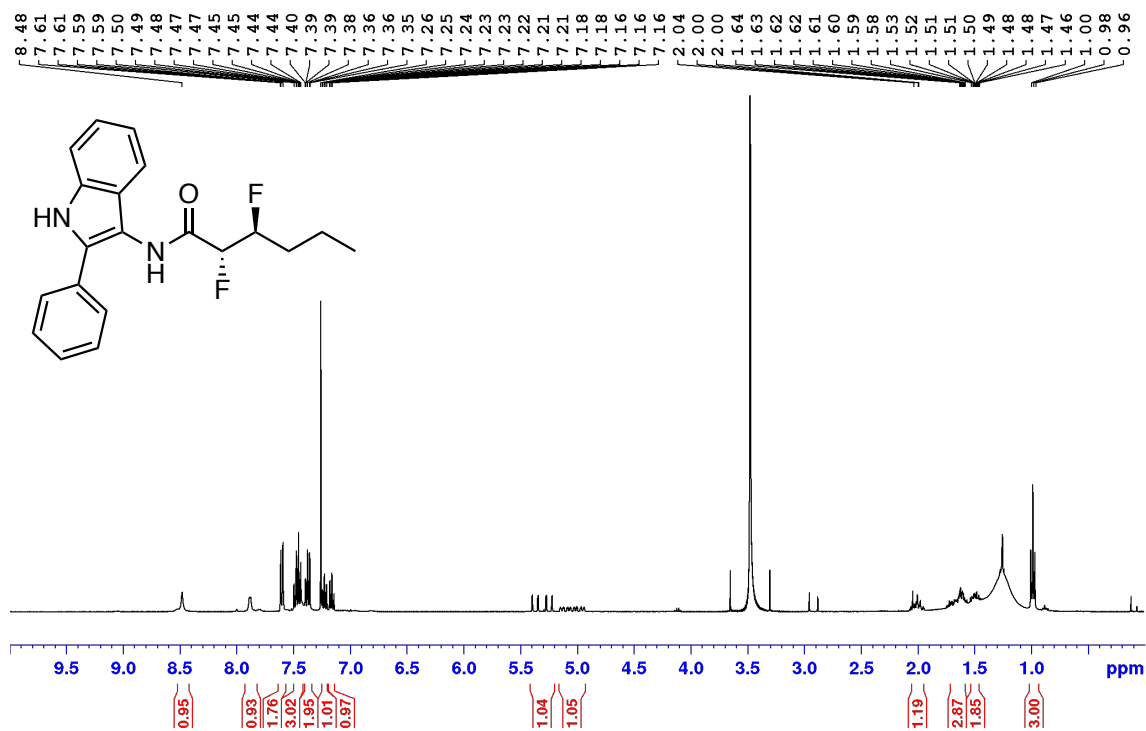
^{19}F NMR (377 MHz, CDCl_3) of **3c**



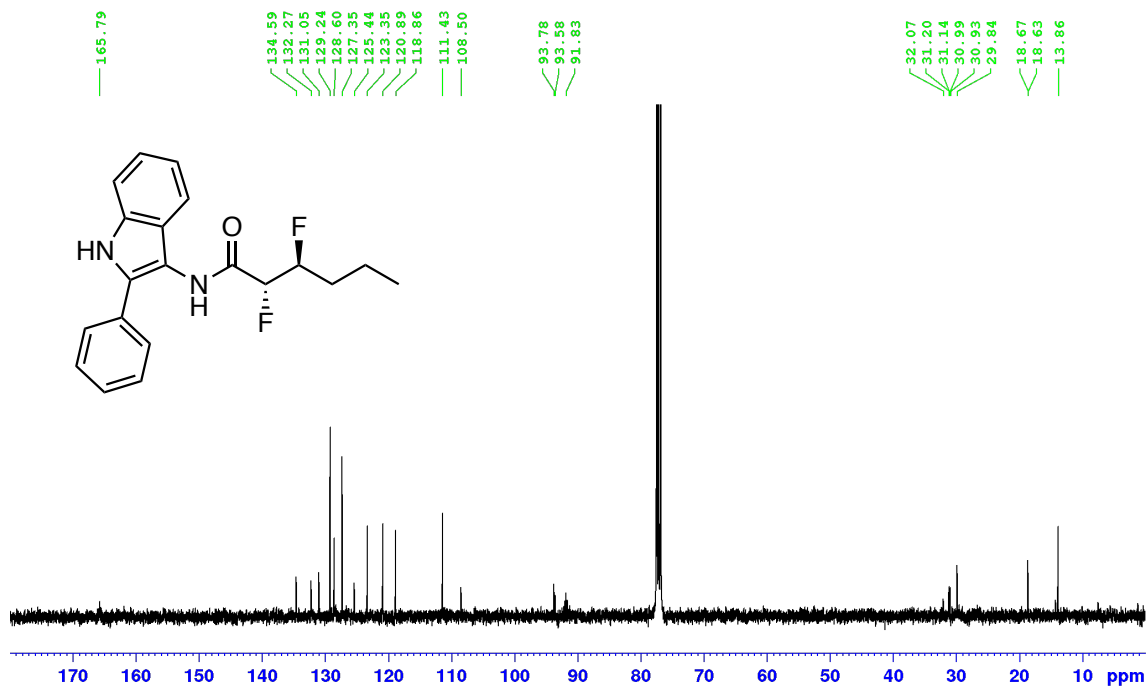
$^{19}\text{F}\{^1\text{H}\}$ NMR (377 MHz, CDCl_3) of **3c**



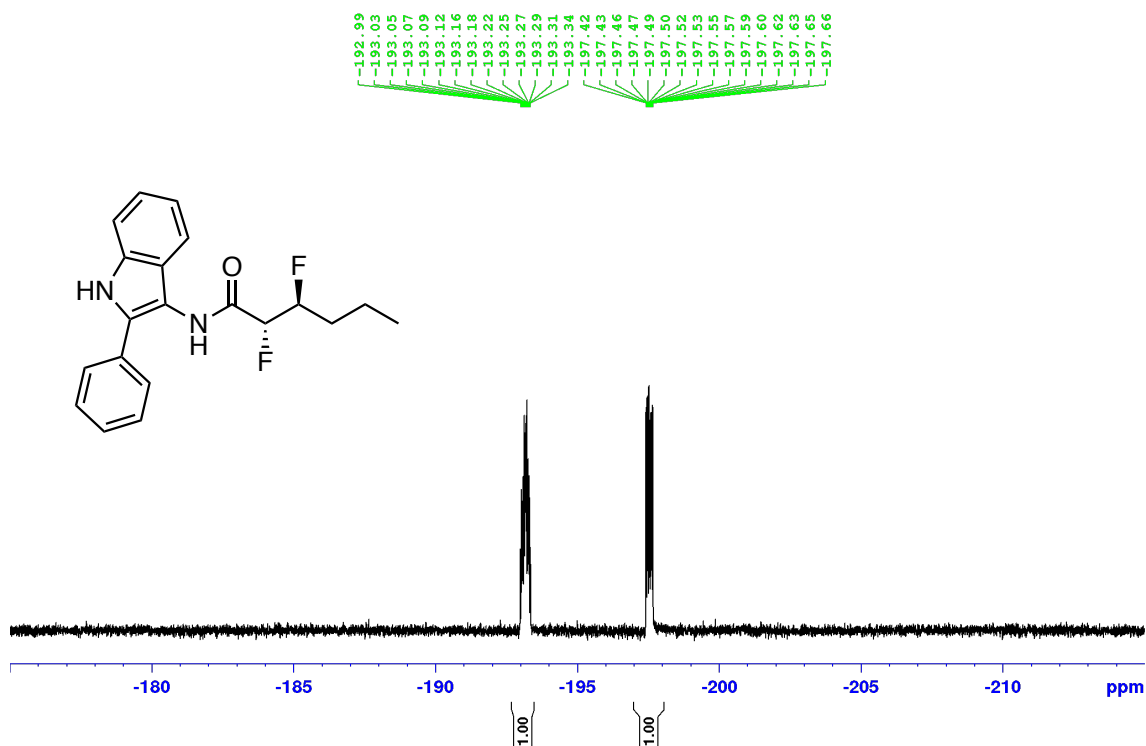
^1H NMR (400 MHz, CDCl_3) of **3e**



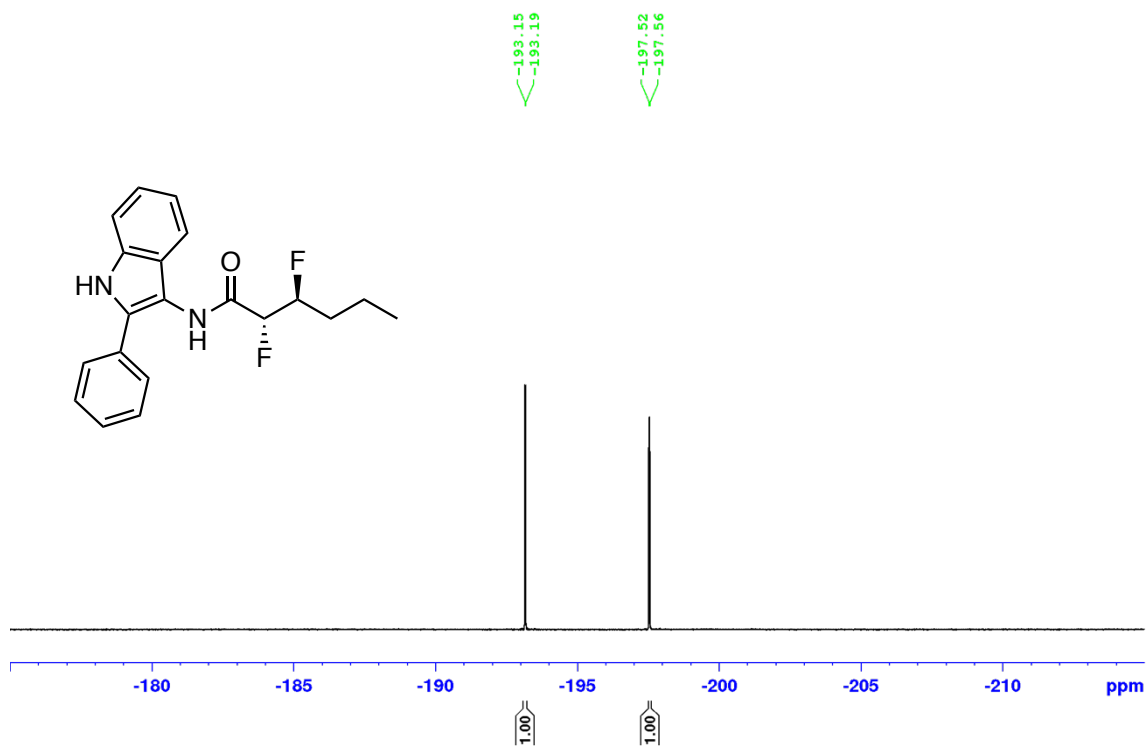
$^{13}\text{C}\{^1\text{H}\}$ NMR (101 MHz, CDCl_3) of **3e**



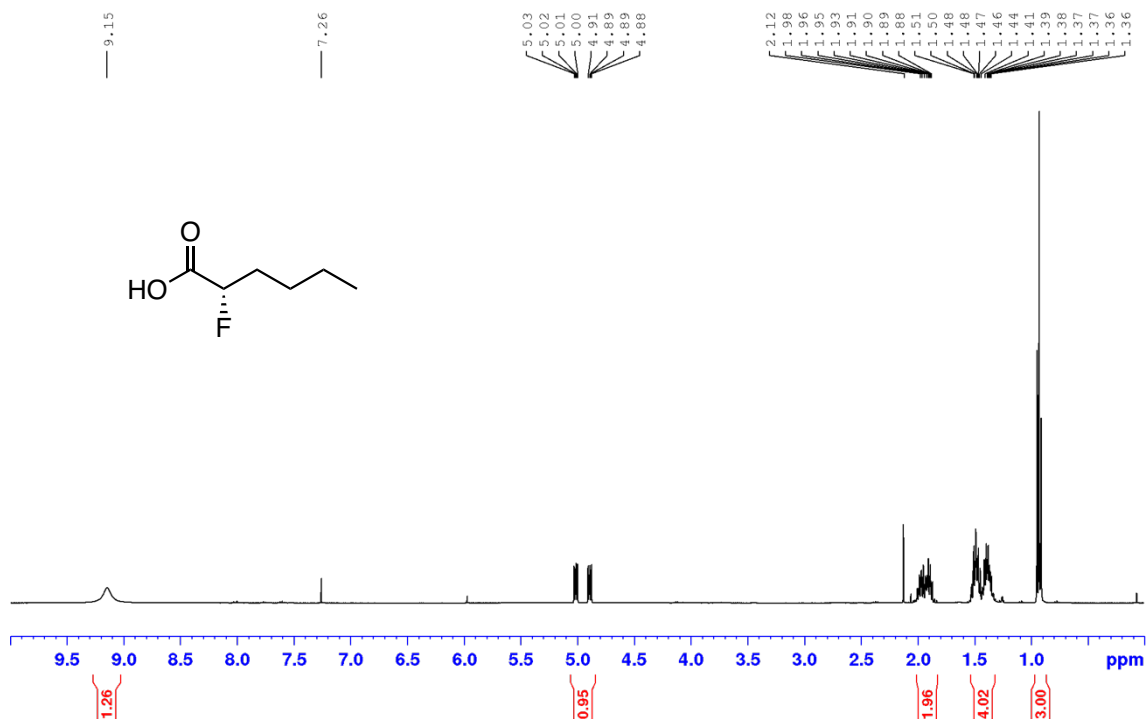
^{19}F NMR (377 MHz, CDCl_3) of **3e**



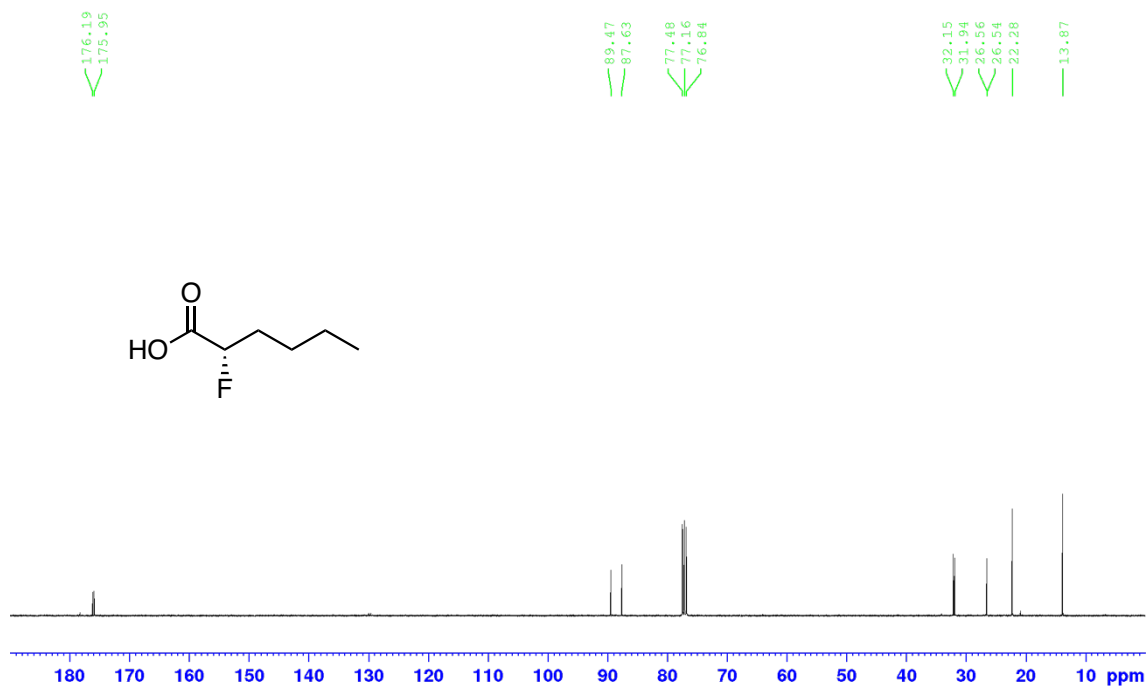
$^{19}\text{F}\{^1\text{H}\}$ NMR (377 MHz, CDCl_3) of **3e**



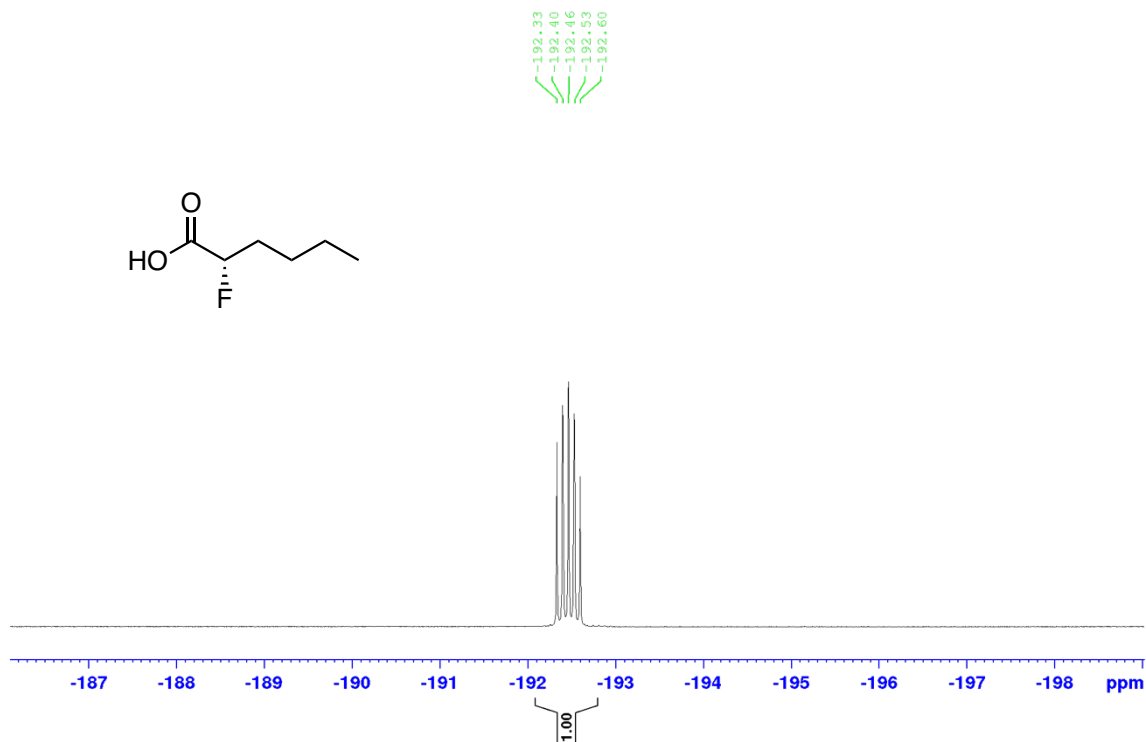
¹H NMR (400 MHz, CDCl₃) of 5



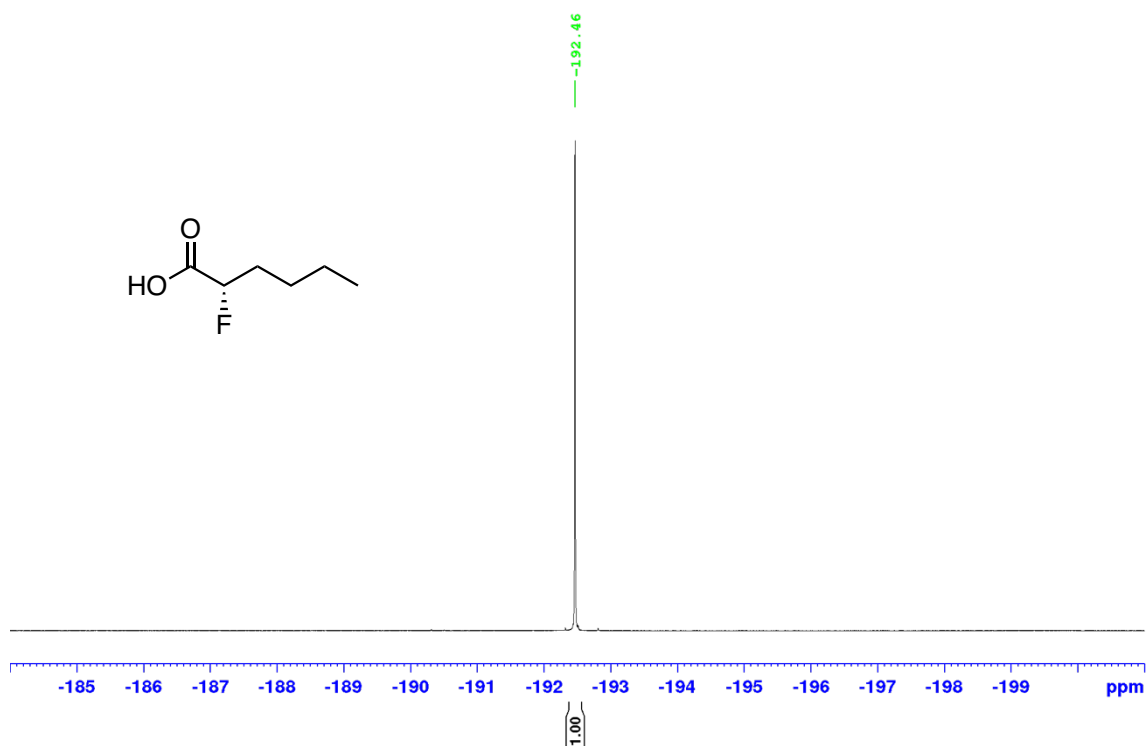
¹³C{¹H} NMR (101 MHz, CDCl₃) of 5



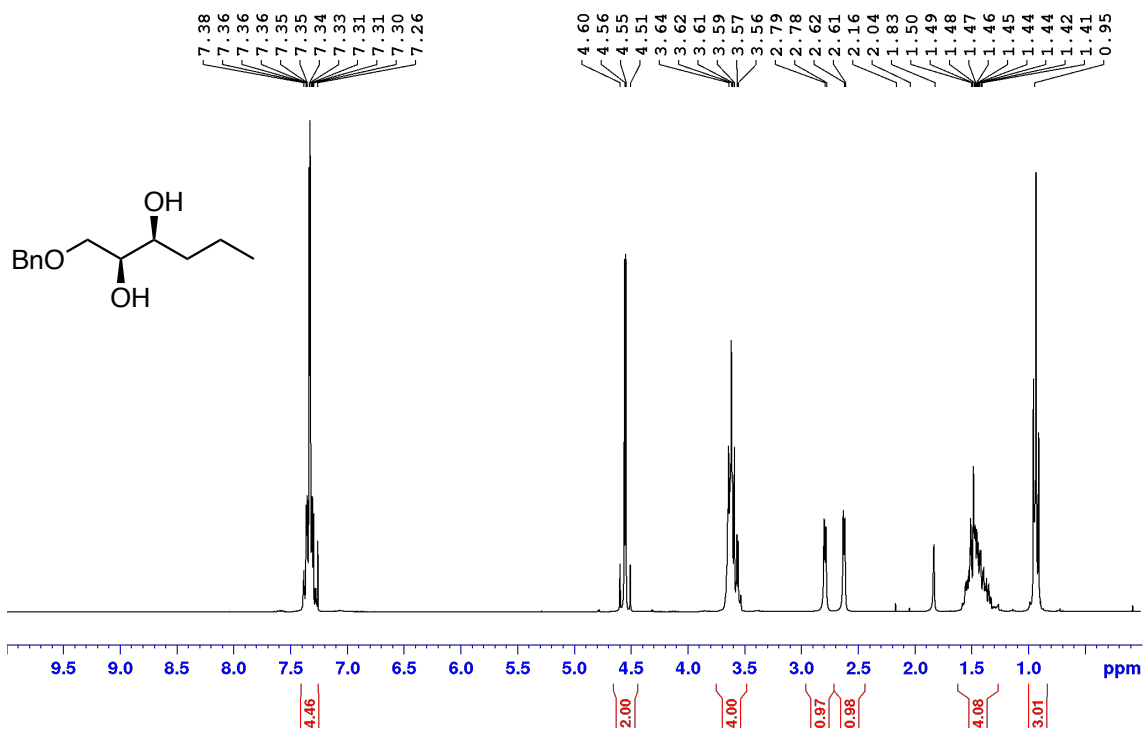
^{19}F NMR (376 MHz, CDCl_3) of **5**



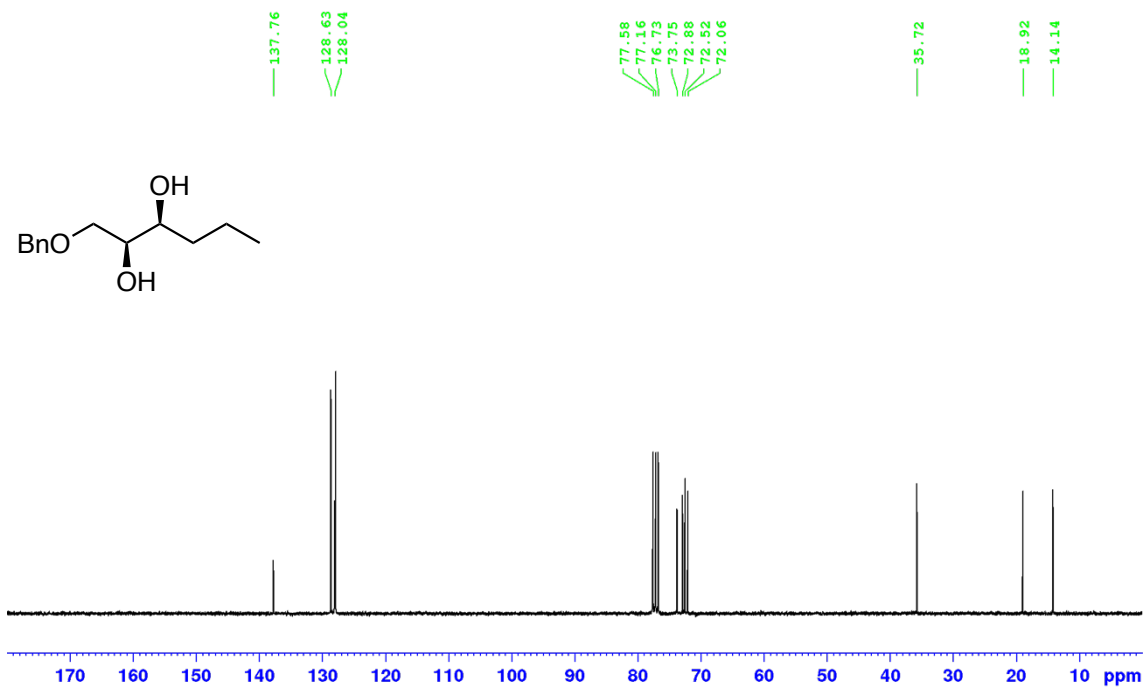
$^{19}\text{F}\{^1\text{H}\}$ NMR (376 MHz, CDCl_3) of **5**



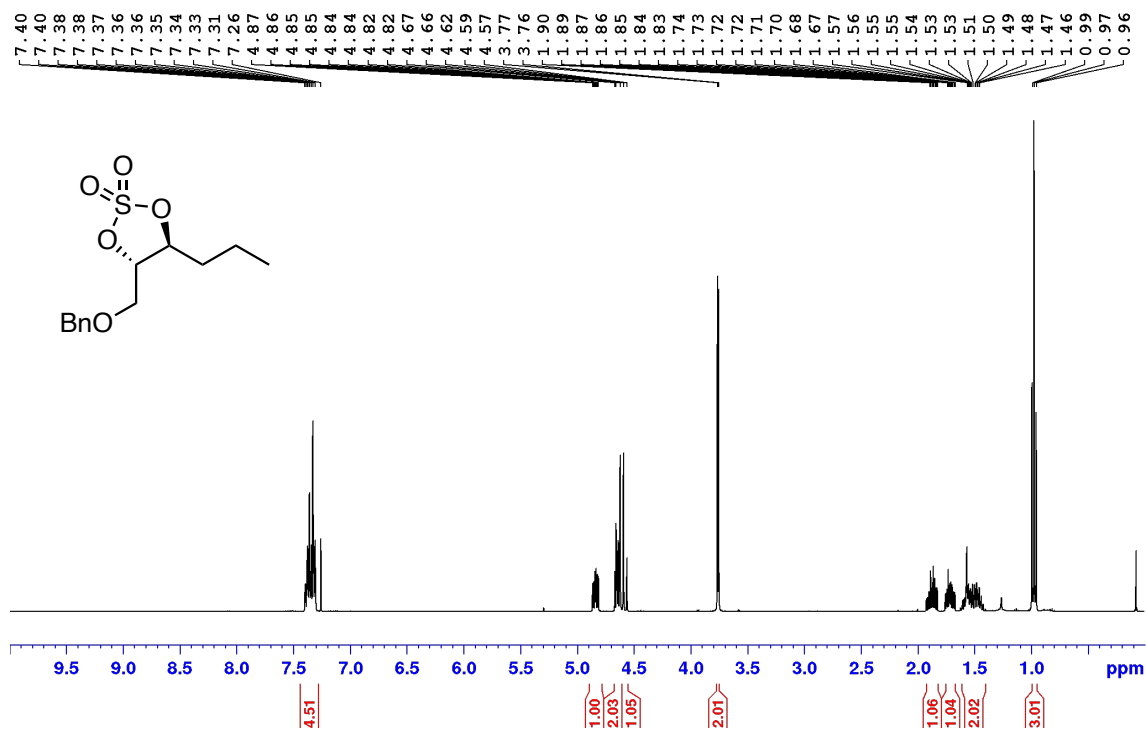
^1H NMR (300 MHz, CDCl_3) of **7**



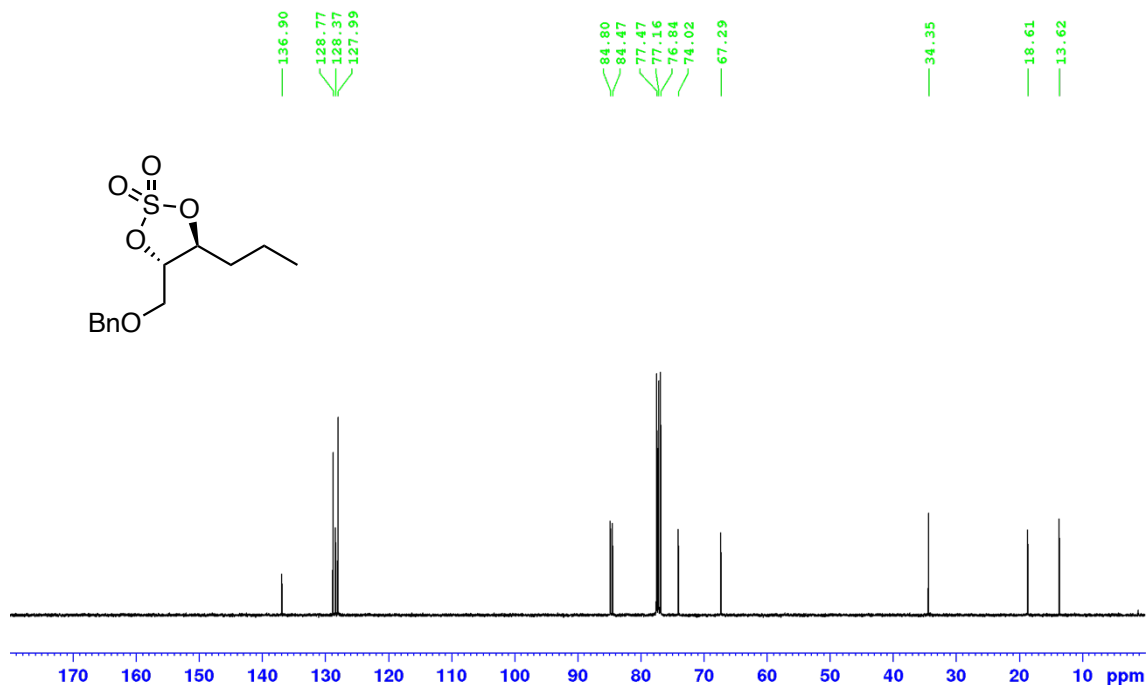
$^{13}\text{C}\{^1\text{H}\}$ NMR (76 MHz, CDCl_3) of **7**



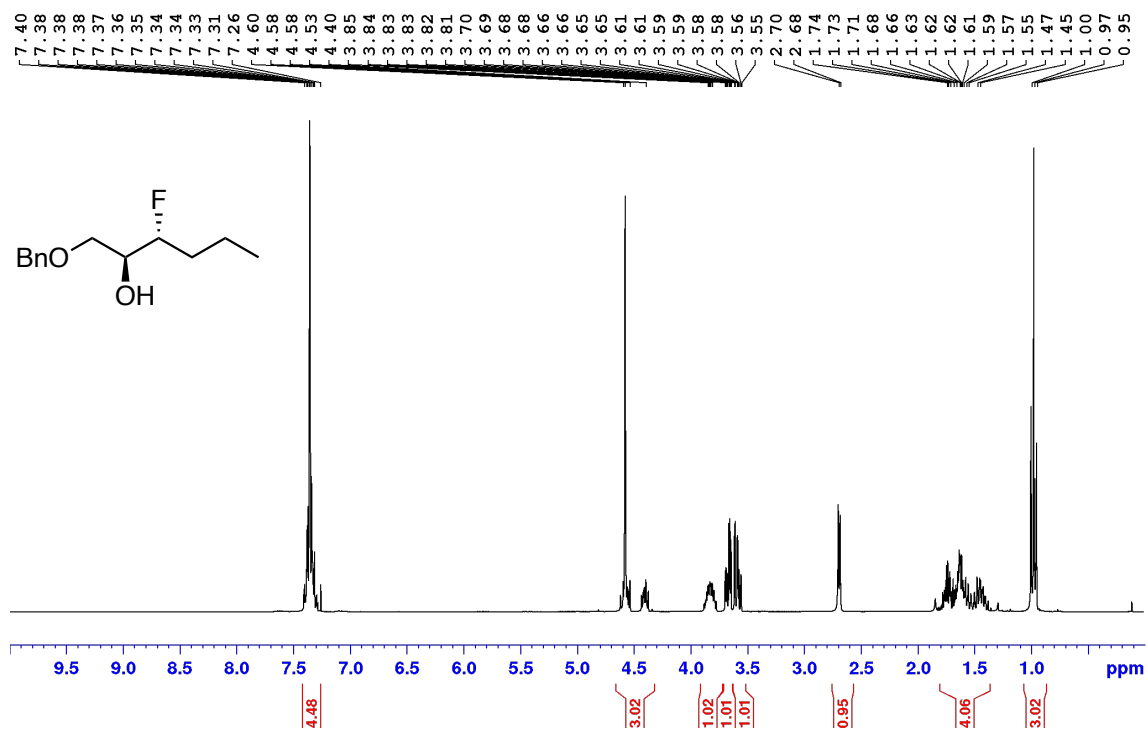
^1H NMR (400 MHz, CDCl_3) of **8**



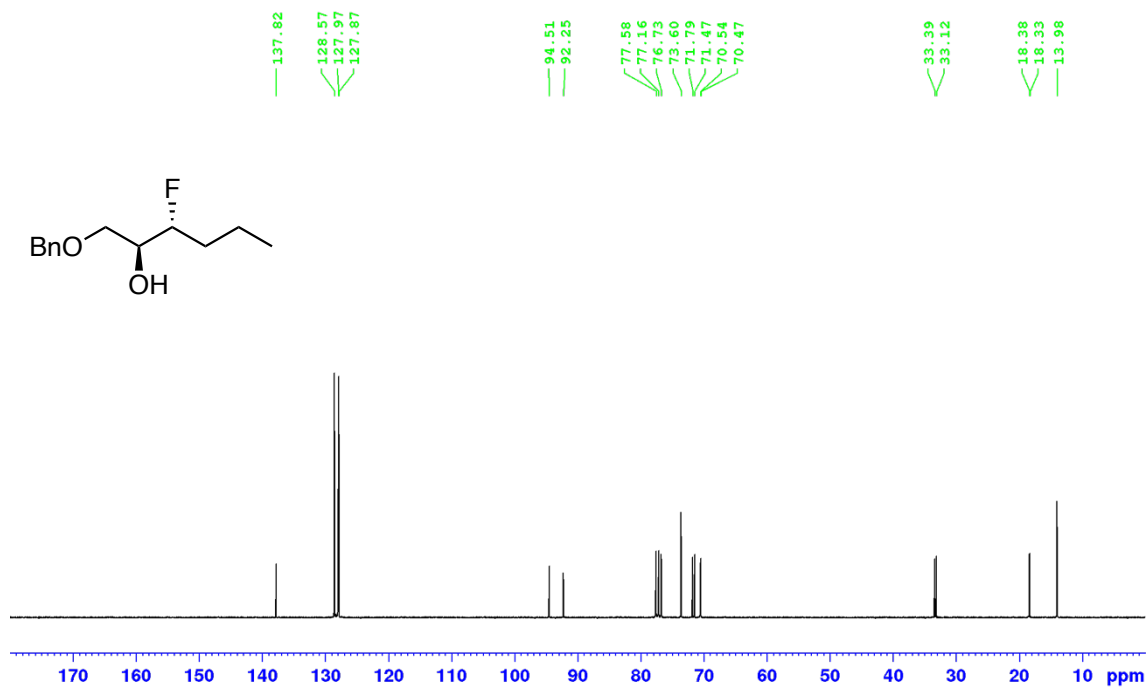
$^{13}\text{C}\{^1\text{H}\}$ NMR (101 MHz, CDCl_3) of **8**



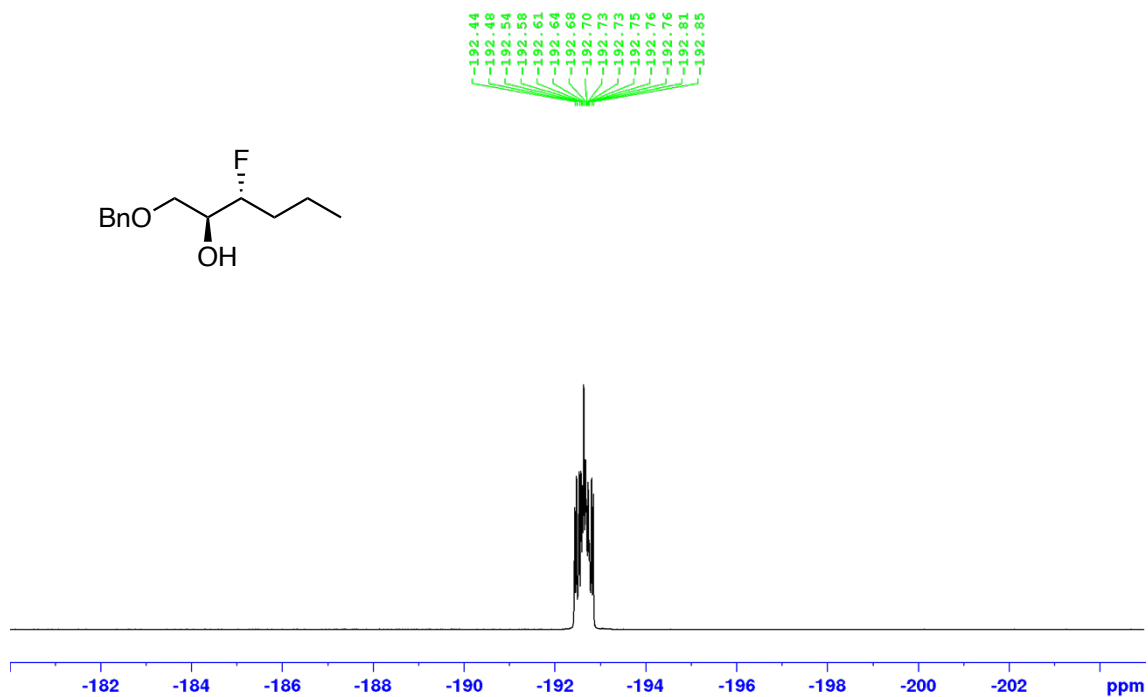
^1H NMR (300 MHz, CDCl_3) of **9**



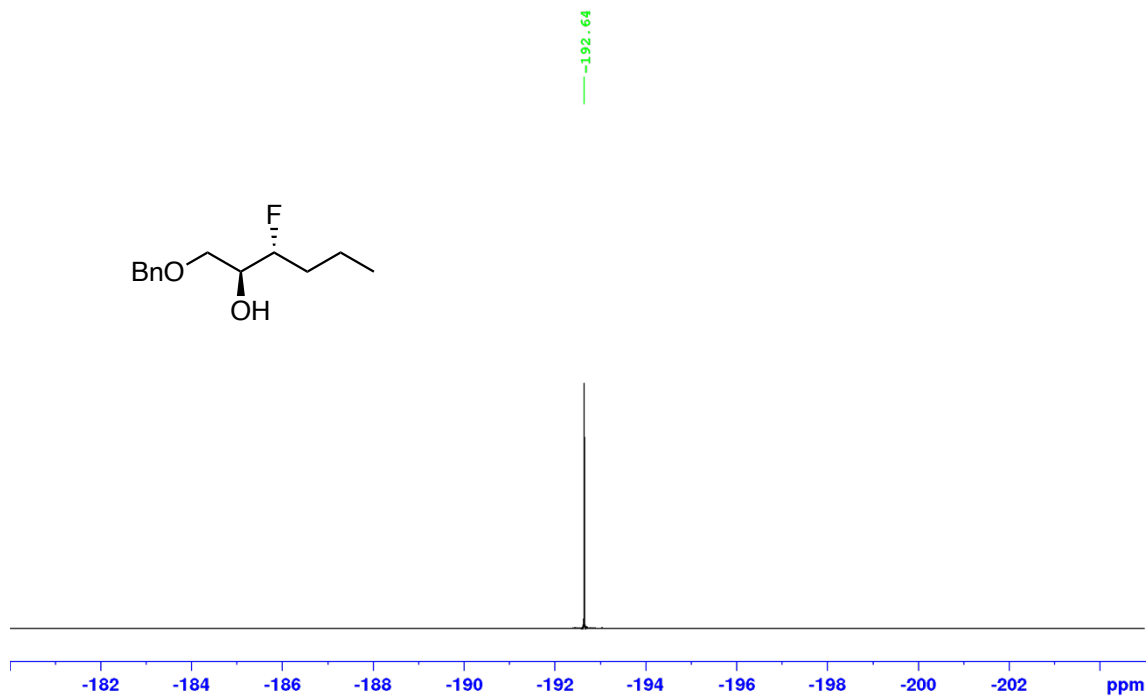
$^{13}\text{C}\{^1\text{H}\}$ NMR (76 MHz, CDCl_3) of **9**



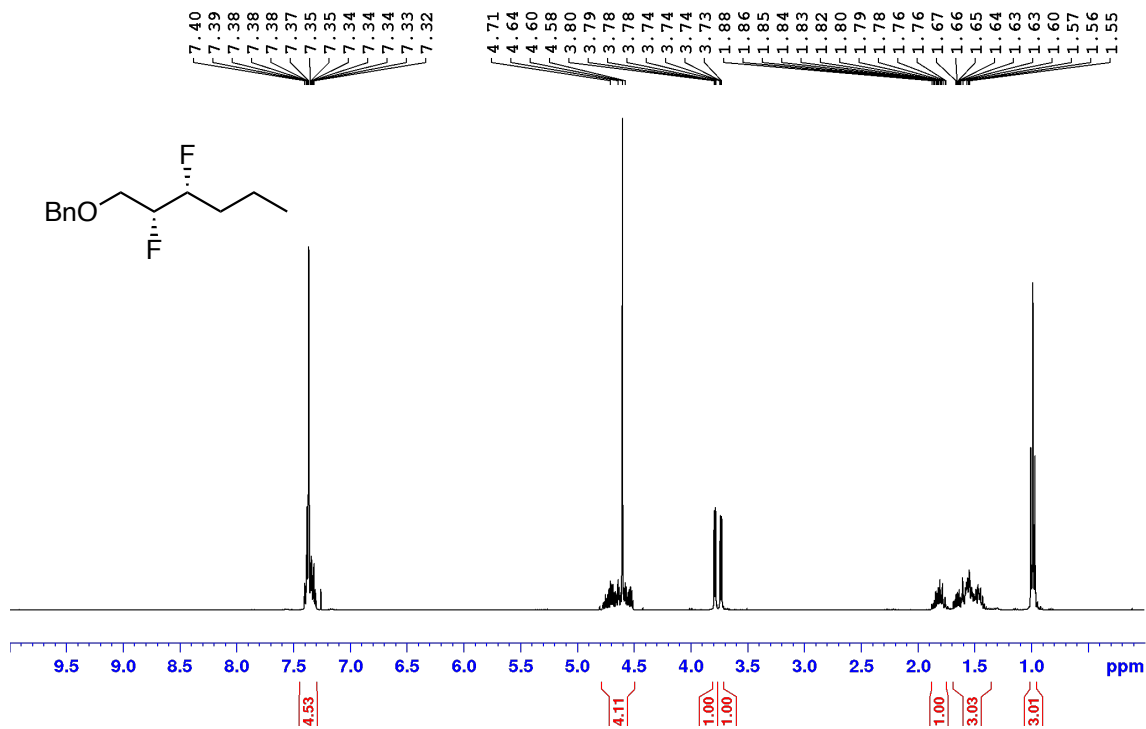
^{19}F NMR (283 MHz, CDCl_3) of **9**



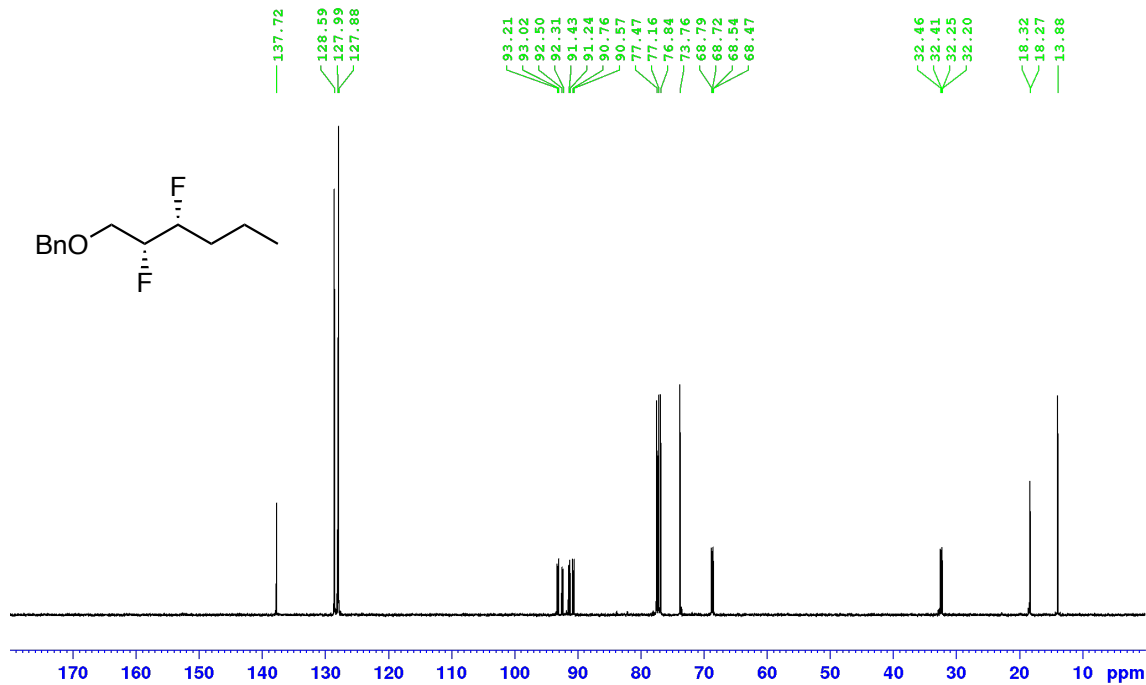
$^{19}\text{F}\{^1\text{H}\}$ NMR (283 MHz, CDCl_3) of **9**



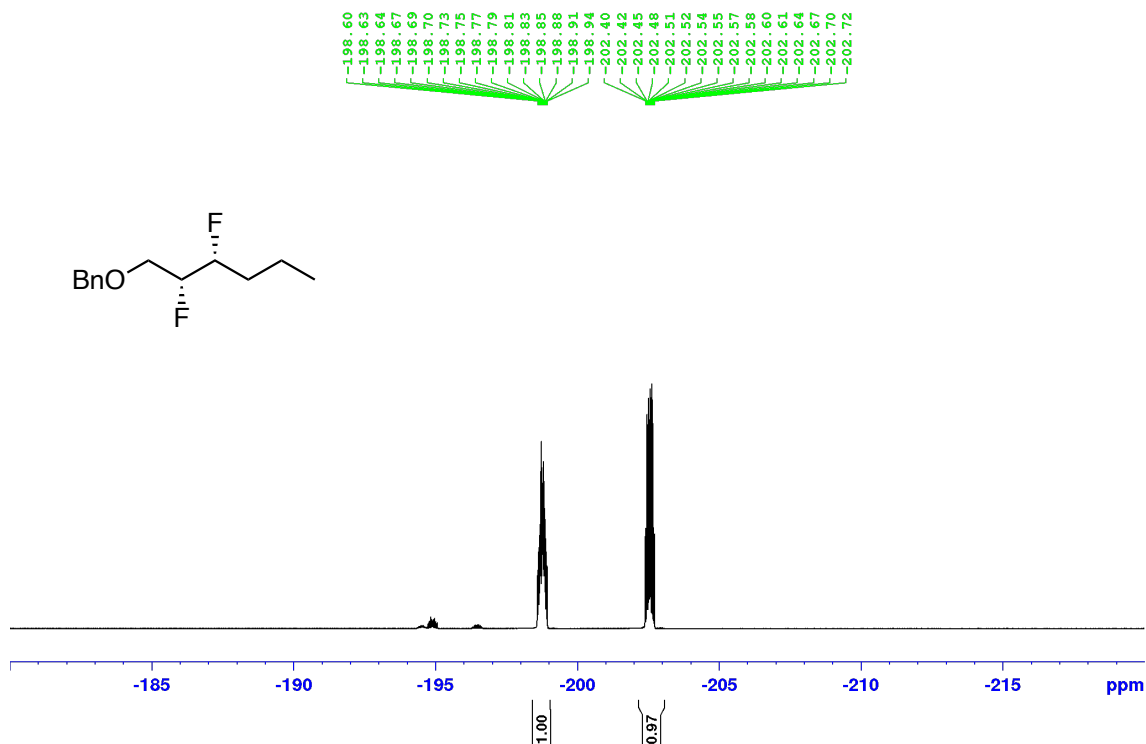
^1H NMR (400 MHz, CDCl_3) of **10**



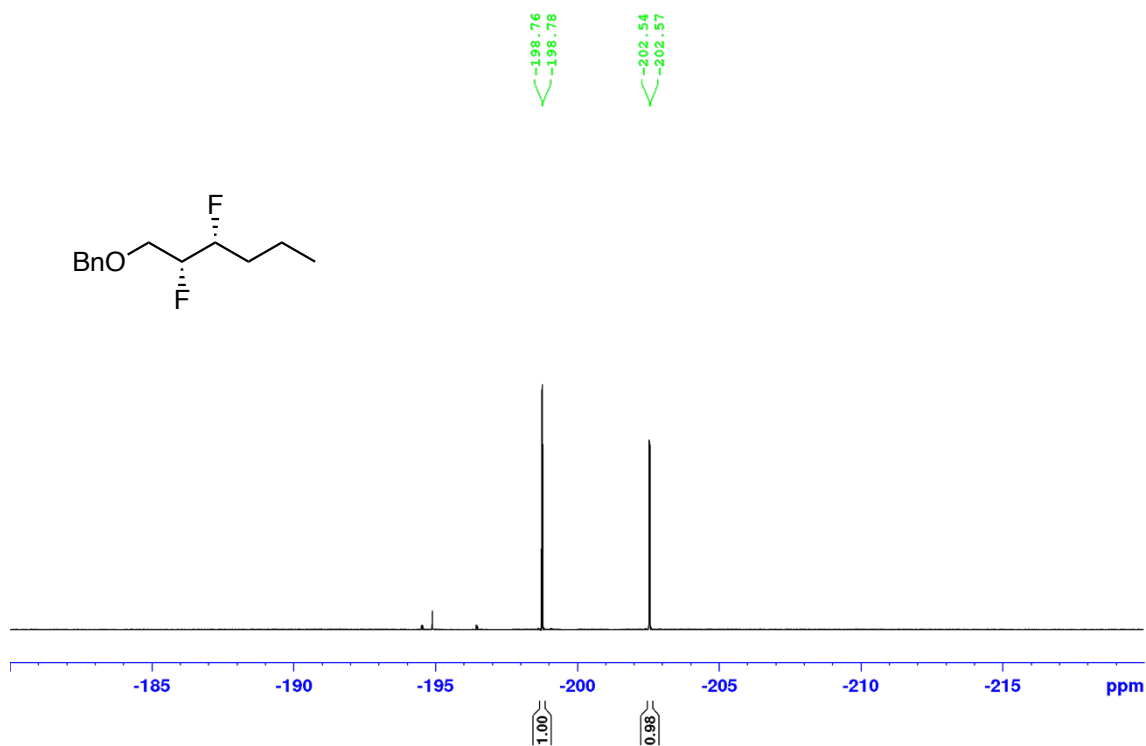
$^{13}\text{C}\{^1\text{H}\}$ NMR (101 MHz, CDCl_3) of **10**



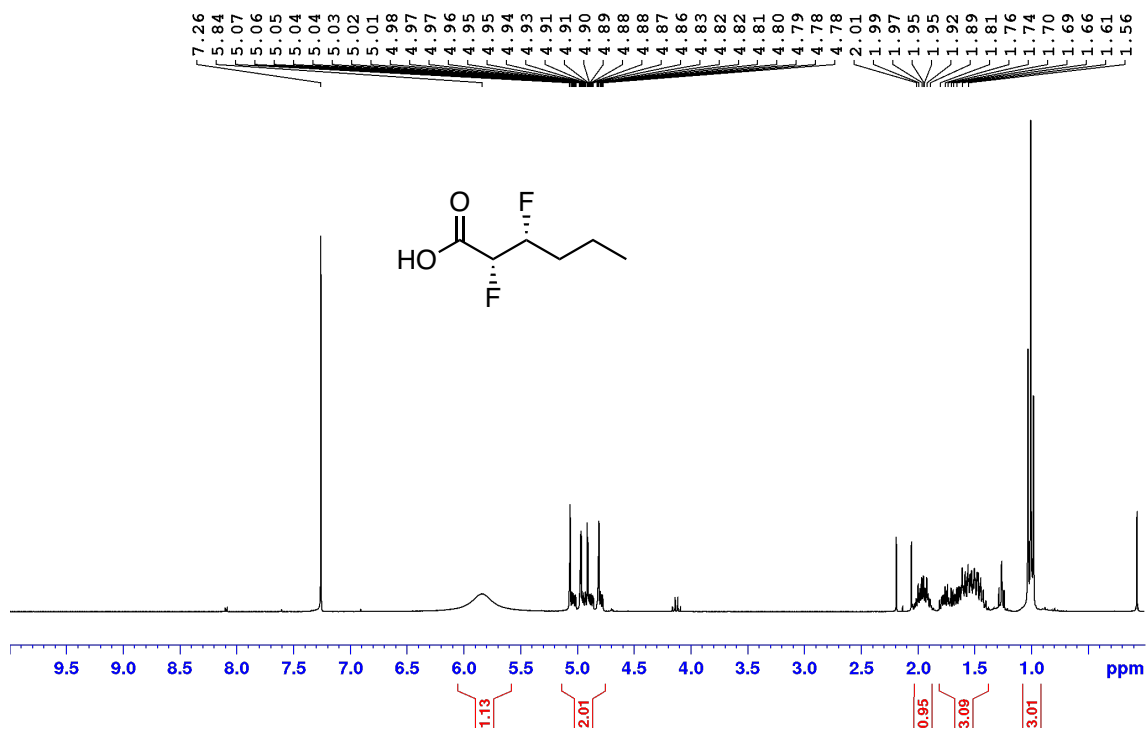
^{19}F NMR (377 MHz, CDCl_3) of **10**



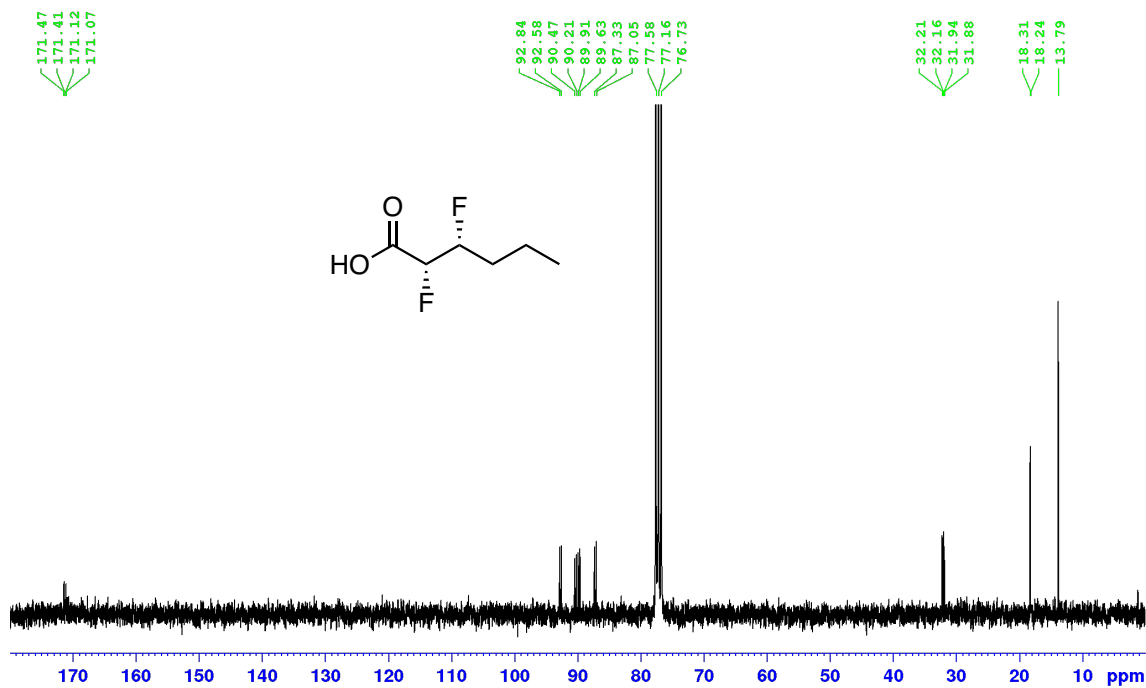
$^{19}\text{F}\{^1\text{H}\}$ NMR (377 MHz, CDCl_3) of **10**



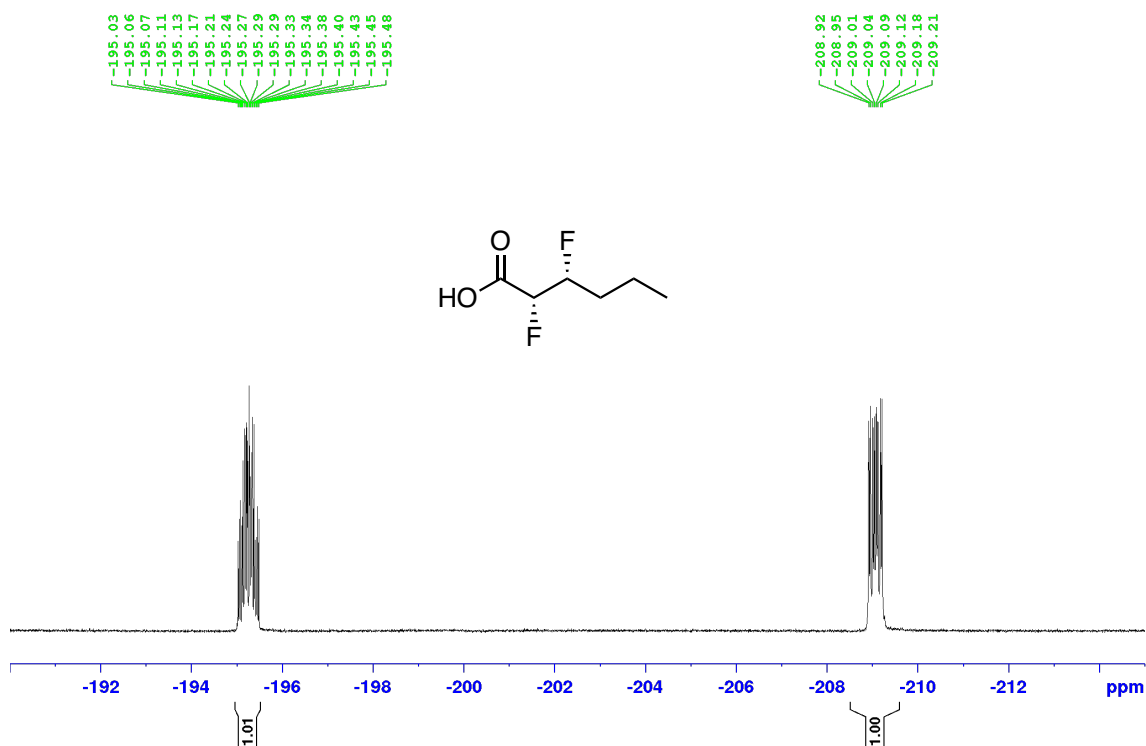
¹H NMR (300 MHz, CDCl₃) of 11



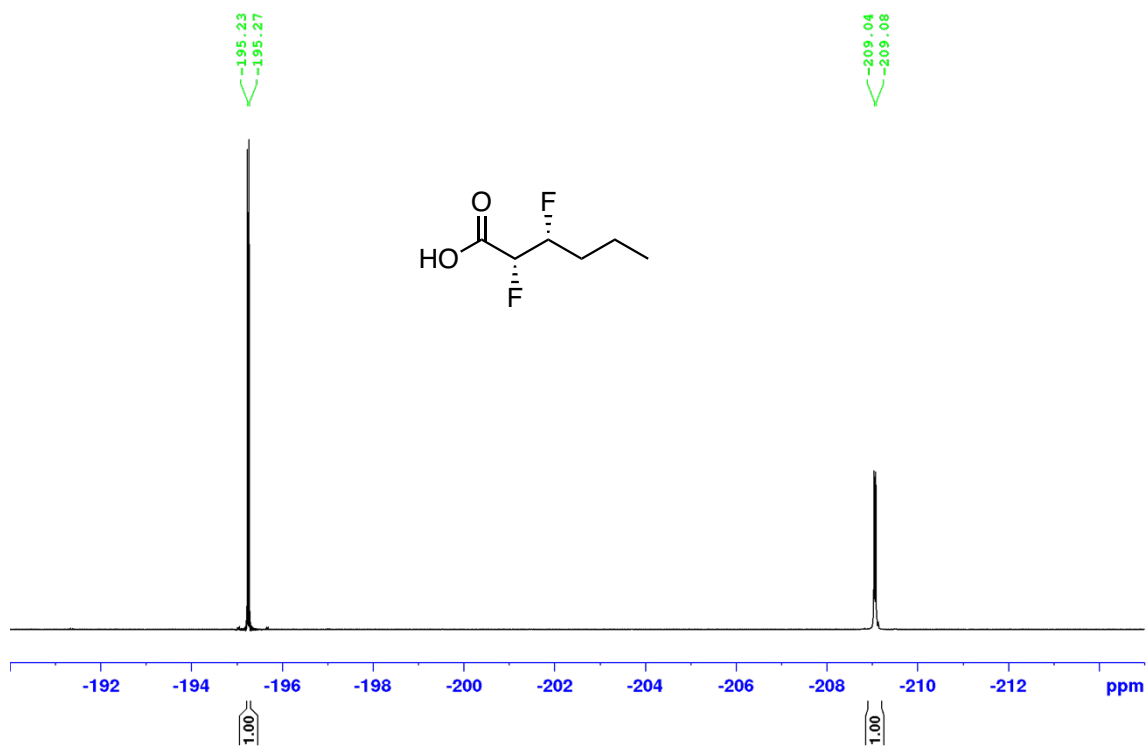
¹³C{¹H} NMR (76 MHz, CDCl₃) of 11



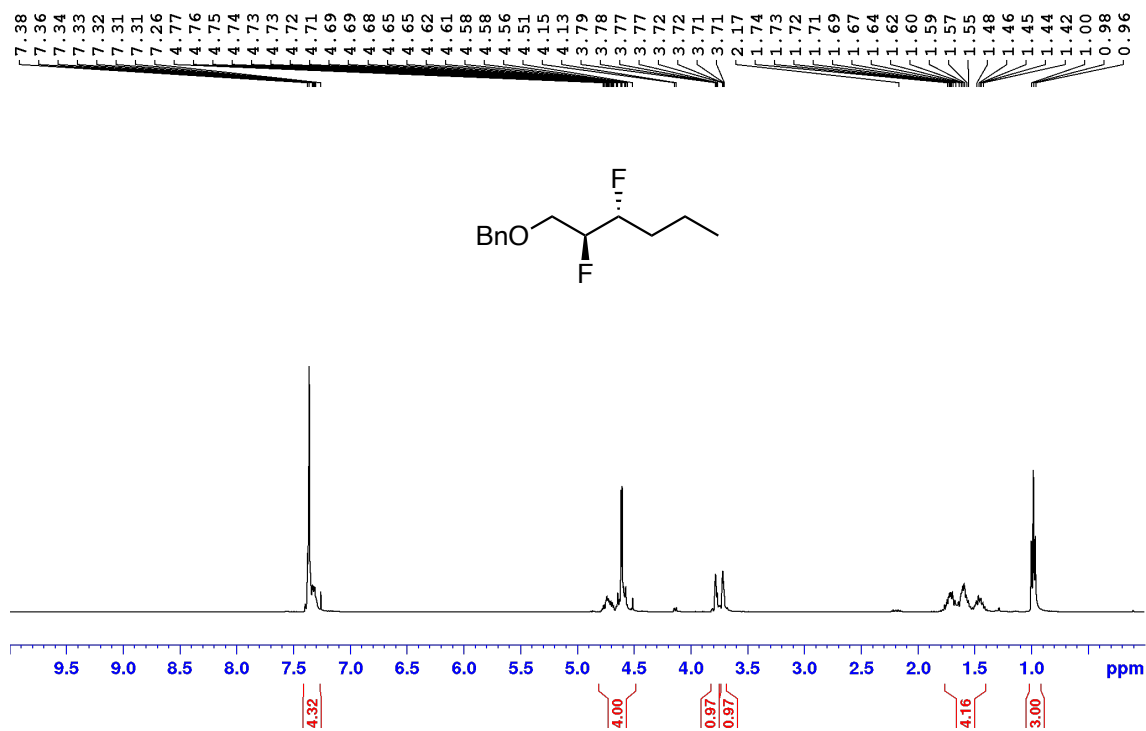
¹⁹F NMR (283 MHz, CDCl₃) of 11



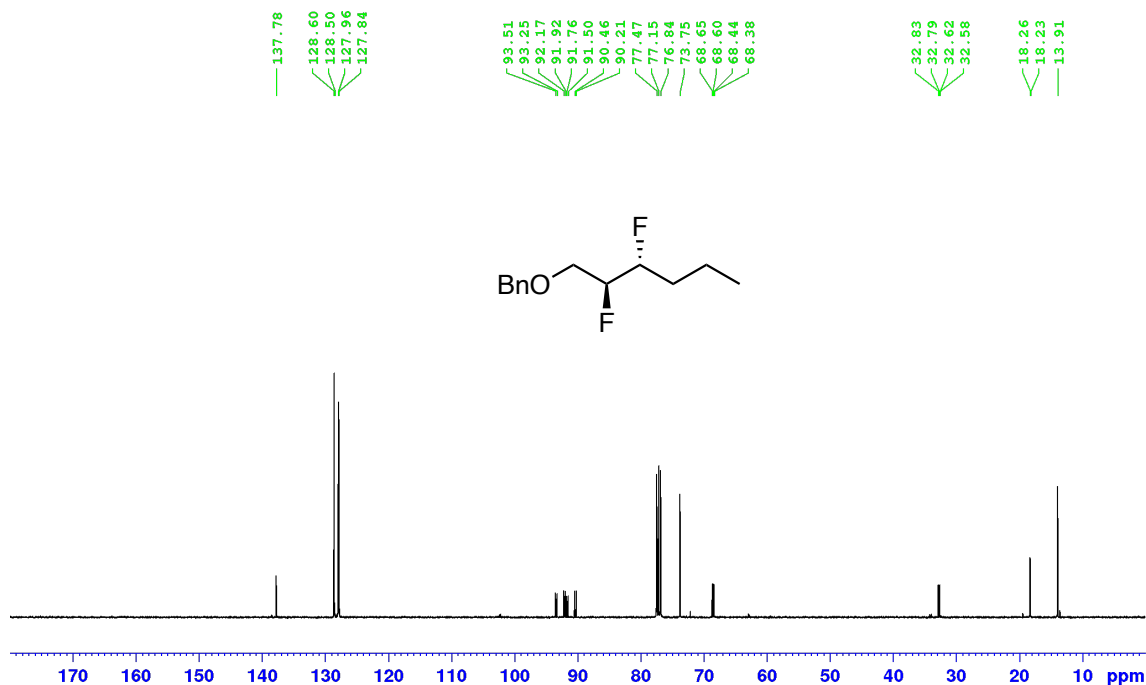
¹⁹F NMR (283 MHz, CDCl₃) of 11



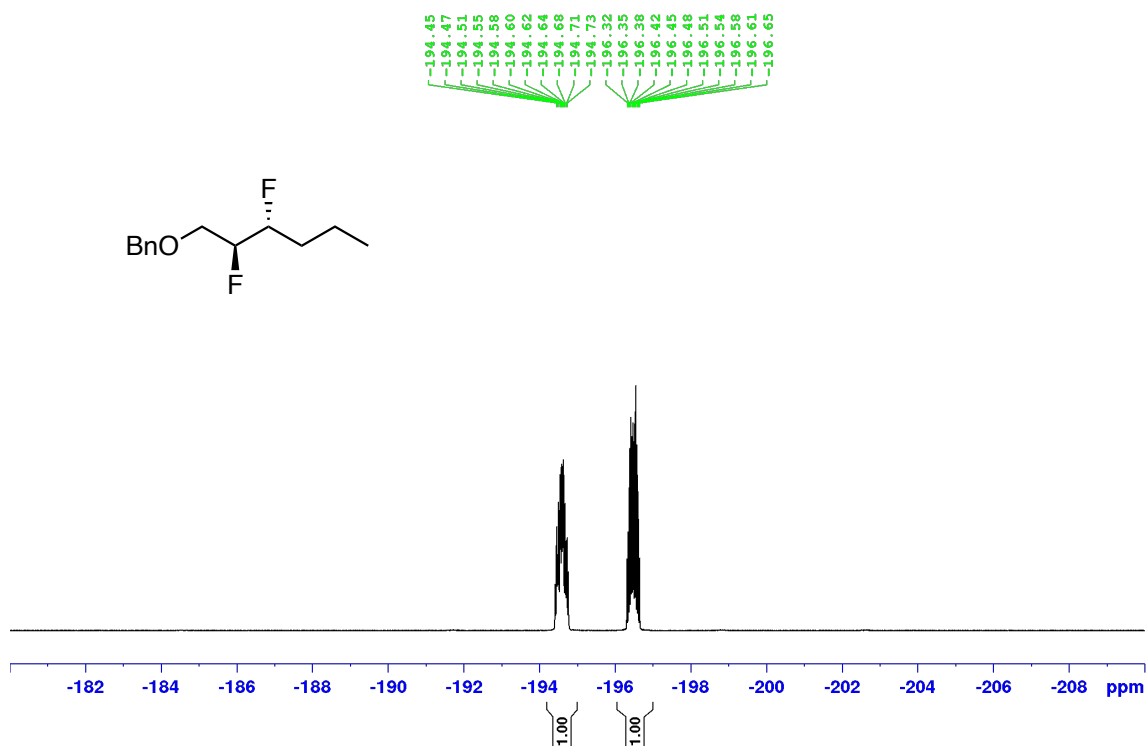
^1H NMR (400 MHz, CDCl_3) of **12**



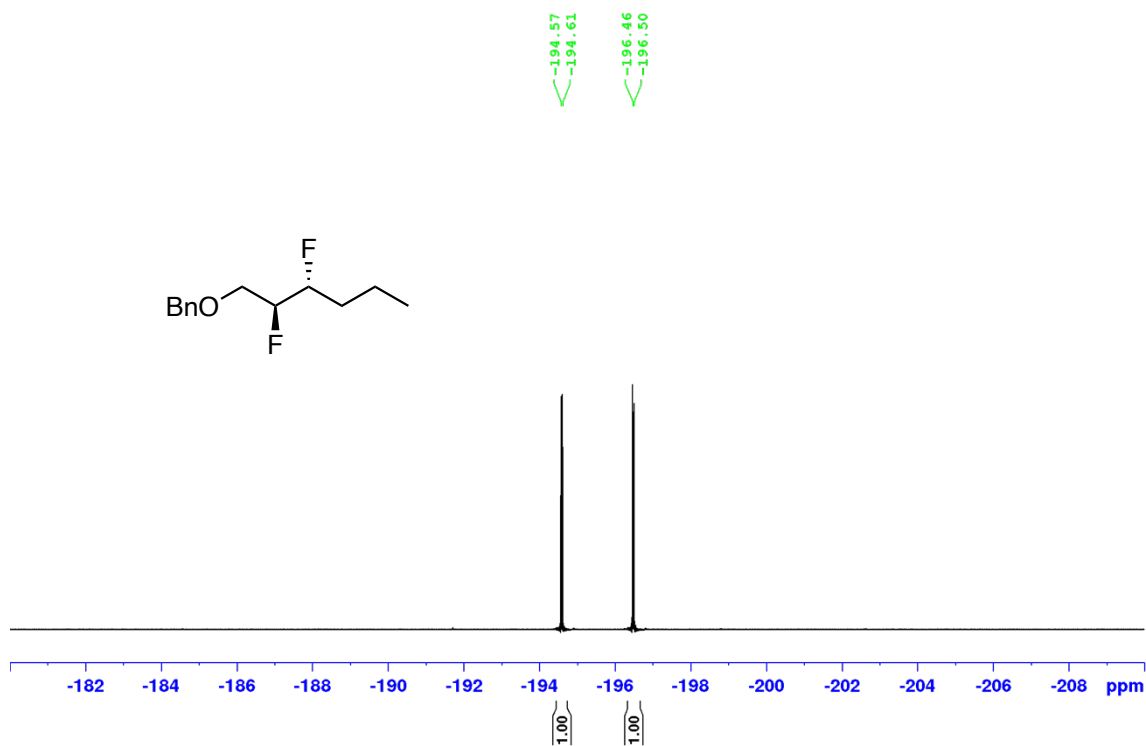
$^{13}\text{C}\{^1\text{H}\}$ NMR (101 MHz, CDCl_3) of **12**



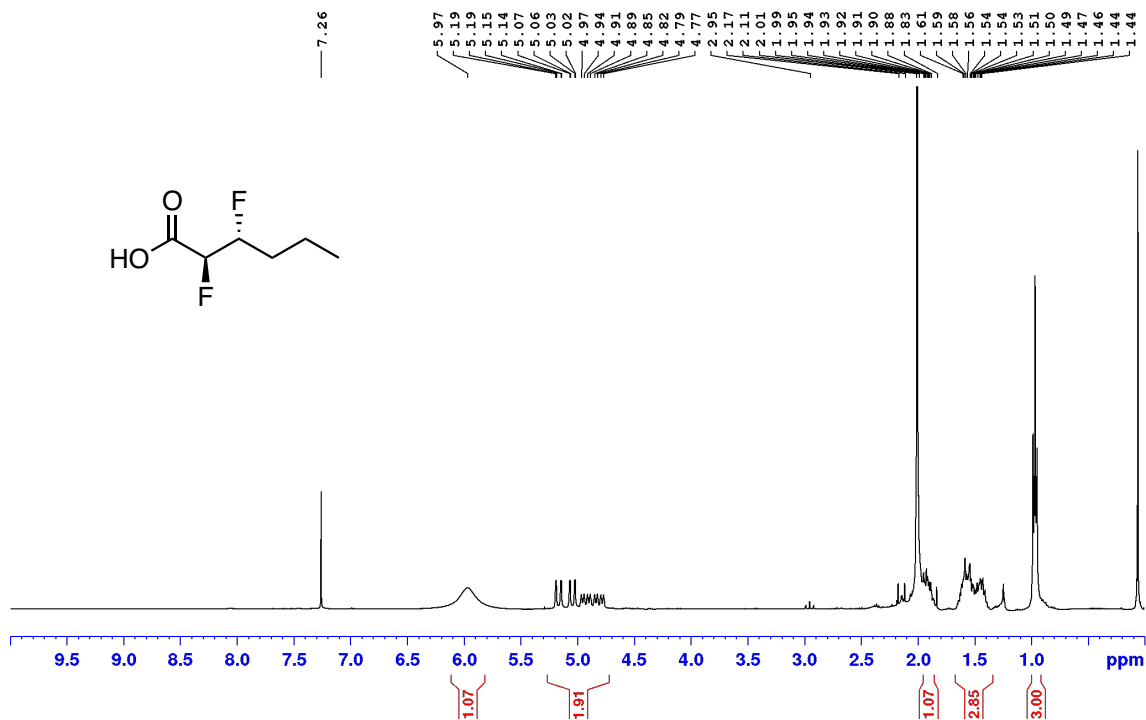
^{19}F NMR (377 MHz, CDCl_3) of **12**



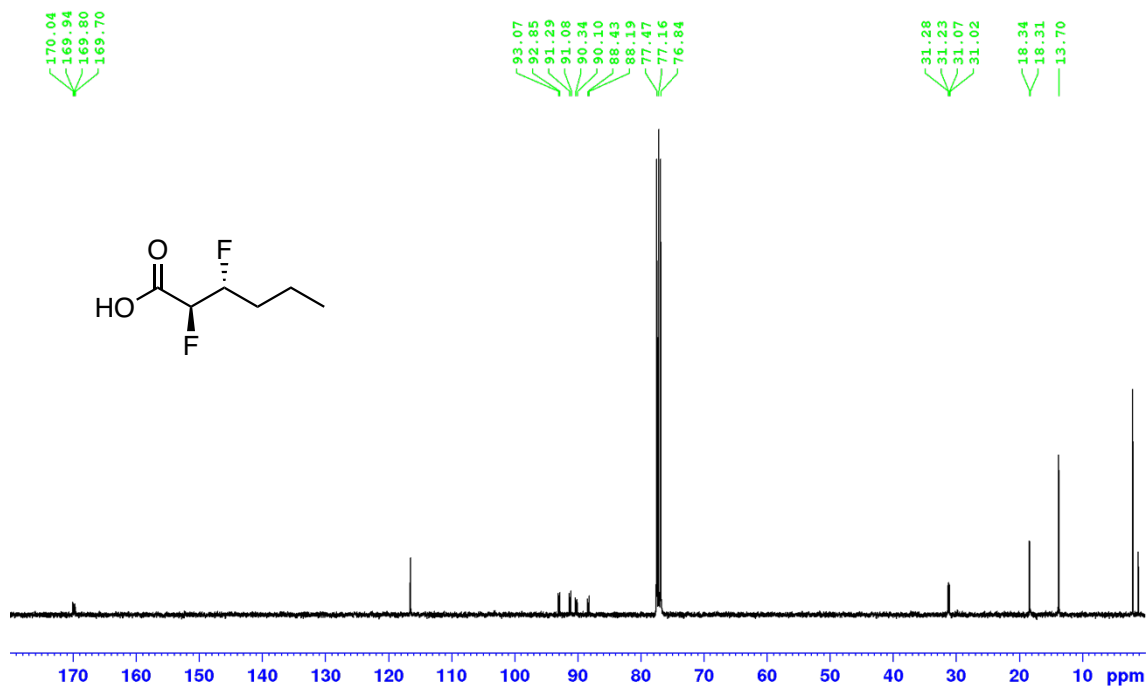
$^{19}\text{F}\{^1\text{H}\}$ NMR (377 MHz, CDCl_3) of **12**



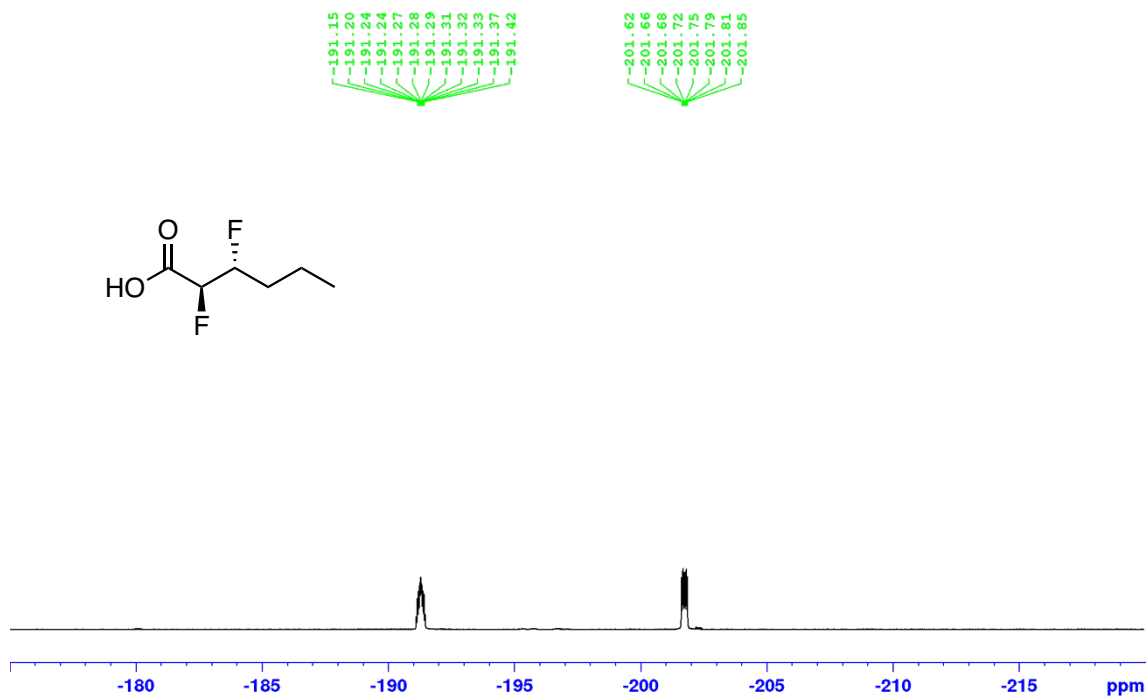
^1H NMR (400 MHz, CDCl_3) of **13**



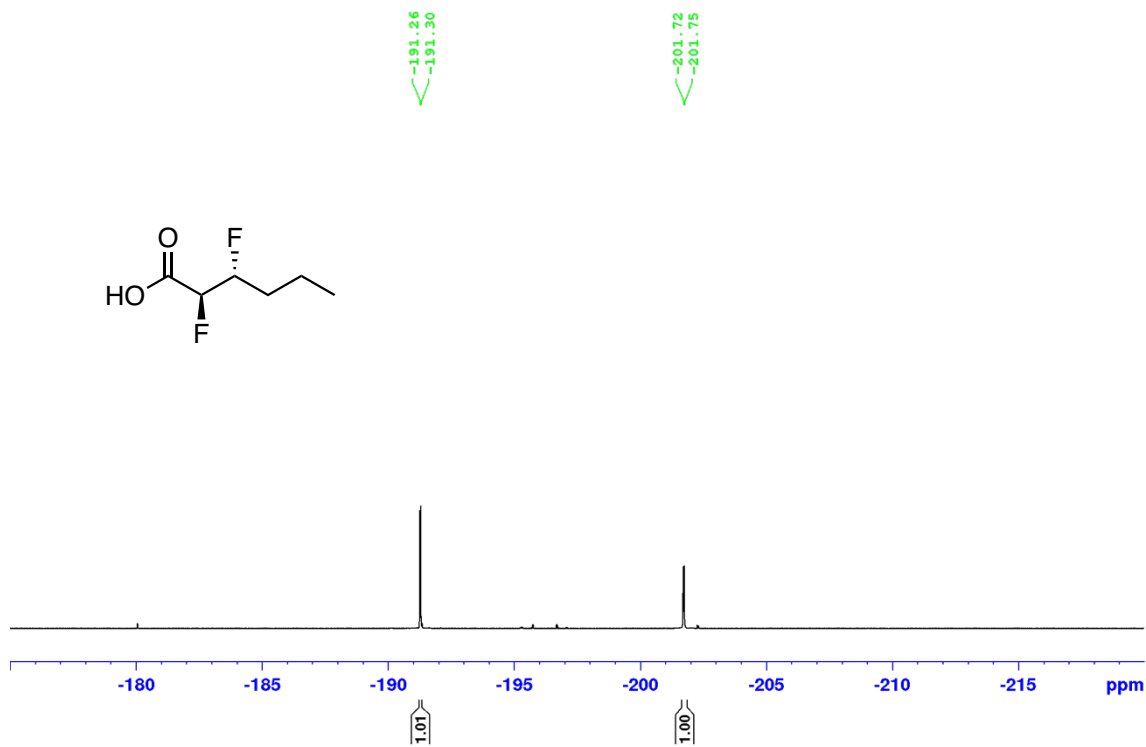
$^{13}\text{C}\{^1\text{H}\}$ NMR (101 MHz, CDCl_3) of **13**



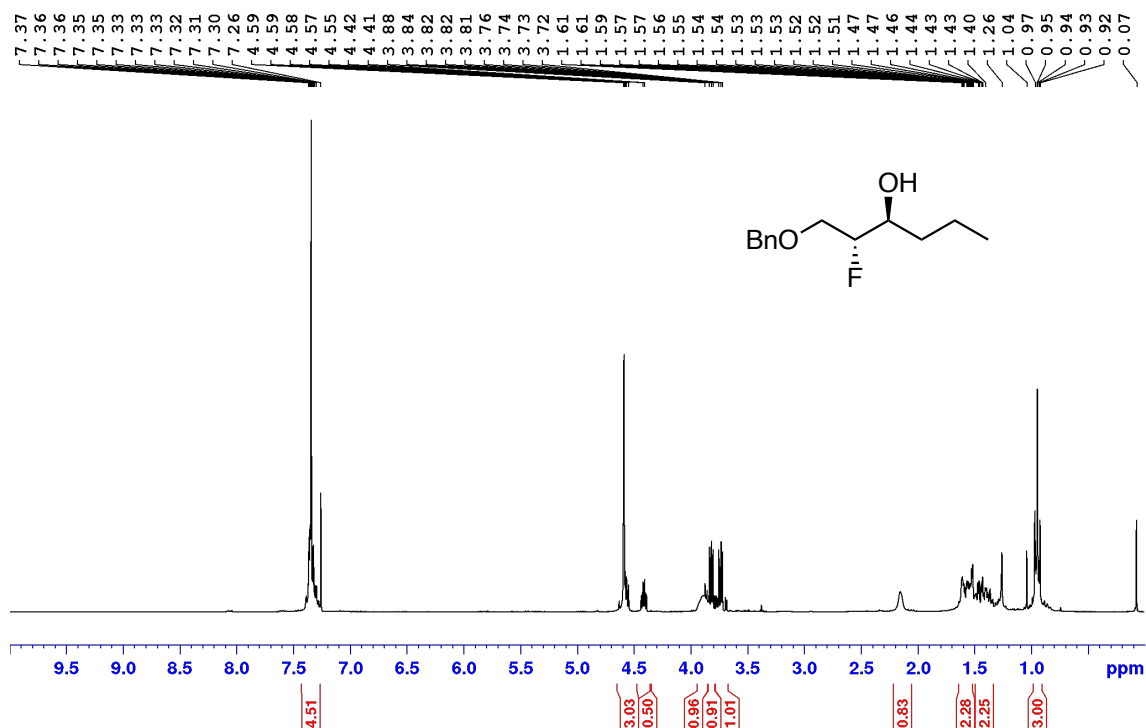
^{19}F NMR (377 MHz, CDCl_3) of **13**



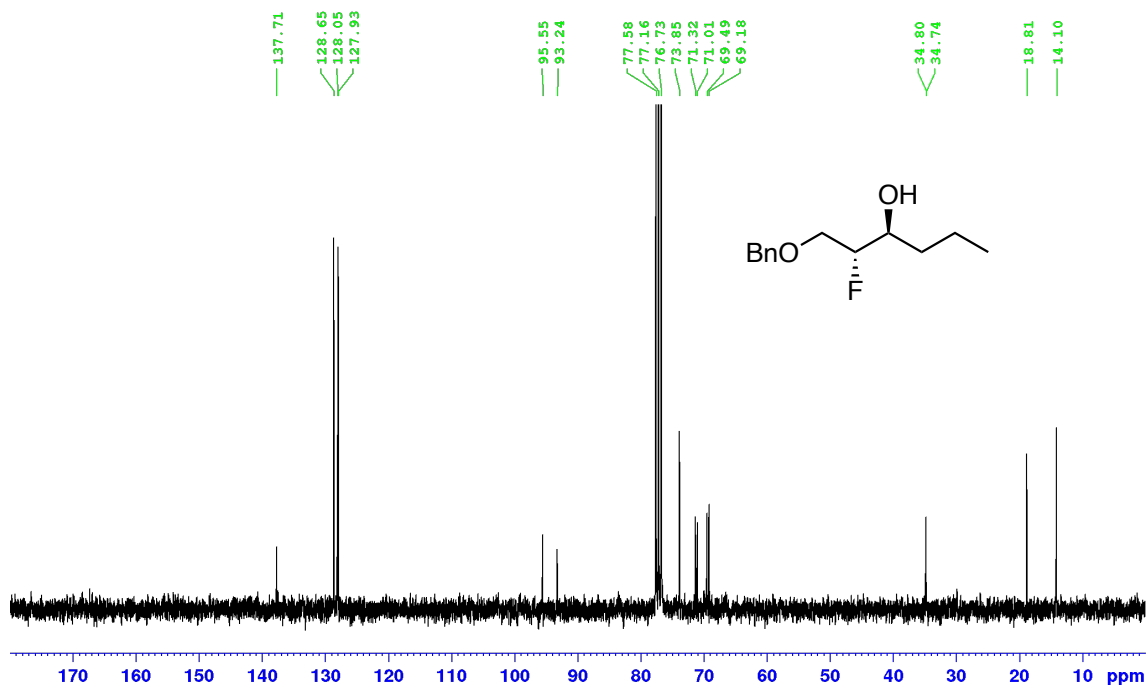
$^{19}\text{F}\{^1\text{H}\}$ NMR (377 MHz, CDCl_3) of **13**



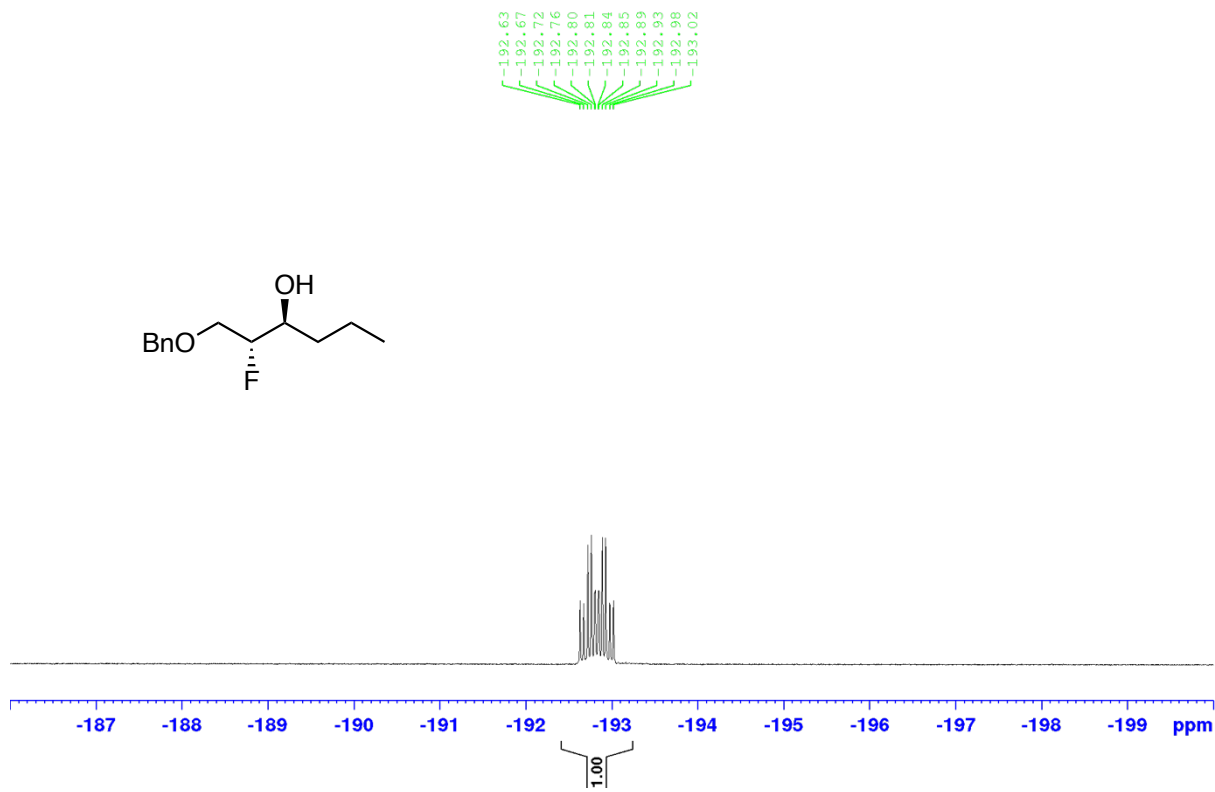
^1H NMR (300 MHz, CDCl_3) of **15**



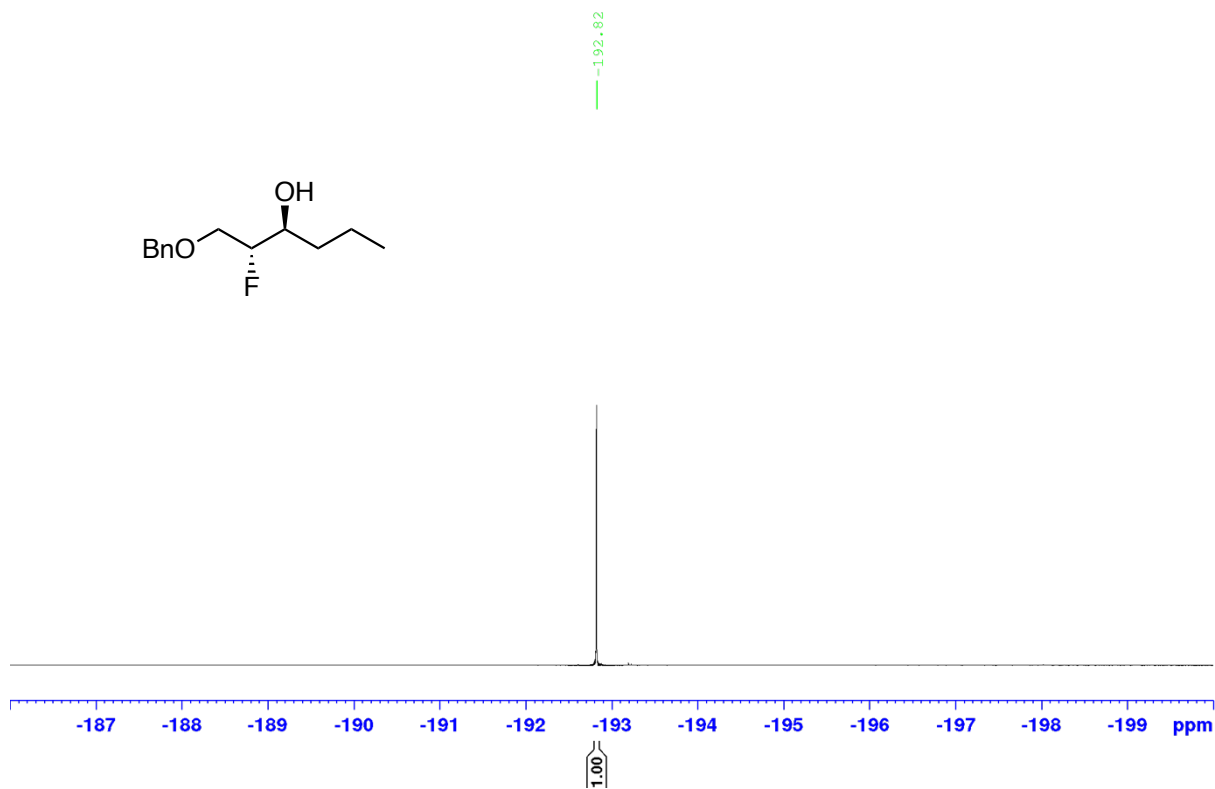
$^{13}\text{C}\{^1\text{H}\}$ NMR (76 MHz, CDCl_3) of **15**



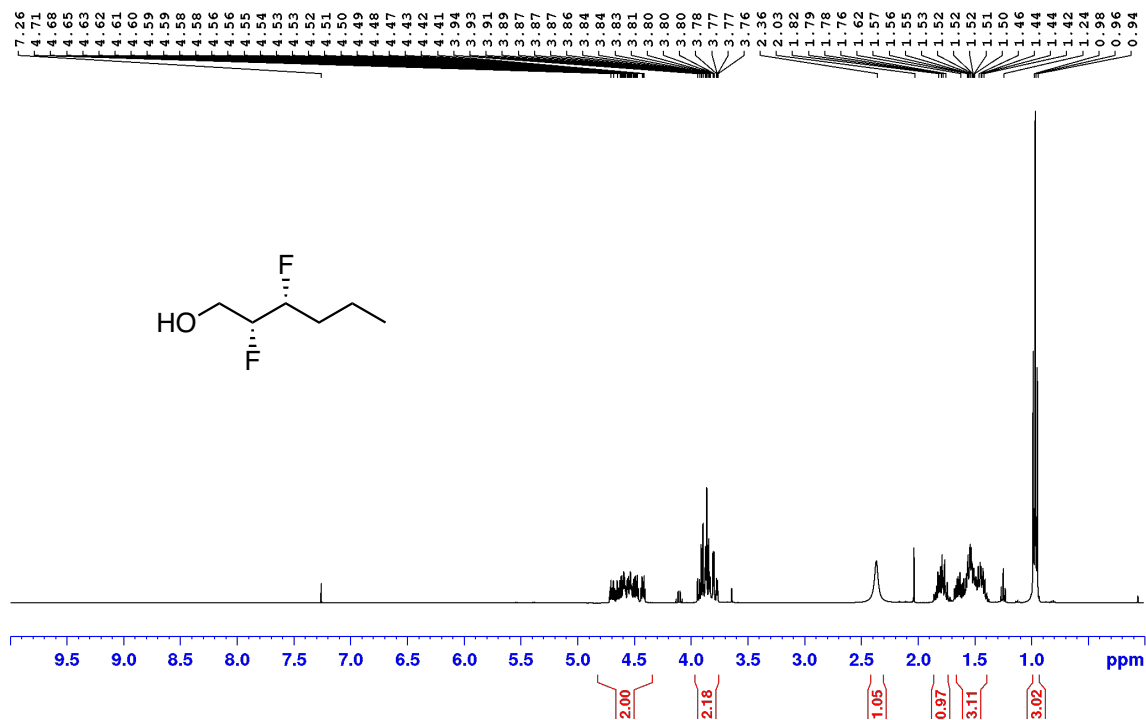
¹⁹F NMR (283 MHz, CDCl₃) of 15



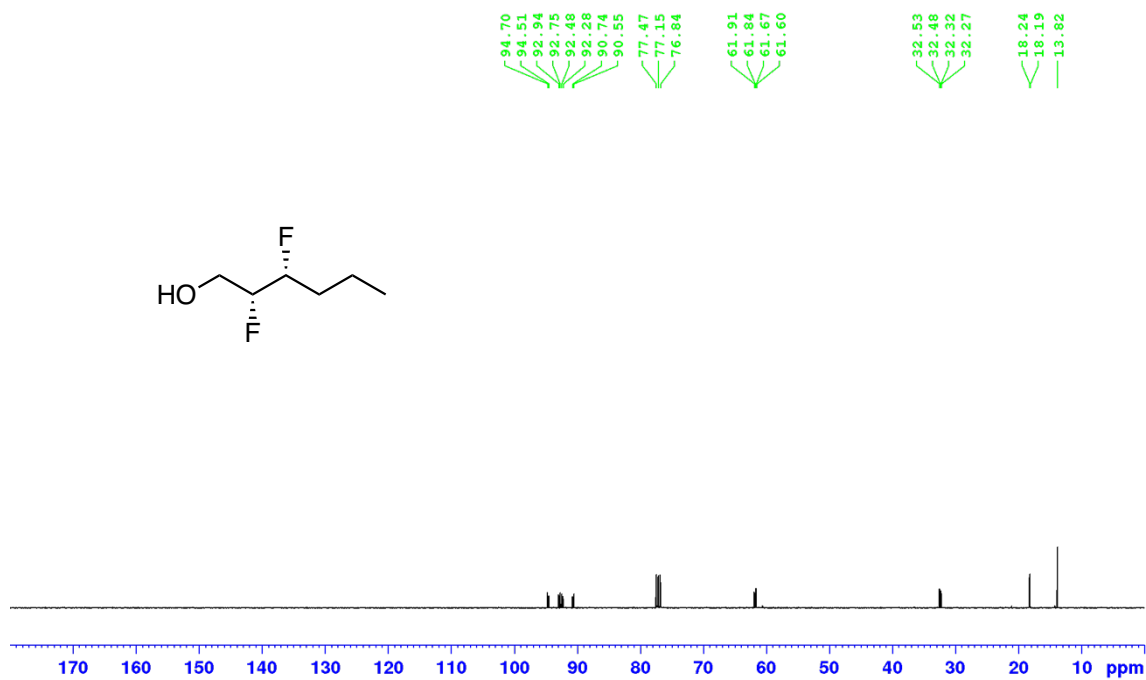
¹⁹F{¹H} NMR (283 MHz, CDCl₃) of 15



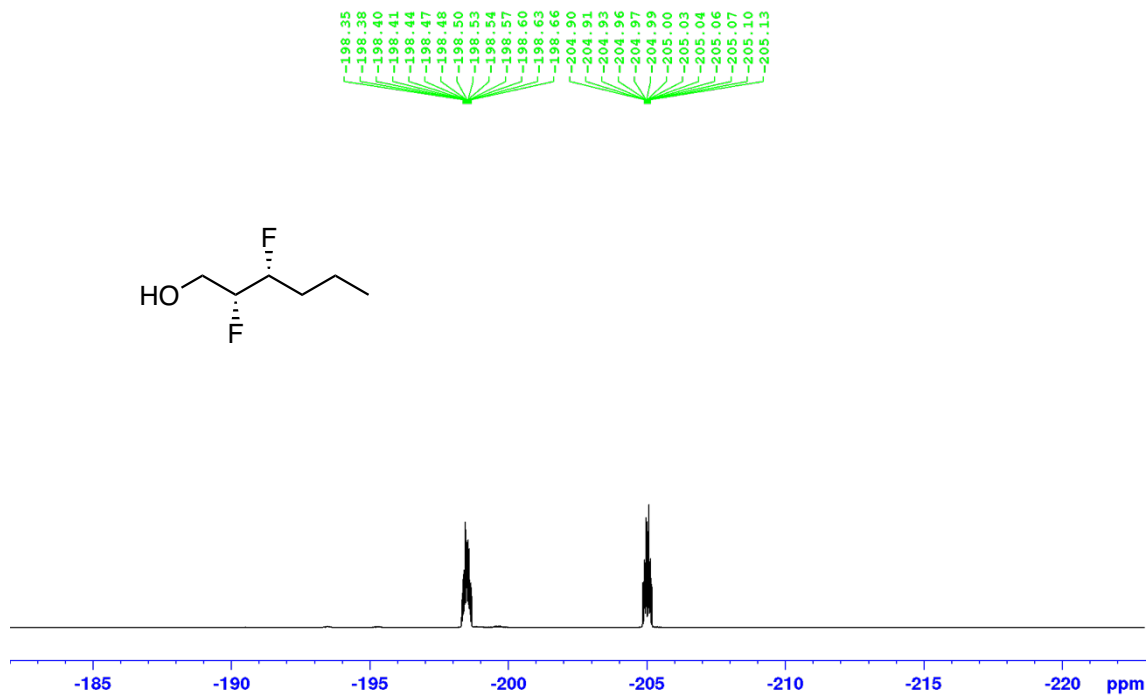
^1H NMR (400 MHz, CDCl_3) of 16



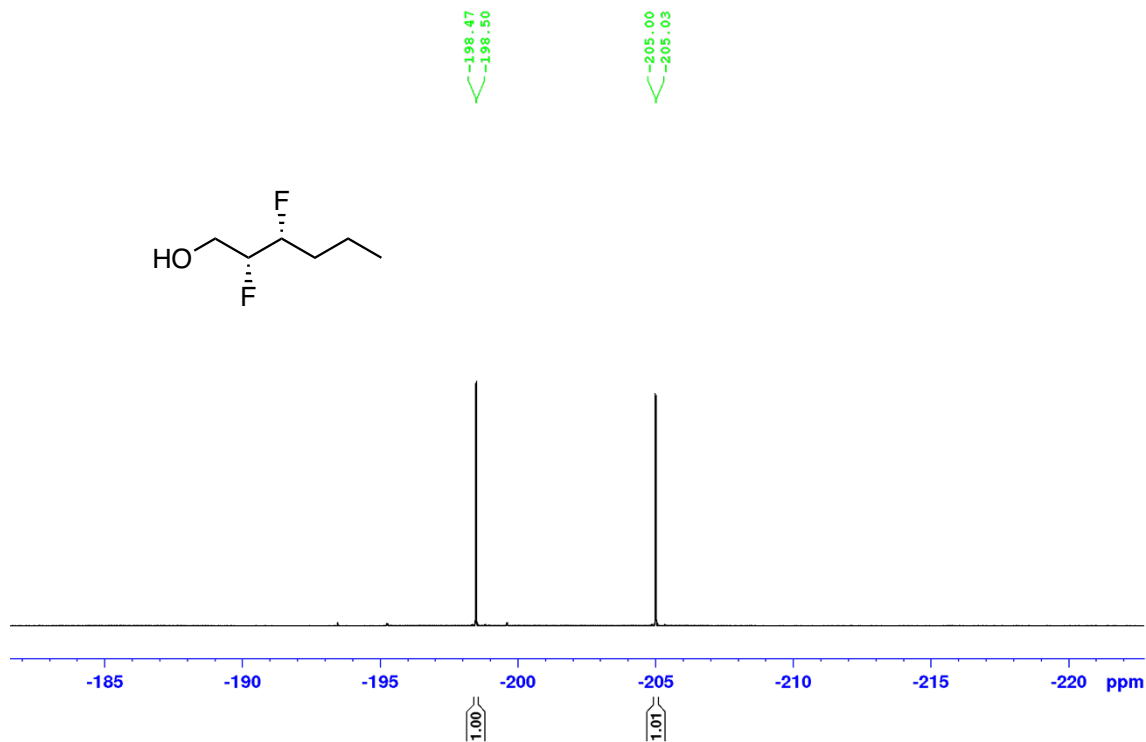
$^{13}\text{C}\{^1\text{H}\}$ NMR (101 MHz, CDCl_3) of 16



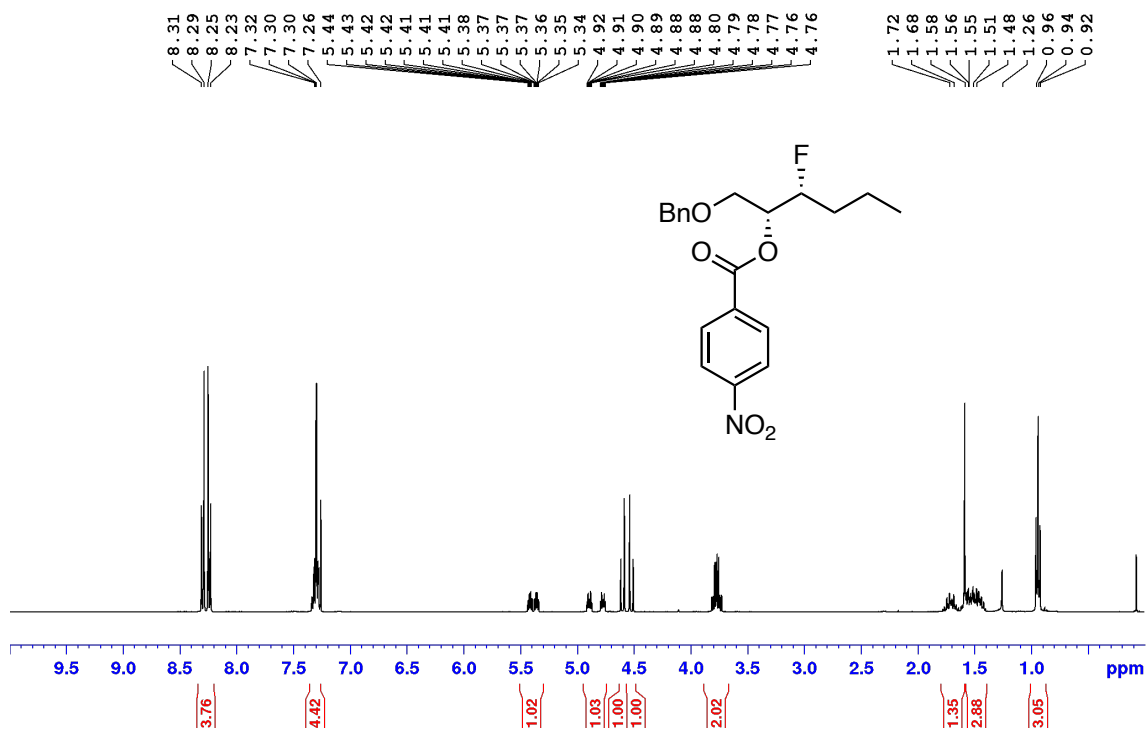
^{19}F NMR (377 MHz, CDCl_3) of 16



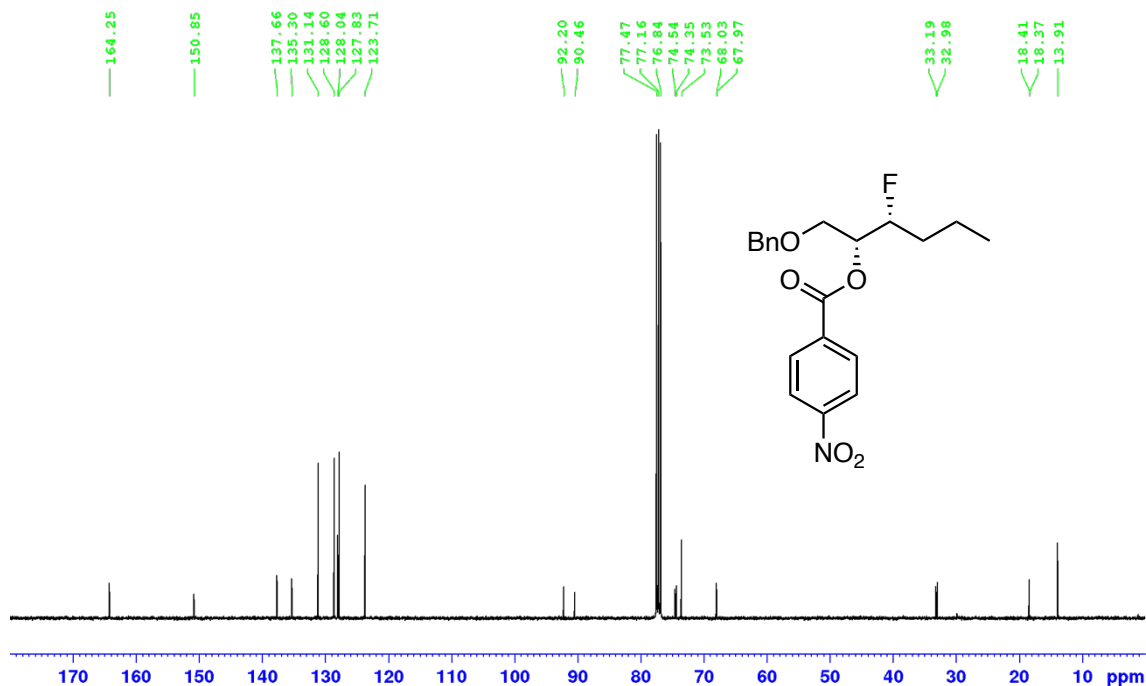
$^{19}\text{F}\{^1\text{H}\}$ NMR (377 MHz, CDCl_3) of 16



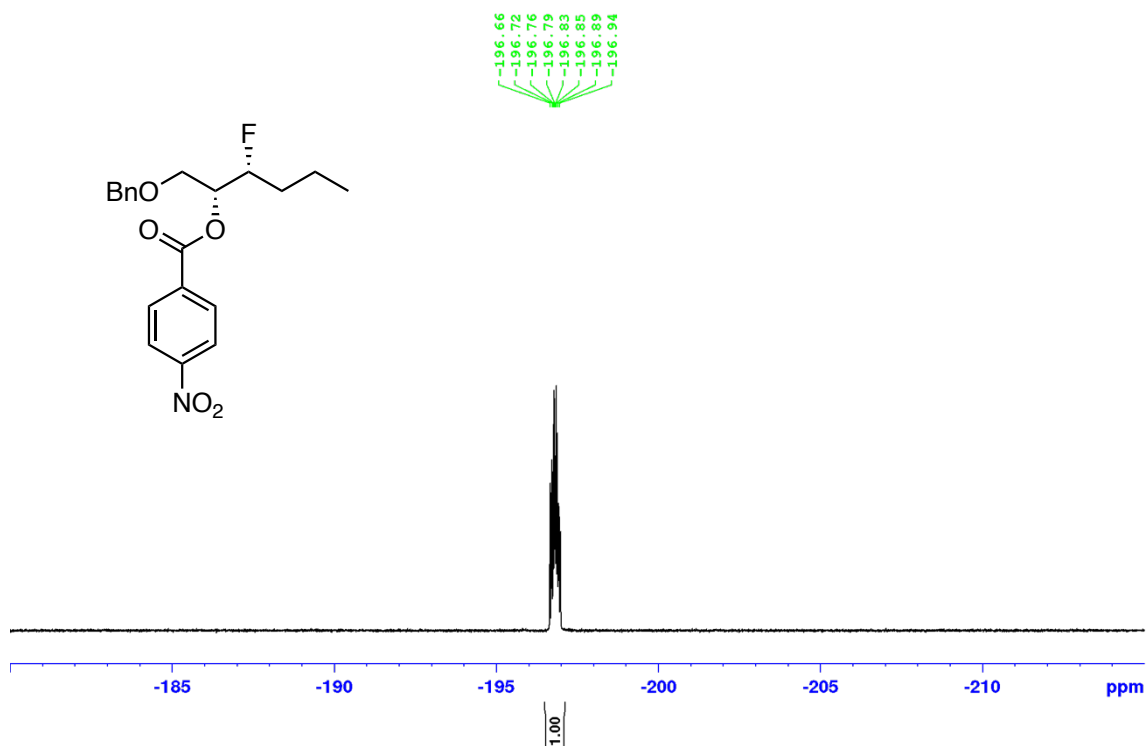
^1H NMR (400 MHz, CDCl_3) of 17



$^{13}\text{C}\{^1\text{H}\}$ NMR (101 MHz, CDCl_3) of 17



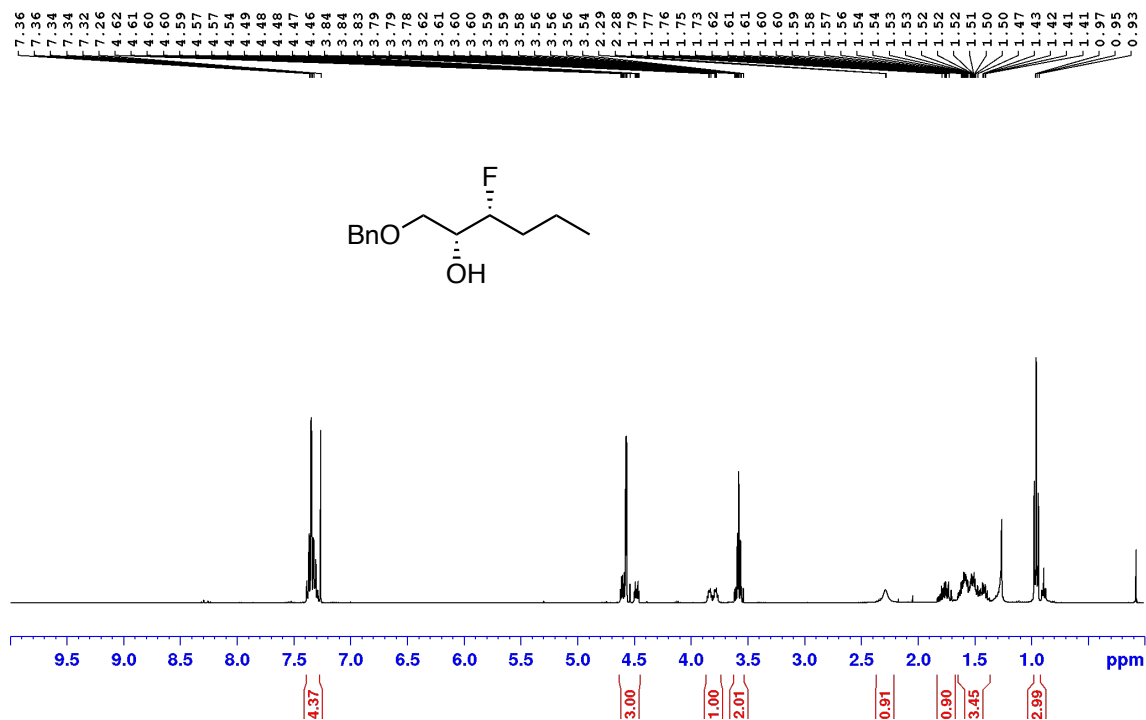
^{19}F NMR (377 MHz, CDCl_3) of 17



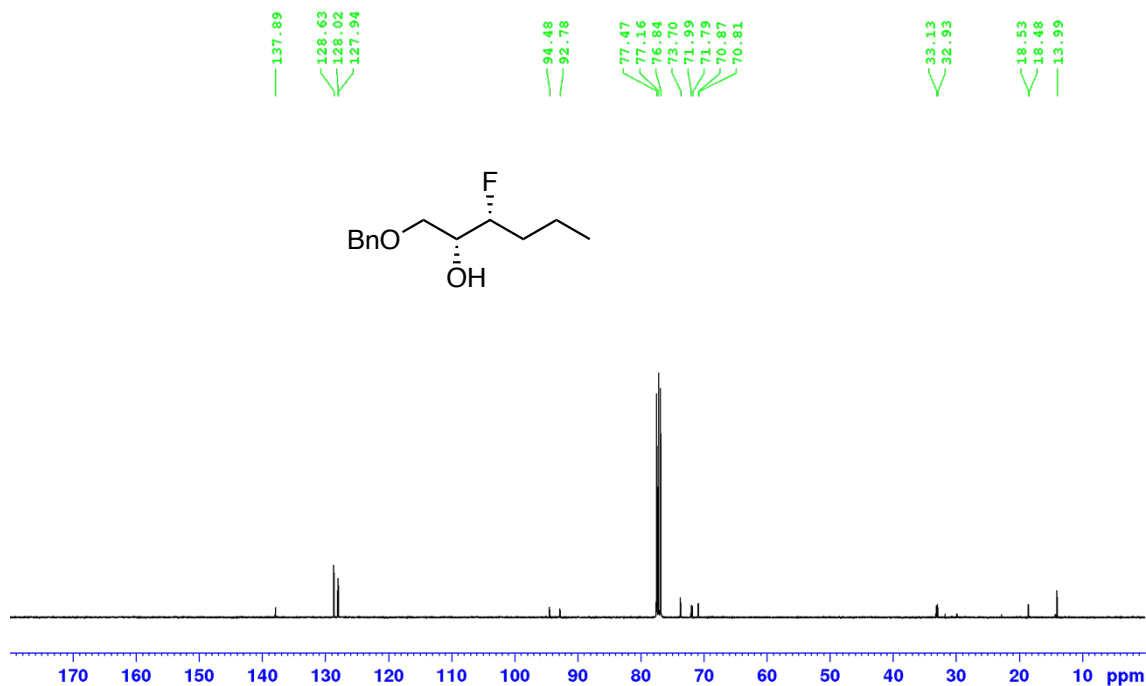
$^{19}\text{F}\{^1\text{H}\}$ NMR (377 MHz, CDCl_3) of 17



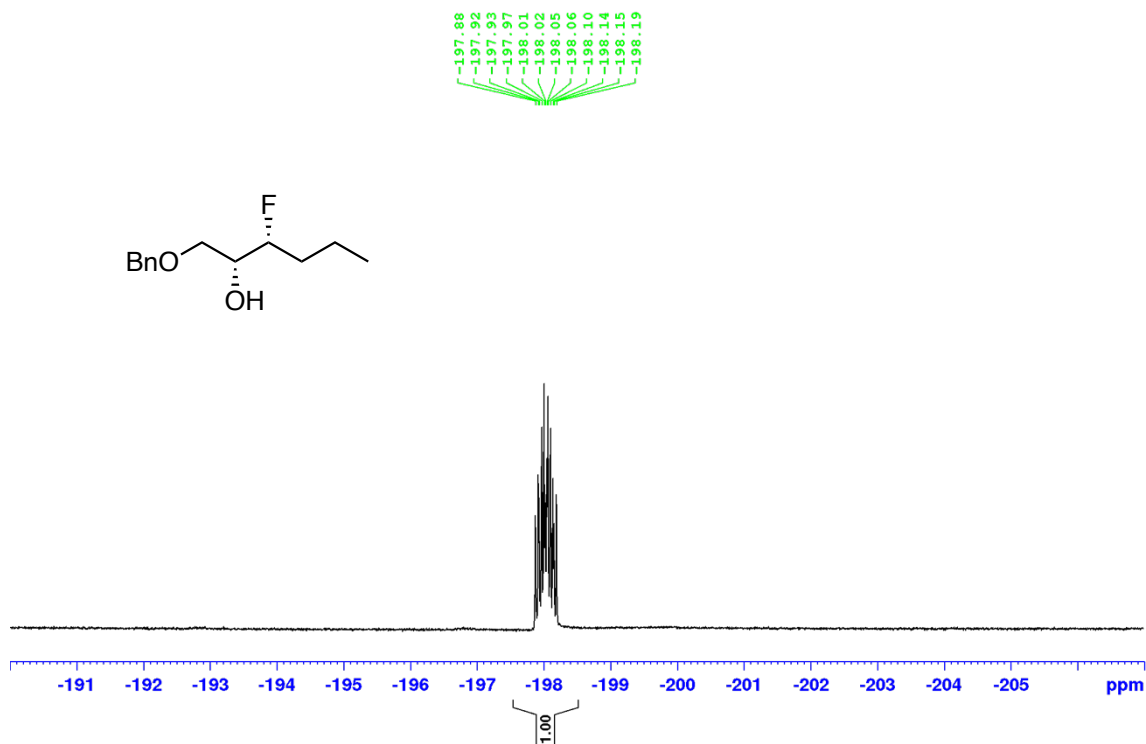
^1H NMR (400 MHz, CDCl_3) of **18**



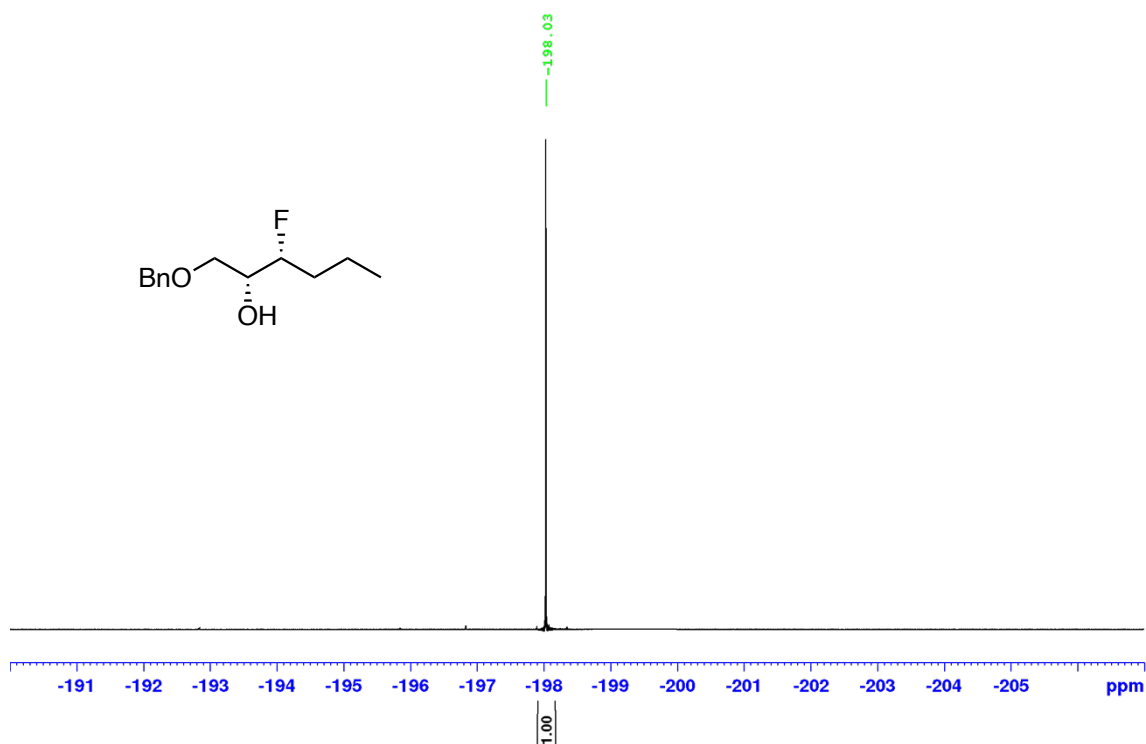
$^{13}\text{C}\{^1\text{H}\}$ NMR (101 MHz, CDCl_3) of **18**



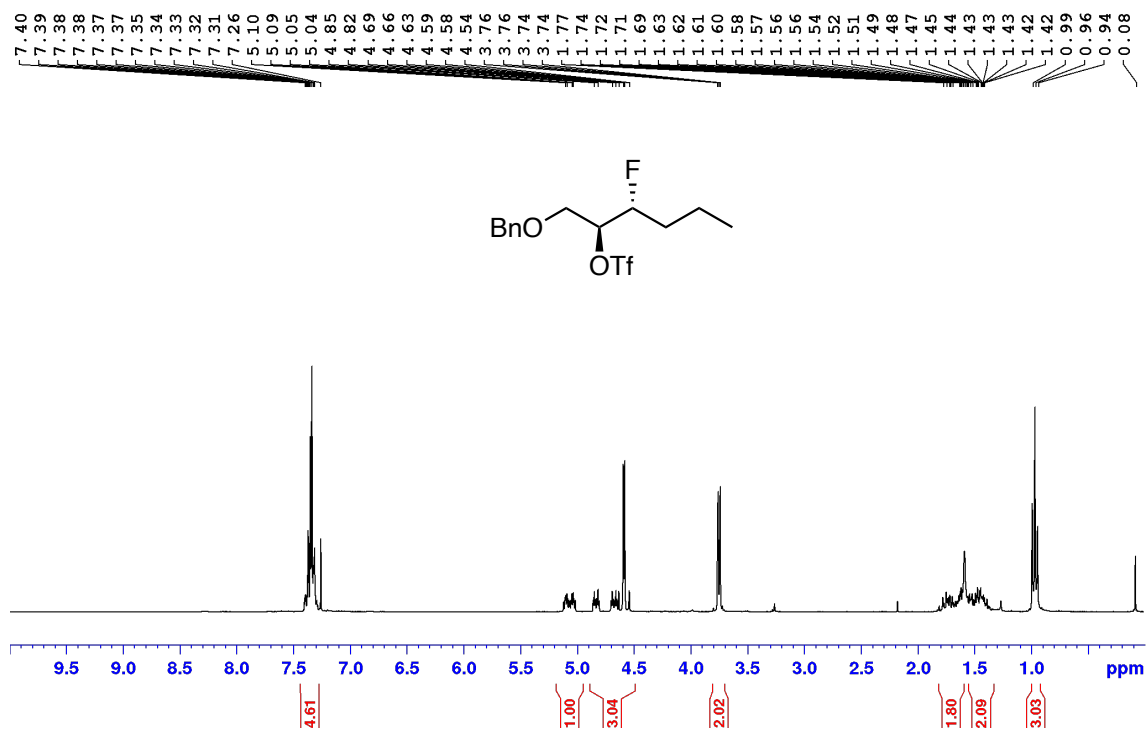
^{19}F NMR (377 MHz, CDCl_3) of **18**



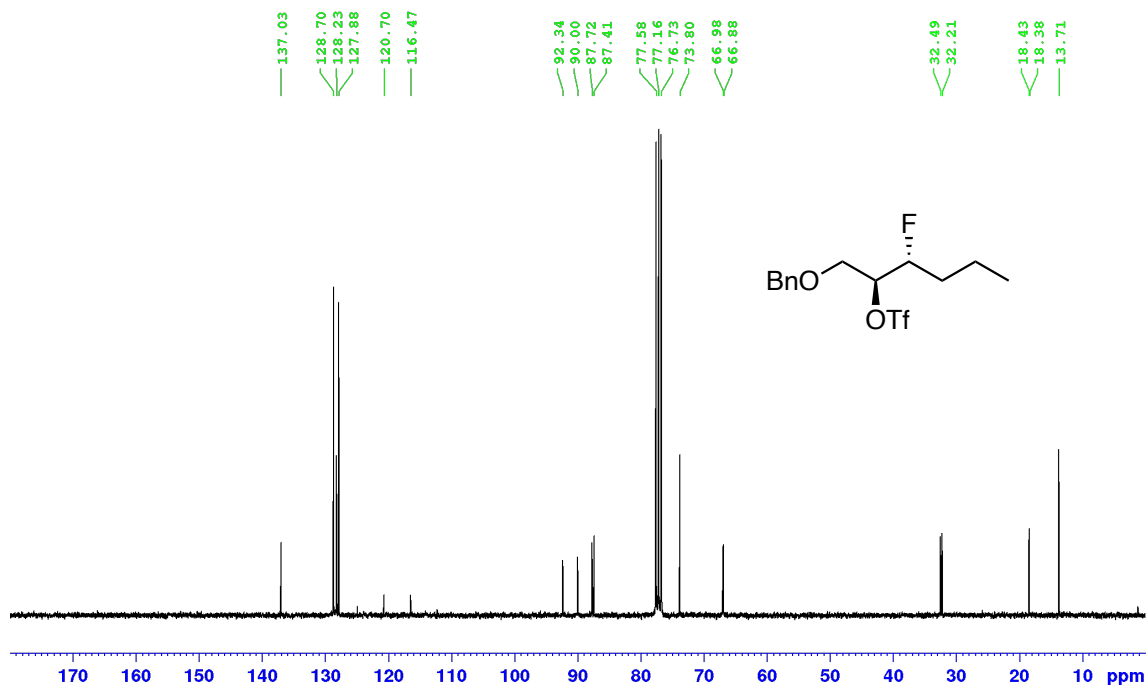
$^{19}\text{F}\{^1\text{H}\}$ NMR (377 MHz, CDCl_3) of **18**



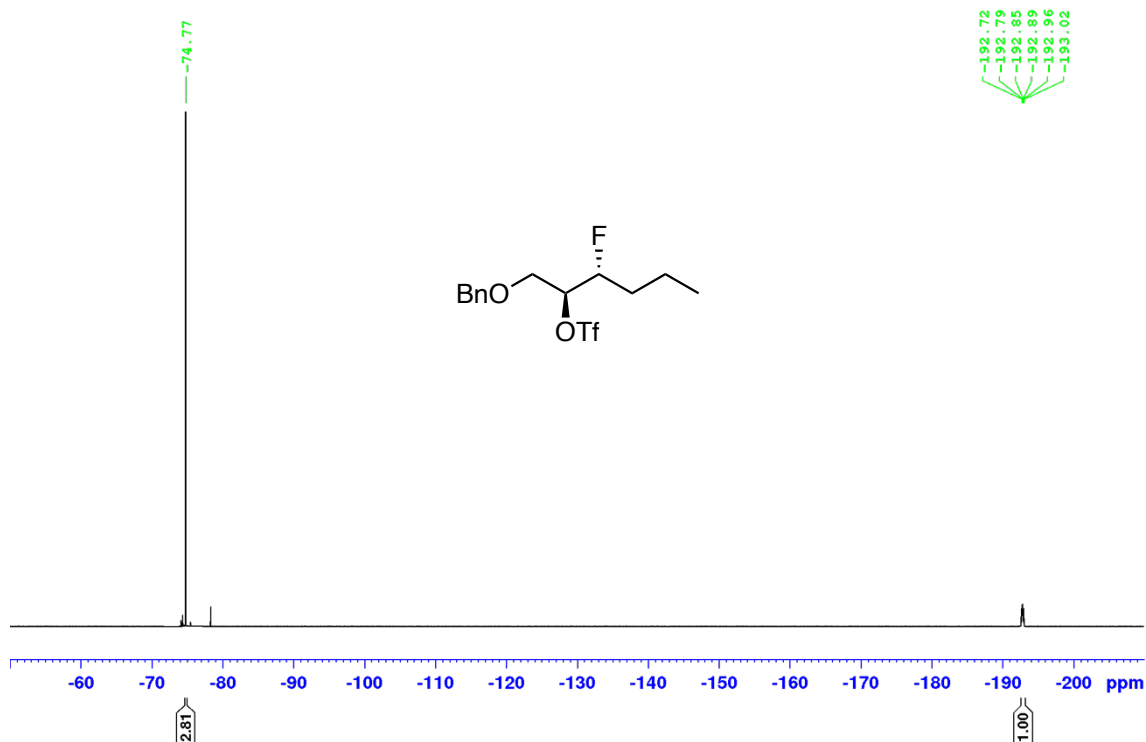
^1H NMR (300 MHz, CDCl_3) of **19**



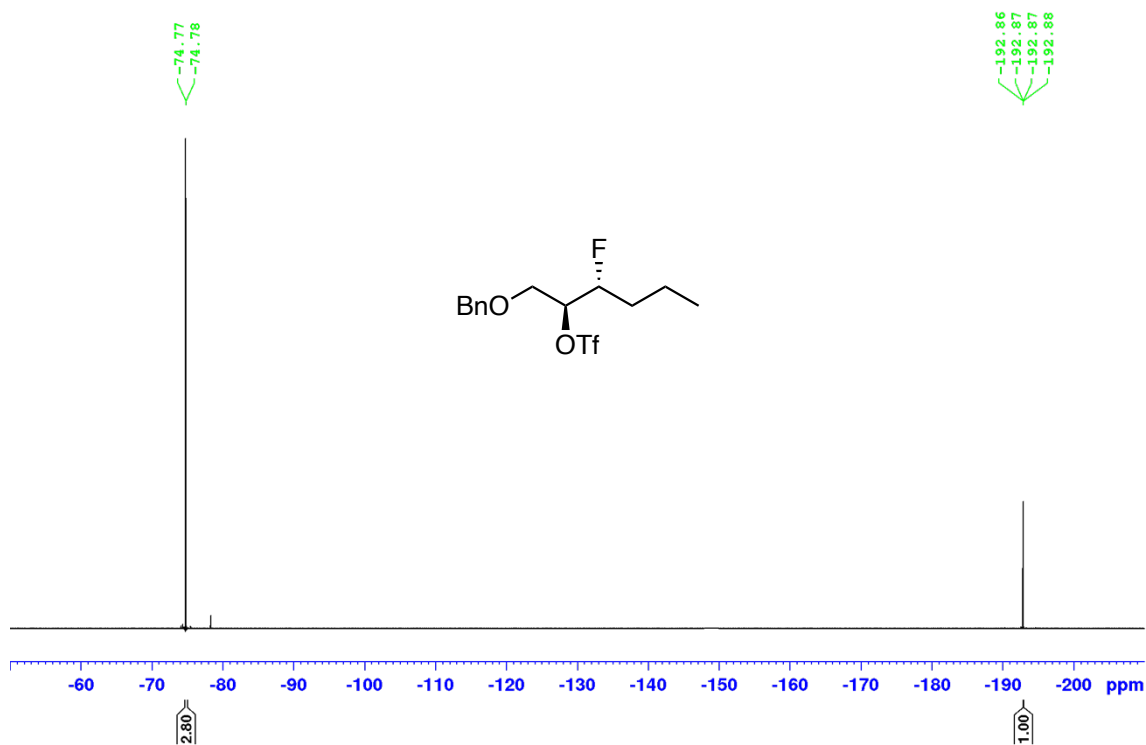
$^{13}\text{C}\{^1\text{H}\}$ NMR (76 MHz, CDCl_3) of **19**



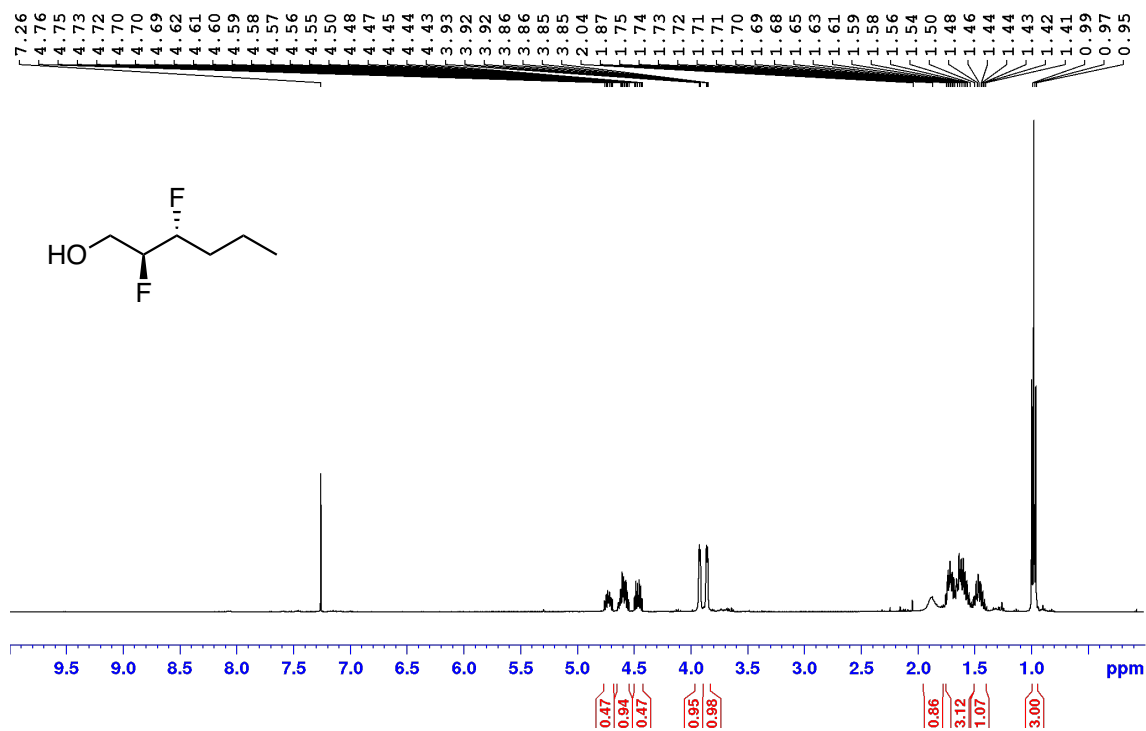
^{19}F NMR (283 MHz, CDCl_3) of **19**



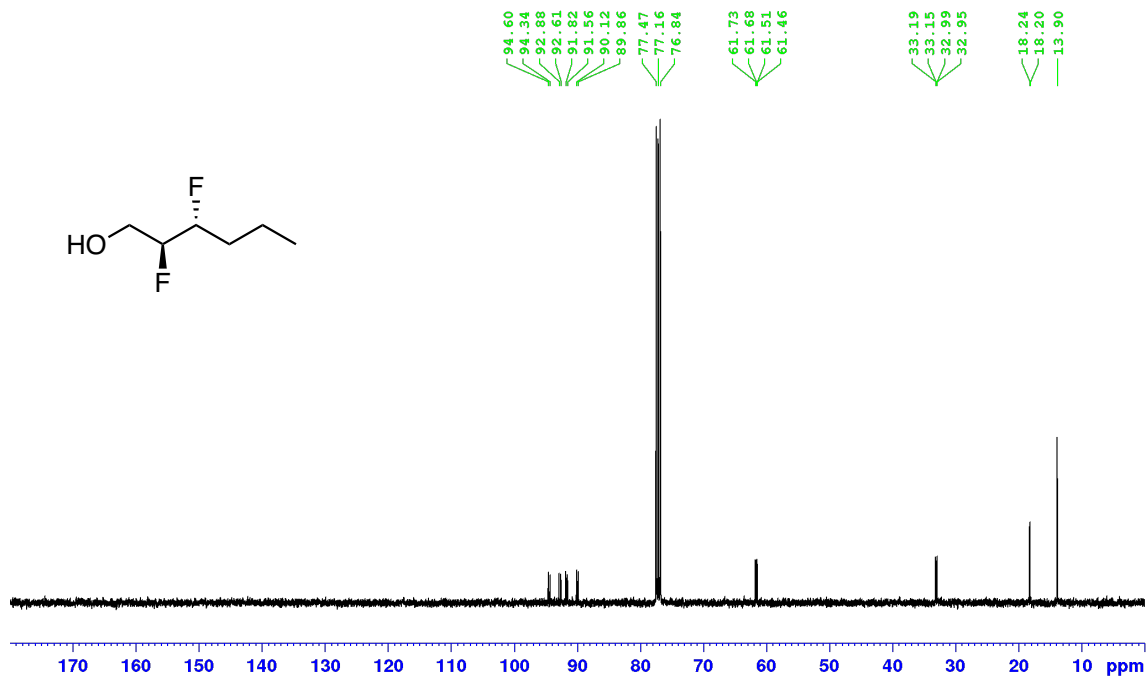
$^{19}\text{F}\{^1\text{H}\}$ NMR (283 MHz, CDCl_3) of **19**



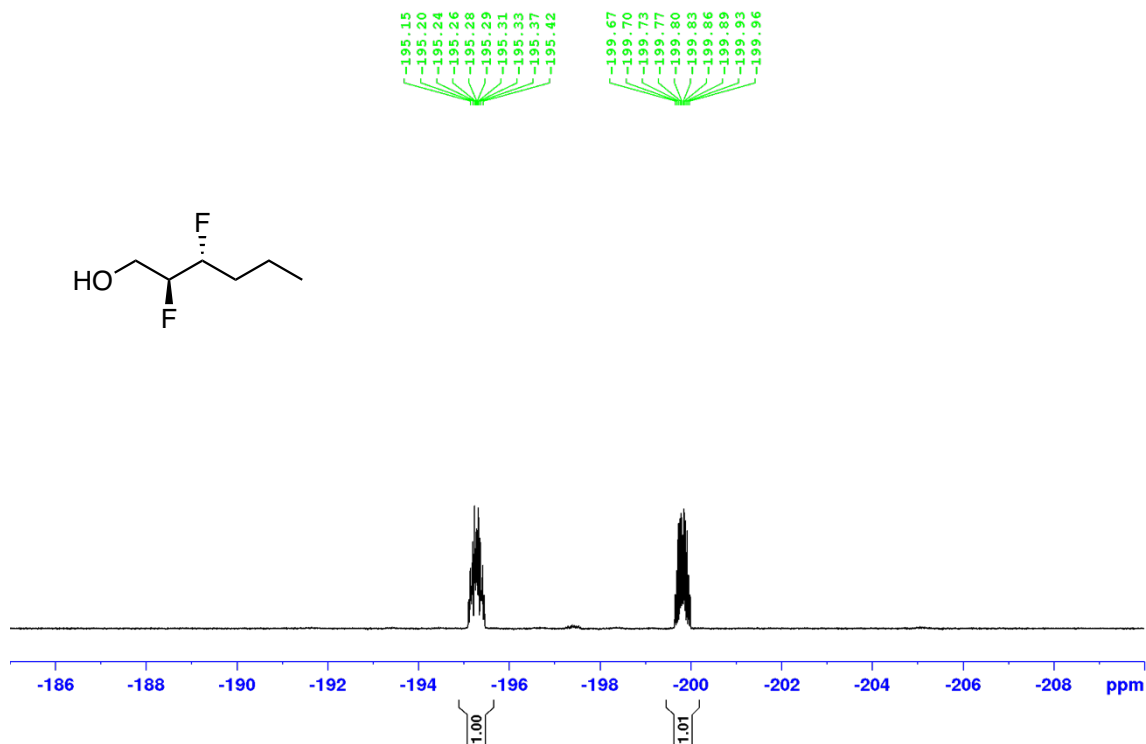
^1H NMR (400 MHz, CDCl_3) of **20**



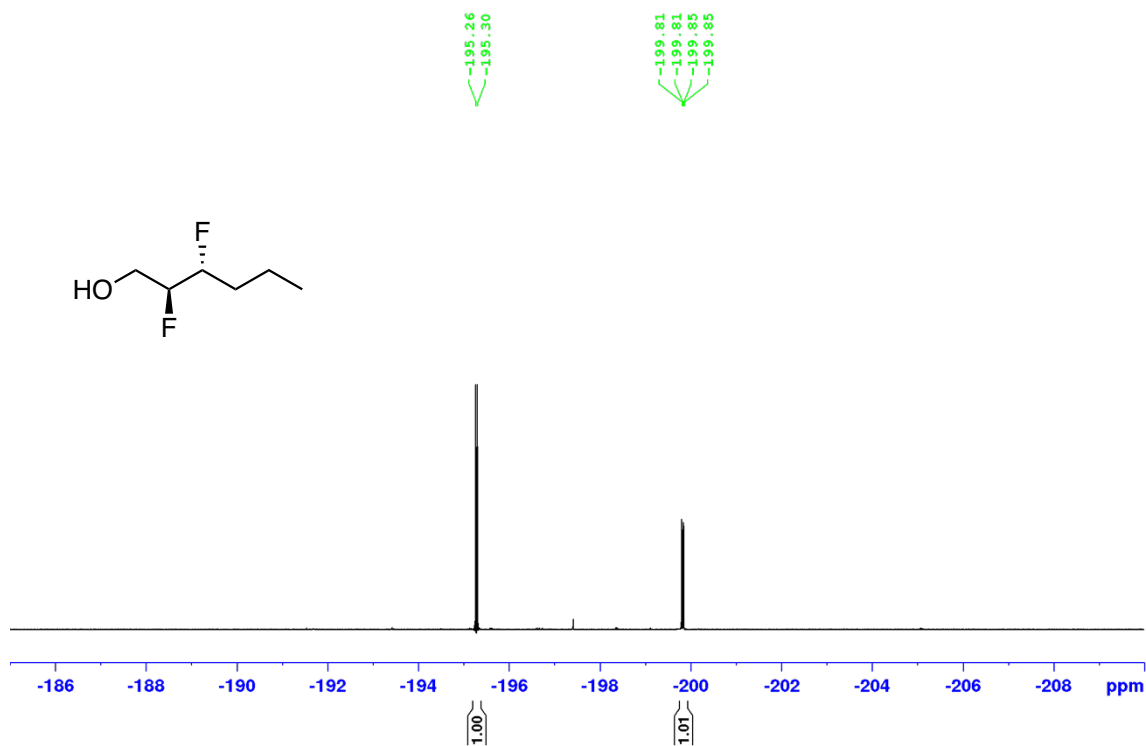
$^{13}\text{C}\{^1\text{H}\}$ NMR (101 MHz, CDCl_3) of **20**



^{19}F NMR (377 MHz, CDCl_3) of **20**



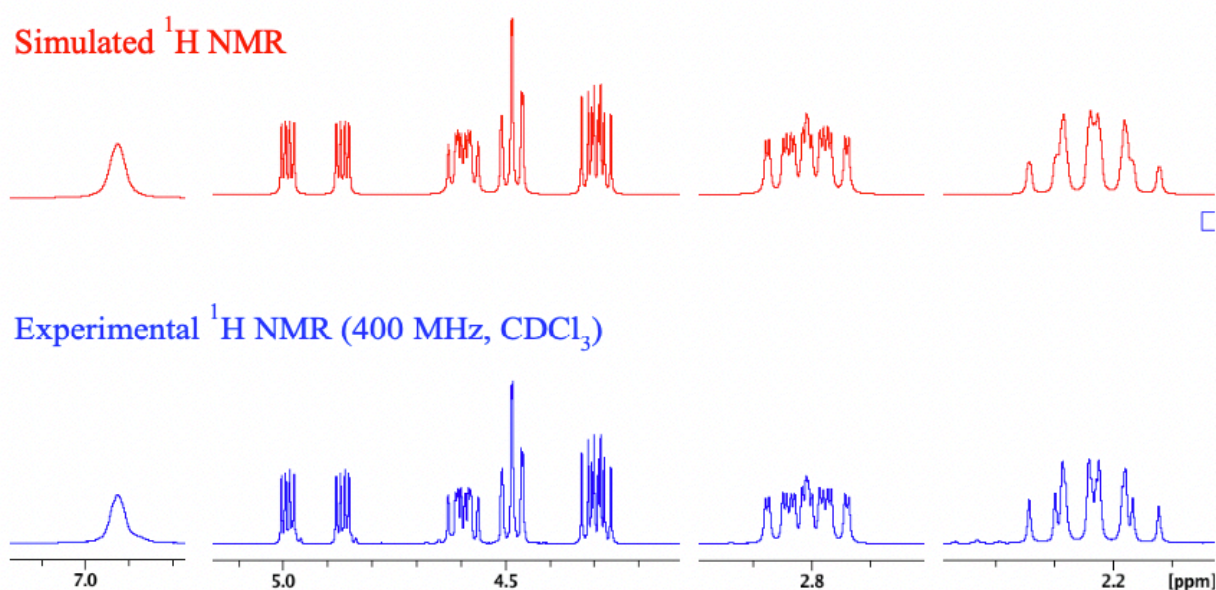
$^{19}\text{F}\{^1\text{H}\}$ NMR (377 MHz, CDCl_3) of **20**



5. NMR *J*-based analysis methodology

Accurate *J*-values for compounds **2a–f** and **3a–f** were determined by simulating the experimental ¹H NMR spectra using the DAISY module of the Bruker TopSpin software. The results are depicted in Figures S3–S11 below. For enantiomeric pairs (*i.e.* **3a/b**, **3c/d**, **3e/f**), data is only presented for one of the pair.

(a)

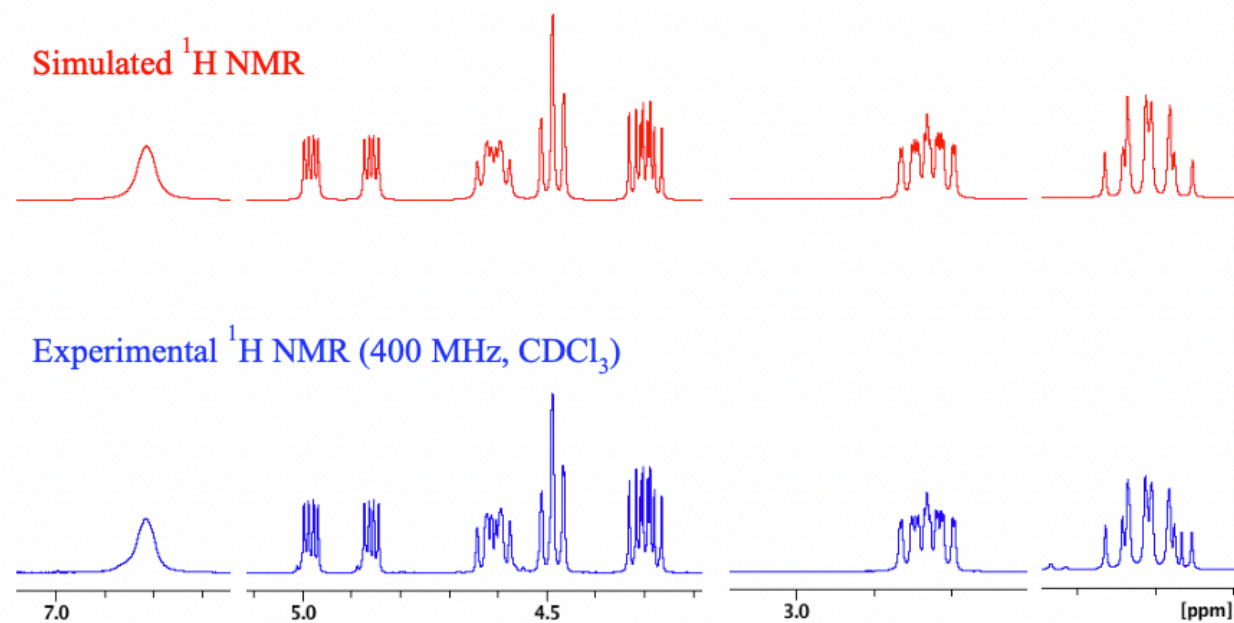


(b)

Spins	3	4	5	6
1	30.9	3.7		
2	14.6	7.7		
3		49.5	4.0	
4			0.5	
5				6.5

Figure S3: (a) Simulated and experimental ¹H NMR spectra of **2a**; (b) Elucidated spin-spin coupling constants (Hz).

(a)



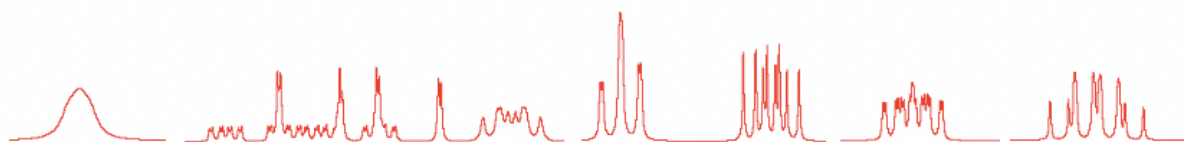
(b)

Spins	3	4	5	6
1	3.7	30.9		
2	7.7	14.6	0.7	
3		49.5	0.5	
4			4.0	
5				6.5

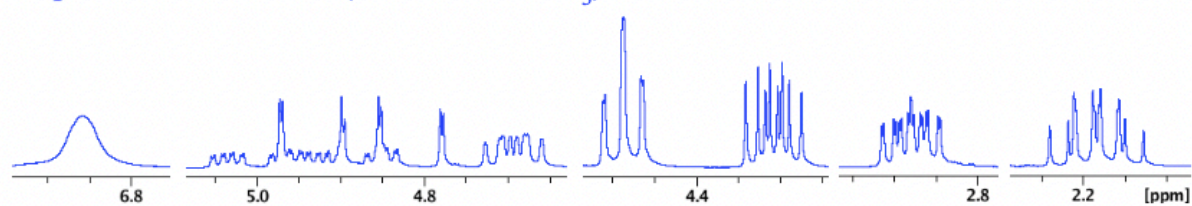
Figure S4: (a) Simulated and experimental ^1H NMR spectra of **2b**; (b) Elucidated spin-spin coupling constants (Hz).

(a)

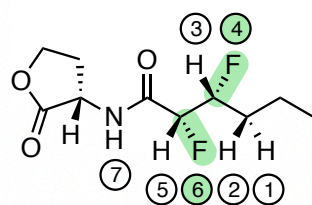
Simulated ^1H NMR



Experimental ^1H NMR (400 MHz, CDCl_3)



(b)

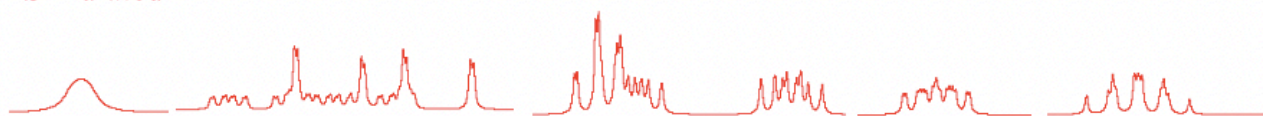


Spins	2	3	4	5	6	7
1	12.0	9.0	9.1			
2		4.9	19.5			
3			45.6	1.4	28.0	
4				29.7	11.2	
5					47.2	
6						4.0

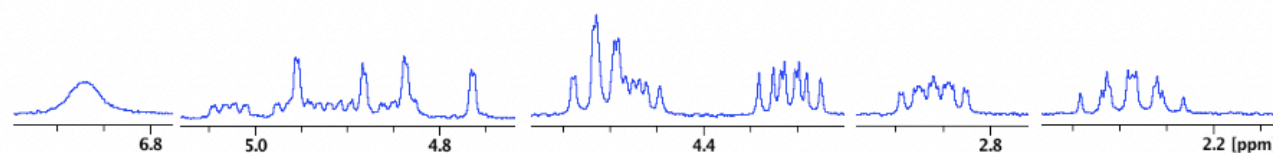
Figure S5: (a) Simulated and experimental ^1H NMR spectra of **2c**; (b) Elucidated spin-spin coupling constants (Hz).

(a)

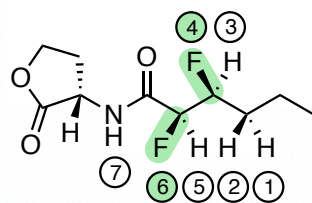
Simulated



Experimental ¹H NMR (400 MHz, CDCl₃)



(b)

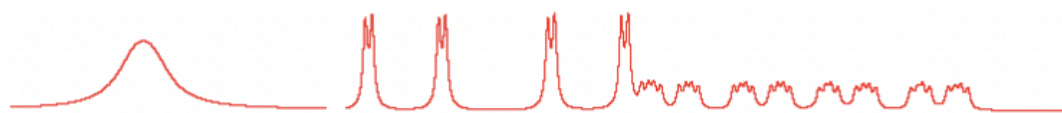


Spins	2	3	4	5	6	7
1	12.0	5.0				
2		9.1	10.0			
3			45.4	1.5	27.5	
4				29.0	10.0	
5					47.4	
6						3.0

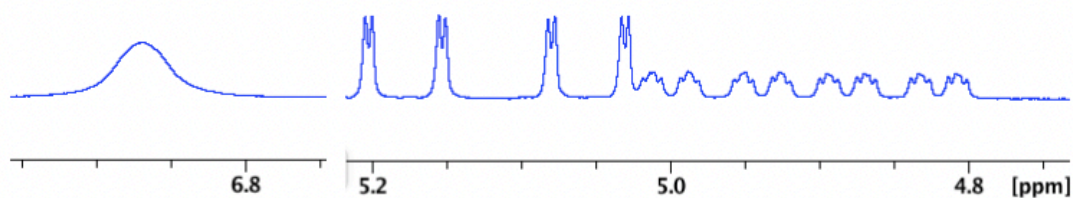
Figure S6: (a) Simulated and experimental ¹H NMR spectra of **2d**; (b) Elucidated spin-spin coupling constants (Hz).

(a)

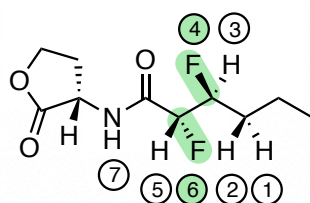
Simulated ^1H NMR



Experimental ^1H NMR (400 MHz, CDCl_3)



(b)

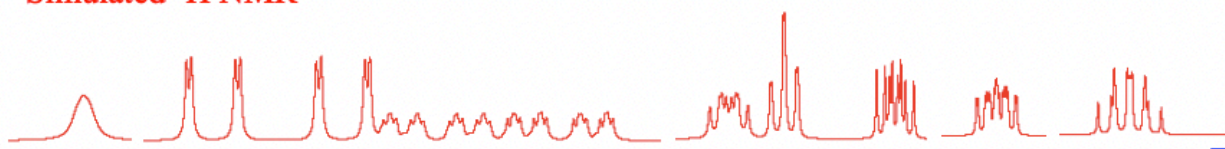


Spins	2	3	4	5	6	7
1	12.0	3.3	23.0			
2		10.1	13.5			
3			47.6	1.8	24.6	
4				19.7	12.9	
5					49.0	
6						4.5

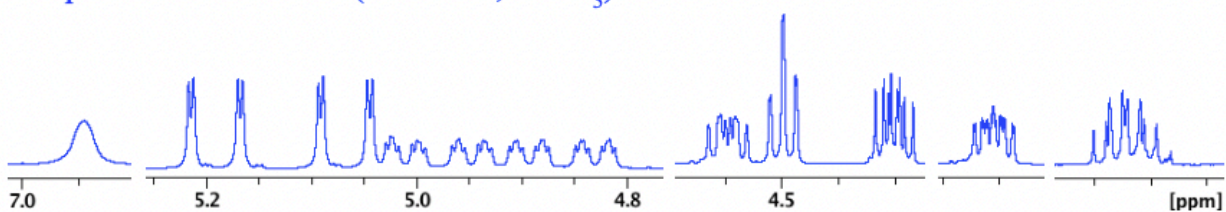
Figure S7: (a) Simulated and experimental ^1H NMR spectra of **2e**; (b) Elucidated spin-spin coupling constants (Hz).

(a)

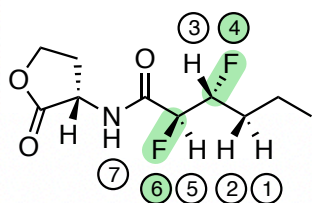
Simulated ^1H NMR



Experimental ^1H NMR (400 MHz, CDCl_3)



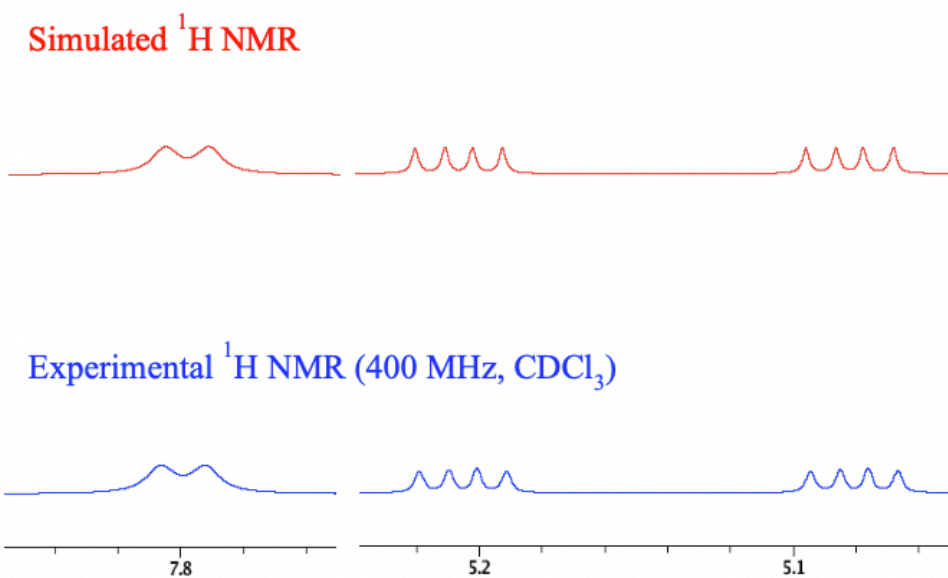
(b)



Spins	2	3	4	5	6	7
1	12.0	10.3	7.0			
2		2.9	25.0			
3			47.1	1.9	25.2	
4				18.5	12.7	
5					49.4	0.5
6						4.0

Figure S8: (a) Simulated and experimental ^1H NMR spectra of **2f**; (b) Elucidated spin-spin coupling constants (Hz).

(a)



(b)

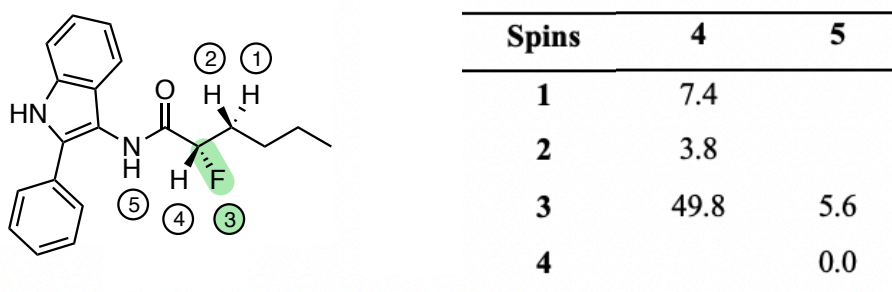
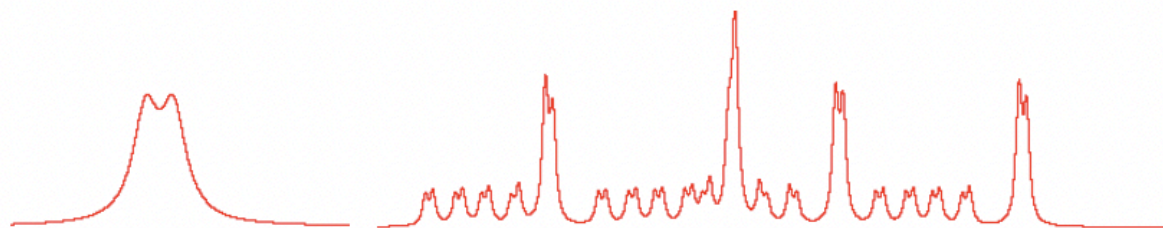


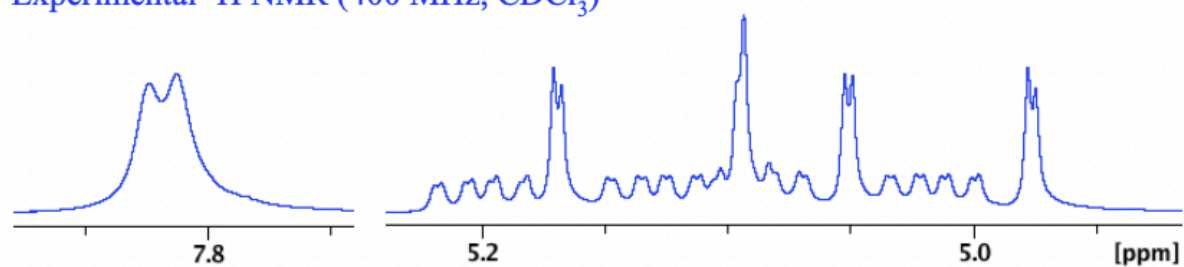
Figure S9: (a) Simulated and experimental ^1H NMR spectra of **3a**; (b) Elucidated spin-spin coupling constants (Hz).

(a)

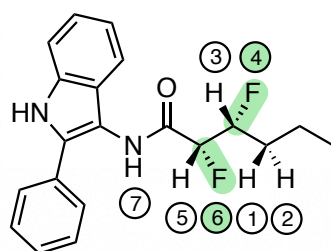
Simulated ^1H NMR



Experimental ^1H NMR (400 MHz, CDCl_3)



(b)

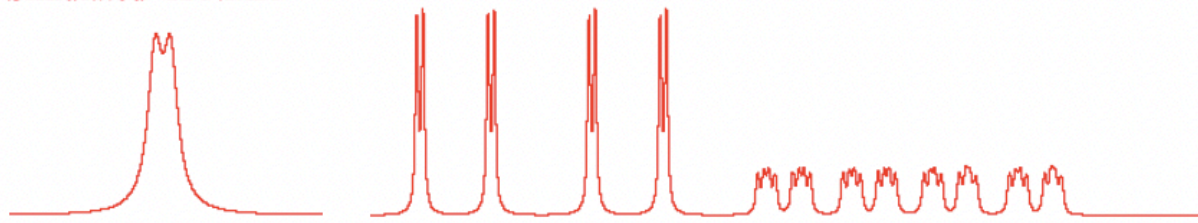


Spins	2	3	4	5	6	7
1		4.9				
2		9.2				
3			45.3	1.2	28.3	
4				29.9	11.6	
5					47.4	0.3
6						4.9

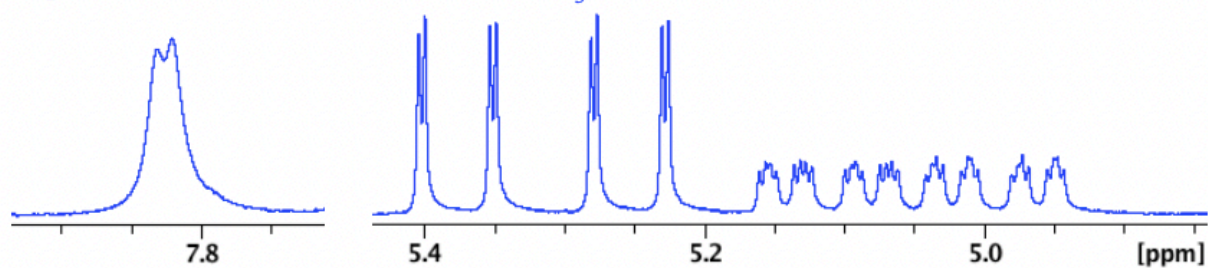
Figure S10: (a) Simulated and experimental ^1H NMR spectra of **3c**; (b) Elucidated spin-spin coupling constants (Hz).

(a)

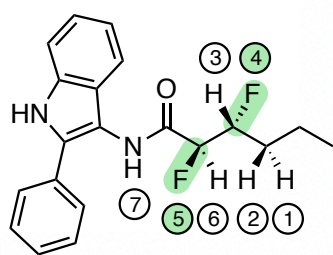
Simulated ^1H NMR



Experimental ^1H NMR (400 MHz, CDCl_3)



(b)



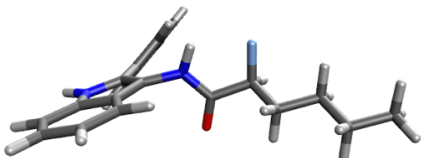
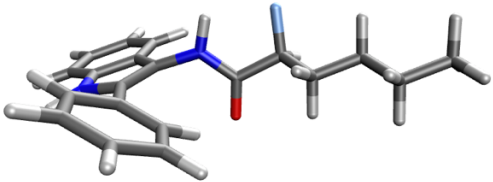
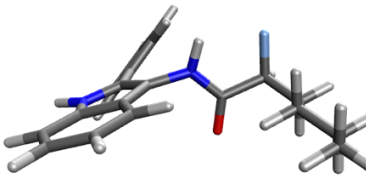
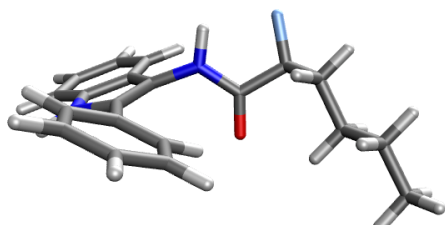
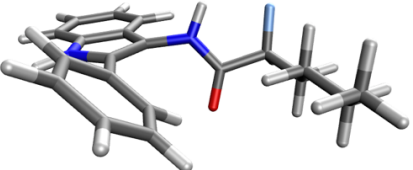
Spins	2	3	4	5	6	7
1		10.4				
2		3.1				
3			47.6	24.5	1.8	
4				13.0	20.3	
5					49.3	4.8
6						0.0

Figure S11: (a) Simulated and experimental ^1H NMR spectra of **3f**; (b) Elucidated spin-spin coupling constants (Hz).

6. DFT study

In order to confirm the solution state conformations assigned by NMR analysis, a DFT study was undertaken. This study was performed with the Gaussian09 suite of programs,^[4] run on the UNSW Katana computational cluster. This study examined compounds **3a**, **3c** and **3f**, which taken together provide a good representation of the conformational space illustrated in the main manuscript, Figure 2. A library of structures was generated by systematically rotating C_{indole}-N, O=C-CHF, CHF-CHF and CHF-CH₂ bonds by 120° increments. These structures were then optimised without restraint at the B3LYP/6-311+G(d,p) level with a SMD chloroform solvent model. The obtained geometries (Tables S1–S3) were identified as stationary points by frequency calculations at the same level of theory (N_{imag} = 0).

Table S1. Calculated geometries of **3a** and their relative energies (B3LYP/6-311+G(d,p)).

ID	3D geometry	E + ZPE (kJ/mol)
3a-I		0
3a-II		1.1111
3a-III		2.3280
3a-IV		5.9709
3a-V		7.0816

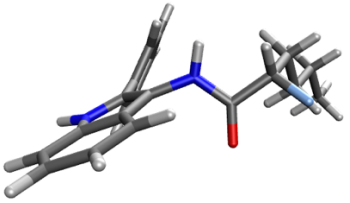
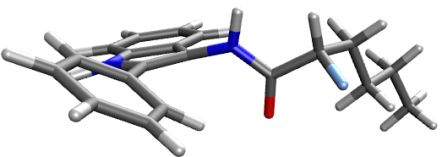
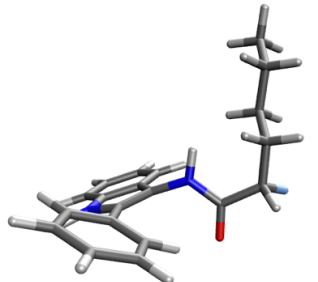
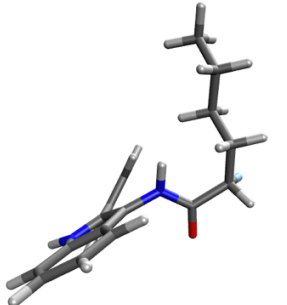
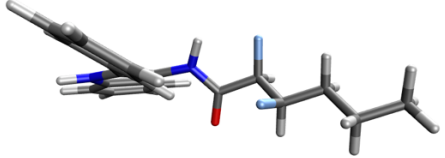
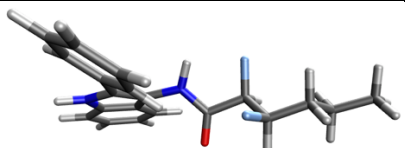
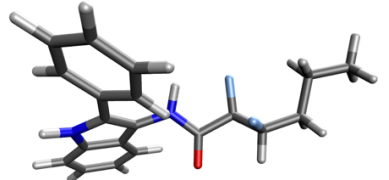
3a-VI		22.4038
3a-VII		26.6422
3a-VIII		29.2592
3a-IX		30.9384

Table S2. Calculated geometries of **3c** and their relative energies (B3LYP/6-311+G(d,p)).

ID	Geometry	E + ZPE (kJ/mol)
3c-I		0
3c-II		2.4040
3c-III		9.4108

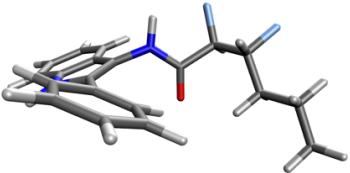
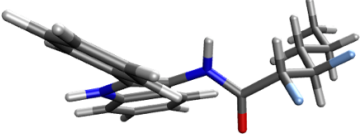
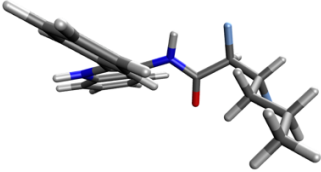
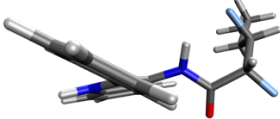
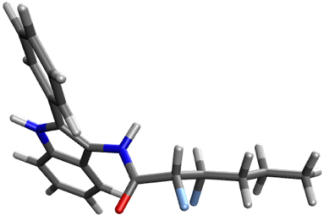
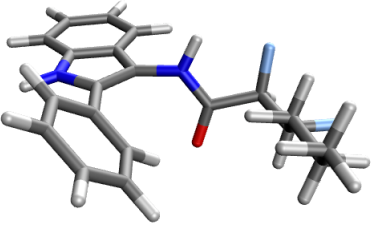
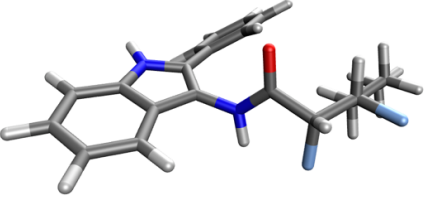
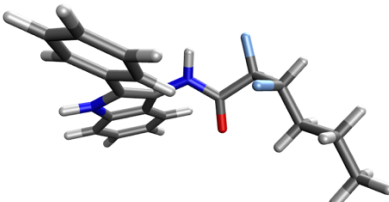
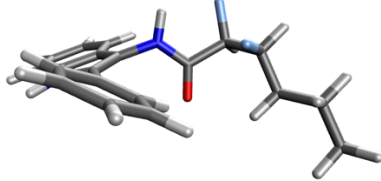
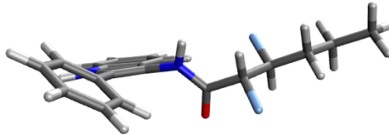
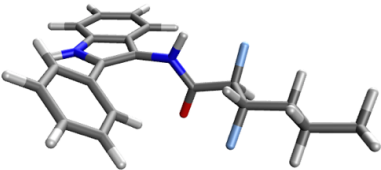
3c-IV		11.9582
3c-V		17.0932
3c-VI		18.3809
3c-VII		20.6509
3c-VIII		21.4799

Table S3. Calculated geometries of **3f** and their relative energies (B3LYP/6-311+G(d,p)).

ID	Geometry	E + ZPE (kJ/mol)
3f-I		0
3f-II		0.4251

3f-III		1.3341
3f-IV		3.2419
3f-V		11.3354
3f-VI		11.5904

The lowest energy conformer for all three compounds features an approximately planar α -fluoroamide moiety with a short N-H...F contact (*ca.* 2.1 Å). This is consistent with the NMR results. Conformers featuring synclinal carbonyl and fluorine groups were substantially disfavoured; the lowest energy conformer that had a *gauche* O–C–C–F torsion (*i.e.* **3f-V**) was 11 kJ/mol higher in energy than the global minimum (*i.e.* **3f-I**).

The lowest energy structures of **3a** and **3c** feature a zigzag carbon chain with (O)C–C–C–C torsions of 174° and 181°, respectively. This is consistent with the NMR results. For **3f**, conformers with both possible *gauche* F–C–C–F torsions are energetically accessible: conformer **3f-I** features an F–C–C–F torsion of –72° and the slightly higher-energy **3f-III** features a torsion of 70°. As a result, these conformers both exhibit bent carbon chains. This is consistent with the NMR results.

To provide an additional cross-check between theory and experiment, NMR coupling constants were calculated for all low-energy conformers using the GIAO method at the B3LYP/6-311+G(d,p) level with SMD chloroform solvation. Using the ‘mixed’ option in Gaussian09, the basis set was augmented with tight polarisation functions for the calculation of the Fermi contact contribution.^[5] Obtained *J*-values were weighted according to their prominence in the calculated thermal Boltzmann distribution and then averaged. The resulting values were then compared with the experimental *J*-

values (Figures S12–S14). A reasonable match between theory and experiment was obtained, providing confidence that the conformational characteristics of the test compounds were well understood.

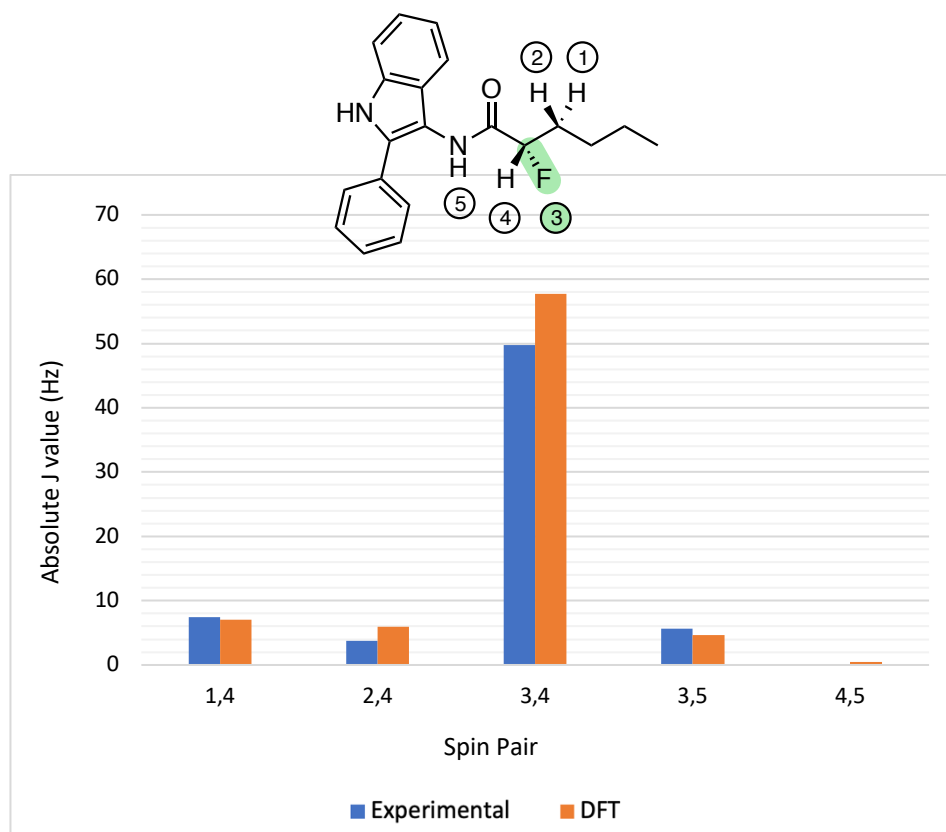


Figure S12. Comparison of calculated and experimentally observed J coupling values for 3a.

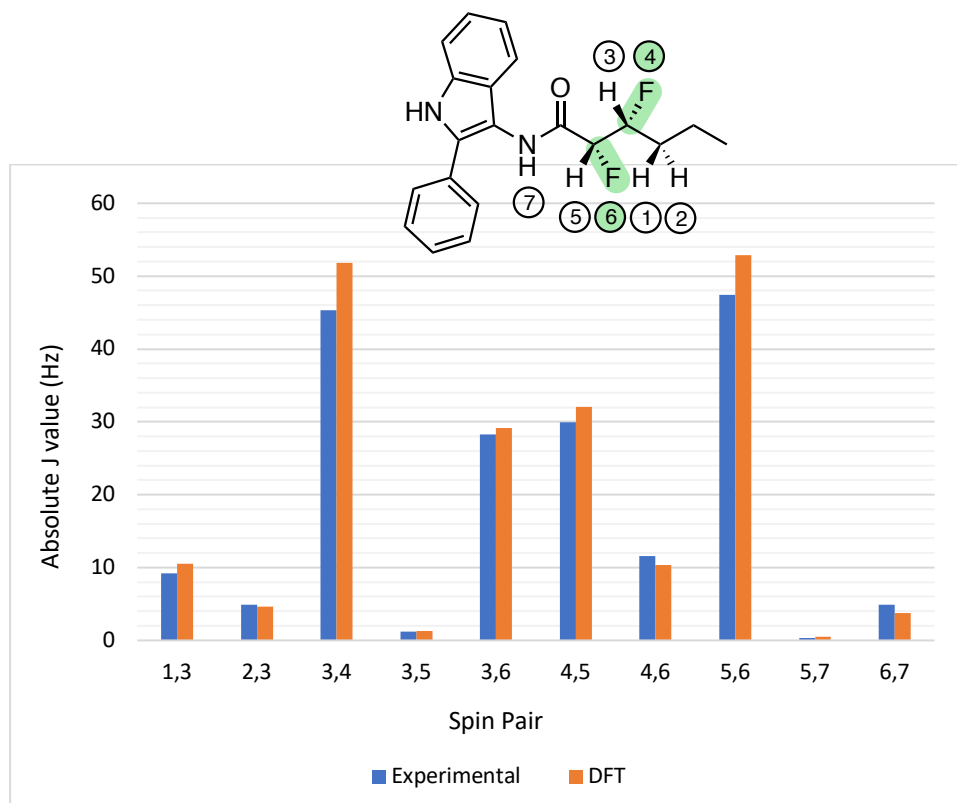


Figure S13. Comparison of calculated and experimentally observed J coupling values for **3c**.

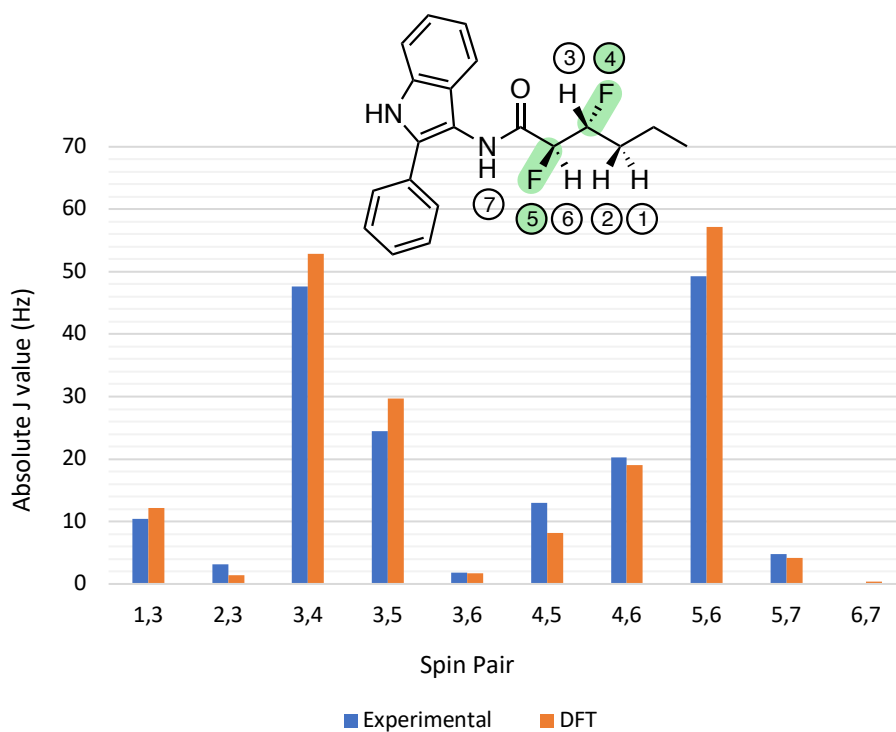


Figure S14. Comparison of calculated and experimentally observed J coupling values for **3f**.

7. Biological assay details

To assess the QS inhibitory activity of the synthesised fluorinated indoles and lactones on QS signalling, the *P. aeruginosa* MH602 PlasB::gfp(ASV) reporter strain, which harbors a chromosomal fusion of the *lasB* promoter to an unstable *gfp* gene and responds to the AHL 3-oxo-dodecanoyl homoserine lactone (3oxo-C12-HSL), was used.^[6] An overnight culture was prepared in Luria-Bertani (LB10) media supplemented with gentamycin (40 μ M). The culture was then diluted (1:100) in AB medium supplemented with 0.25% tryptone, 0.13% yeast extract and gentamycin (40 μ M), and 200 μ L aliquots were dispensed to flat bottom 96-well plate wells (Costar). The culture was supplemented with varying concentrations of synthetic compounds dissolved in DMSO. Control cultures were supplemented with equal amounts of DMSO (1%). Wells with bacterial culture but no compound were used as negative control while wells supplemented with furanone (Fu-30) was used as positive controls. Plates were sealed with self-adhesive microplate sealers (TopSeal-A, PerkinElmer) to allow air diffusion and to prevent condensation. Plates were incubated with shaking at 120 rpm for 15 hours at 37 °C and the fluorescence (excitation, 485 nm; emission, 535 nm) and cell growth (OD600) was measured by a plate reader (FLUOstar Omega, BMG Labtech). Each experiment was performed in triplicate and was repeated in three independent experiments.

Percentage growth inhibition of *P. aeruginosa* MH602 in presence of tested compounds at different concentrations (values expressed as mean \pm SEM of at least three independent experiments; 0 = no growth inhibition):

Compound	62.5 μ M	125 μ M	250 μ M
2	0	0	21.8 \pm 4.2
2a	0	14.9 \pm 7.0	36.3 \pm 5.6
2b	0	6.4 \pm 6.8	20.6 \pm 3.5
2c	0	0	24.7 \pm 5.7
2d	0	5.0 \pm 4.6	28.6 \pm 5.7
2e	0	22.5 \pm 6.6	33.6 \pm 4.6
2f	0	12.4 \pm 5.1	25.6 \pm 5.5
3	20.0 \pm 2.9	26.6 \pm 4.3	17.8 \pm 2.7
3a	27.2 \pm 2.1	16.7 \pm 3.9	16.7 \pm 22.9
3b	15.1 \pm 3.3	27.7 \pm 2.3	16.7 \pm 16.5
3c	0	16.0 \pm 1.7	0
3d	0	15.7 \pm 3.8	0
3e	14.2 \pm 4.0	18.7 \pm 3.9	4.6 \pm 10.2
3f	0	22.6 \pm 4.0	0

8. Docking procedures

In silico docking was performed using AutoDock Vina.^[7]

Protein preparation: The crystal structure 2UV0^[8] was downloaded from the Protein Data Bank and opened in Maestro. All molecules except for protein chain E were deleted, polar hydrogens were then added, and the resulting structure was saved as a .pdb file. This file was re-opened in MGLTools, and an appropriate “grid box” for ligand binding was determined (*i.e.* center_x = 23.922, center_y = 16.256, center_z = 81.224, size_x = 10, size_y = 10, size_z = 14, measured with grid spacing = 1.000). The structure was exported as a .pdbqt file.

Ligand preparation: The crystal structure 2UV0 was opened in Maestro. All molecules except for the ligand were deleted. The resulting structure was edited using the “build” functionality in Maestro until the required chemical constitution was obtained. The resulting structure was saved as a .pdb file. This file was re-opened in MGLTools, and designated as the ligand for docking. The default set of rotatable bonds was retained. The structure was exported as a .pdbqt file.

Docking: Docking was performed in AutoDock Vina using the protein.pdbqt and ligand.pdbqt files created above. Default parameters were used, except for one detail: in the config file, “exhaustiveness” was set to 32.

Pose selection: Docking results were visualised in PyMol. For each ligand, the suite of 9 binding poses was inspected to ensure that diversity was obtained both in terms of binding orientation (to confirm that the ligand had sufficient degrees of freedom to rotate) and molecular conformation (to confirm that the ligand had sufficient flexibility to explore its full conformational space and not be biased by the starting conformation). For ligand **2**, pose #2 was identified as the “best” pose on the basis of its close overlay with the crystal structure of the native ligand bound to lasR. For ligand **3**, poses #1 and #3 were identified as equal “best” poses on the basis of their similarity with the binding pose previously identified in a separate docking study using Discovery Studio / GOLD.^[9] For ligands **2a–f** and **3a–f**, poses #1 through to #9 were inspected, and any structures that contained obviously unfavourable torsions (e.g. if O=C–C–F was far from 180°)^[10] were rejected. The top-ranked pose to survive this exclusion process was identified as the “best” pose. As an example of this decision process, poses #1–4 of ligand **2a** featured O=C–C–F torsions of –125°, –57°, 7° and –15° respectively, corresponding to strain energies of approximately 11–30 kJ/mol (see DFT study above and ref. 10) and rendering these poses unrealistic; whereas pose #5 had an O=C–C–F torsion of 174° which was judged to be sufficiently close to the ideal value^[10] for this pose to be retained.

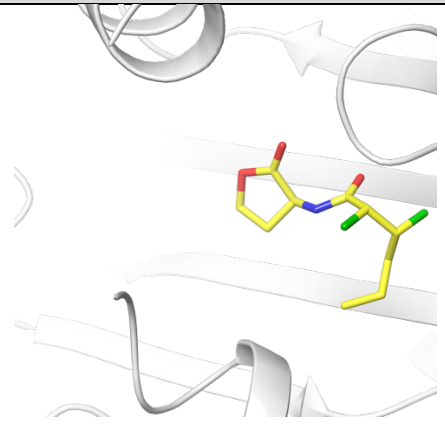
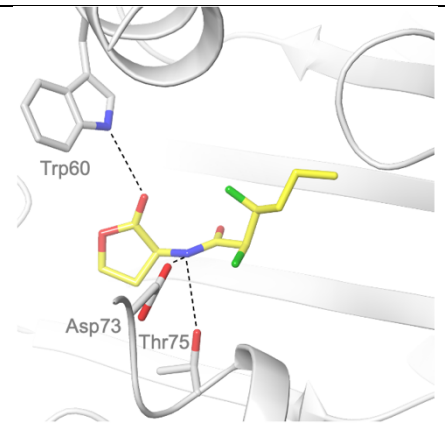
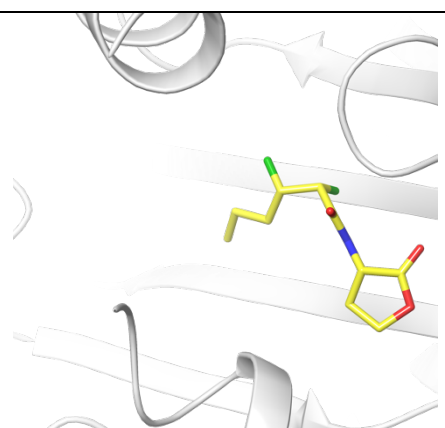
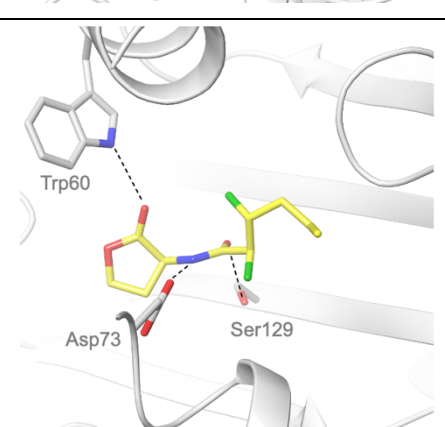
Method validation: The methods described above were validated by docking the native ligand (**1**) back into the protein structure according to the same parameters. A diversity of binding poses was

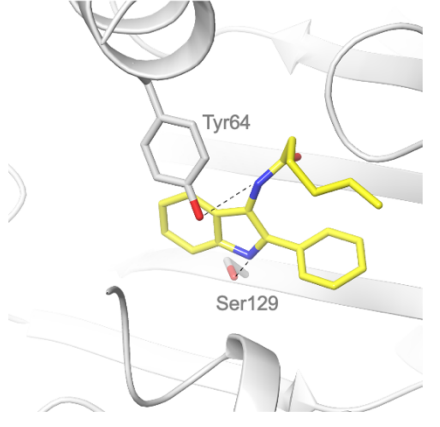
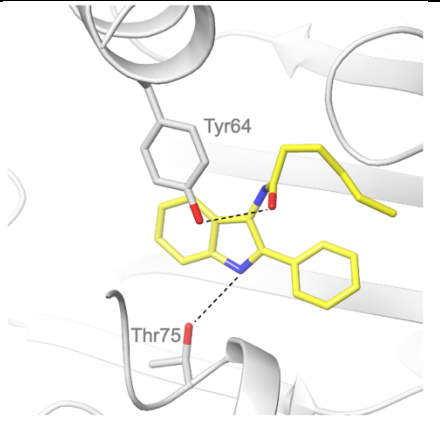

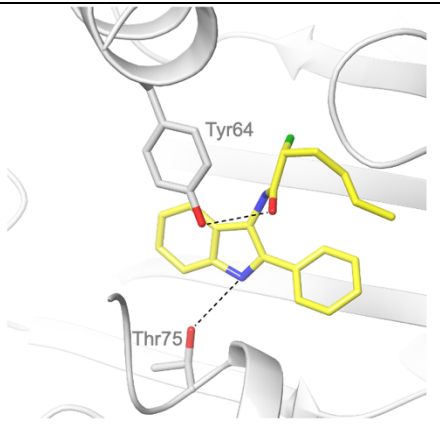
obtained, confirming that the ligand was able to rotate and change conformation during the docking process. The “best” pose, which was pose #1 according to the decision process described above, quite closely matched the pose seen in the crystal structure (see the Table below).

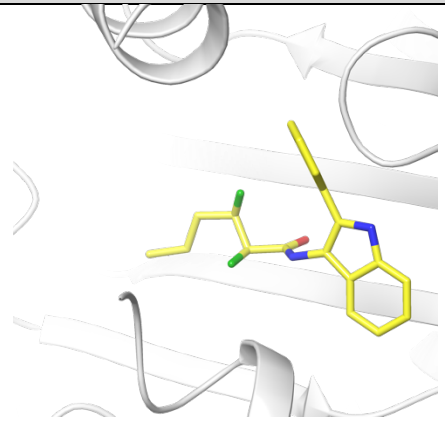
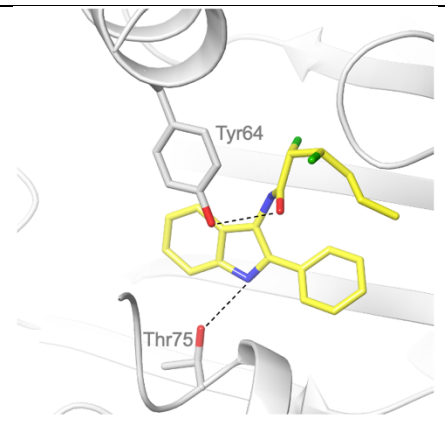
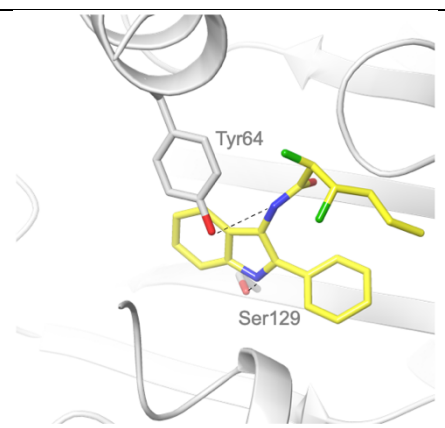
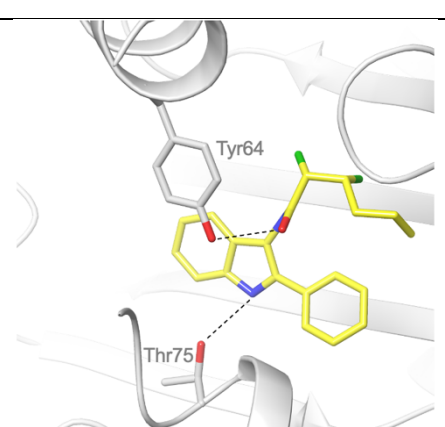
Results: See the Table overleaf.

Analysis of results: For the fluorinated lactones (**2a–f**), Autodock Vina successfully predicts the top three most potent QS inhibitors based on calculated binding affinities (*i.e.* 1st = **2d**; 2nd = **2f**; 3rd = **2b** [albeit equal 3rd]). Another measure of success is that for each of these top three inhibitors, the “best” pose is ranked #1 or #2, whereas for the other compounds in the lactone series (*i.e.* **2a**, **2c**, **2e**), the “best” pose is ranked #4 or lower. The results for the fluorinated indoles (**3a–f**) are not quite as clear. Autodock Vina successfully distinguishes the top four most potent indoles (*i.e.* **3e**, **3f**, **3d**, **3b**) from the two least potent indoles (*i.e.* **3a**, **3c**) based on calculated binding affinities, albeit not in the correct rank order. Another measure of success is that for the top four indoles, the “best” pose is ranked #1 or #2, whereas for the other indoles, the “best” pose is ranked #3 or lower.

Ligand	Pose #	3D geometry of docked pose, with polar interactions highlighted	Predicted binding affinity (kJ/mol)	Comments
1	1		-36.8	The docked pose (yellow) quite closely matches the crystal structure (teal), confirming that the docking method is appropriate. Polar interactions are shown for the docked ligand only.
2	2		-31.8	See manuscript text.
2a	5		-31.4	Poses #1–4 had high-energy OCCF torsions. Pose #5 is a completely different binding mode with no polar interactions. This explains the weak QS inhibitory activity of 2a .
2b	1		-31.4	See manuscript text.

Ligand	Pose #	3D geometry of docked pose, with polar interactions highlighted	Predicted binding affinity (kJ/mol)	Comments
2c	4		-31.0	Poses #1–3 had high-energy OCCF torsions. Pose #4 is a completely different binding mode with no polar interactions. This explains the weak QS inhibitory activity of 2c .
2d	1		-32.2	See manuscript text.
2e	8		-30.5	Poses #1–7 had high-energy OCCF torsions. Pose #8 is a completely different binding mode with no polar interactions. This explains the weak QS inhibitory activity of 2e .
2f	2		-31.8	Similar pose to 2b . The FCCF torsion is not ideal, but the pose is otherwise good and this explains the strong QS inhibitory activity of 2d .

Ligand	Pose #	3D geometry of docked pose, with polar interactions highlighted	Predicted binding affinity (kJ/mol)	Comments
3	1		-31.8	See manuscript text.
3	3		-28.0	See manuscript text. This is the closest to the “best” pose previously identified in a separate docking study using Discovery Studio / GOLD. ^[9]
3a	7		-18.0	Poses #1–6 had high-energy OCCF torsions. Pose #7 is a completely different binding mode. This explains the weak QS inhibitory activity of 3a .
3b	1		-30.1	See manuscript text.

Ligand	Pose #	3D geometry of docked pose, with polar interactions highlighted	Predicted binding affinity (kJ/mol)	Comments
3c	3		-25.1	Poses #1–2 had high-energy OCCF torsions. Pose #3 is a completely different binding mode with no polar interactions. This explains the weak QS inhibitory activity of 3c .
3d	1		-31.0	Similar to pose #3 of ligand 3 . The FCCF torsion is not ideal, but the pose is otherwise good and this explains the quite strong QS inhibitory activity of 3d .
3e	1		-29.7	See manuscript text. Similar to pose #1 of ligand 3 .
3f	2		-29.7	Similar to pose #3 of ligand 3 .

9. References

- [1] T. D. Beeson and D. W. MacMillan, Enantioselective organocatalytic α -fluorination of aldehydes, *J. Am. Chem. Soc.* **2005**, *127*, 8826.
- [2] K. B. Sharpless, W. Amberg, Y. L. Bennani, G. A. Crispino, J. Hartung, K. S. Jeong, H. L. Kwong, K. Morikawa, Z. M. Wang, D. Xu and X.-L. Zhang, The osmium-catalyzed asymmetric dihydroxylation: a new ligand class and a process improvement, *J. Org. Chem.* **1992**, *57*, 2768.
- [3] A. R. S. Vinson, V. K. Davis, K. A. Jesse, R. E. Hamilton, A. C. H. Shattuck, R. G. Iafe and A. G. Wenzel, Gold-catalyzed, S_N1 -type reaction of alcohols to afford ethers and Cbz-protected amines, *Synlett* **2015**, *26*, 265.
- [4] Gaussian 09, Revision A.02, M. J. Frisch, G. W. Trucks, H. B. Schlegel, G. E. Scuseria, M. A. Robb, J. R. Cheeseman, G. Scalmani, V. Barone, G. A. Petersson, H. Nakatsuji, X. Li, M. Caricato, A. Marenich, J. Bloino, B. G. Janesko, R. Gomperts, B. Mennucci, H. P. Hratchian, J. V. Ortiz, A. F. Izmaylov, J. L. Sonnenberg, D. Williams-Young, F. Ding, F. Lipparini, F. Egidi, J. Goings, B. Peng, A. Petrone, T. Henderson, D. Ranasinghe, V. G. Zakrzewski, J. Gao, N. Rega, G. Zheng, W. Liang, M. Hada, M. Ehara, K. Toyota, R. Fukuda, J. Hasegawa, M. Ishida, T. Nakajima, Y. Honda, O. Kitao, H. Nakai, T. Vreven, K. Throssell, J. A. Montgomery, Jr., J. E. Peralta, F. Ogliaro, M. Bearpark, J. J. Heyd, E. Brothers, K. N. Kudin, V. N. Staroverov, T. Keith, R. Kobayashi, J. Normand, K. Raghavachari, A. Rendell, J. C. Burant, S. S. Iyengar, J. Tomasi, M. Cossi, J. M. Millam, M. Klene, C. Adamo, R. Cammi, J. W. Ochterski, R. L. Martin, K. Morokuma, O. Farkas, J. B. Foresman, and D. J. Fox, Gaussian, Inc., Wallingford CT, **2016**.
- [5] T. Bally, and P. R. Rablen, Quantum-chemical simulation of ^1H NMR spectra. 2. Comparison of DFT-based procedures for computing proton–proton coupling constants in organic molecules. *J. Org. Chem.* **2011**, *76*, 4818.
- [6] M. Hentzer, K. Riedel, T. B. Rasmussen, A. Heydorn, J. B. Andersen, M. R. Parsek, S. A. Rice, L. Eberl, S. Molin, N. Høiby, S. Kjelleberg and M. Givskov, Inhibition of quorum sensing in *Pseudomonas aeruginosa* biofilm bacteria by a halogenated furanone compound. *Microbiology (Reading)* **2002**, *148*, 87.
- [7] O. Trott and A. J. Olson, AutoDock Vina: improving the speed and accuracy of docking with a new scoring function, efficient optimization and multithreading, *J. Comput. Chem.* **2010**, *31*, 455.
- [8] M. J. Bottomley, E. Muraglia, R. Bazzo and Andrea Carfi, Molecular insights into quorum sensing in the human pathogen *Pseudomonas aeruginosa* from the structure of the virulence regulator LasR bound to its autoinducer, *J. Biol. Chem.* **2007**, *282*, 13592.

- [9] N. N. Biswas, S. K. Kutty, N. Barraud, G. M. Iskander, R. Griffith, S. A. Rice, M. Willcox, D. StC. Black and N. Kumar, Indole-based novel small molecules for the modulation of bacterial signalling pathways, *Org. Biomol. Chem.* **2015**, *13*, 925.
- [10] J. W. Banks, A. S. Batsanov, J. A. K. Howard, D. O'Hagan, H. S. Rzepa and S. Martin-Santamaria, The preferred conformation of α -fluoroamides, *J. Chem. Soc. Perkin Trans. 2* **1999**, 2409.